To the Graduate Council:

I am submitting herewith a dissertation written by Robert Mark Worden entitled "Dynamics of a Biological Fixed Film for Phenol Degradation." I have examined the final copy of this dissertation for form and content and recommend that it be accepted in partial fulfillment of the requirements for the degree of Doctor of Philosophy, with a major in Chemical Engineering.

Terrence L. Donaldson

Terrence L. Donaldson, Major Professor

We have read this dissertation
and recommend its acceptance:

Duane D Bruns

George C. Frazier

Joseph F. Perna

David W. Watt

Charles D. Scott

Accepted for the Council:

Lee Minkel

Vice Provost
and Dean of The Graduate School

DYNAMICS OF A BIOLOGICAL FIXED FILM FOR PHENOL DEGRADATION

A Dissertation

Presented for the

Doctor of Philosophy

Degree

The University of Tennessee, Knoxville

Robert Mark Worden

March 1986

ACKNOWLEDGEMENT

I would like to thank my principal advisor, Dr. Terry Donaldson, for providing the support, guidance and resources which were invaluable during this endeavor. I also am indebted to Dr. Jerry Strandberg for his technical expertise and daily companionship. Despite having other obligations, these two always found the time when I needed them.

Special thanks go to my parents and my wife, Debbie, whose unfaltering support, interest, and encouragement have made the task an enjoyable one.

This research was supported in part by the Oak Ridge National Laboratory, which made available the facilities, equipment, and supplies used in this study. Fellowship support was provided by Union Carbide.

ABSTRACT

Experimental and modeling studies were conducted to analyze the dynamic-response behavior of a phenol-oxidizing fixed film. A differential, fluidized-bed bioreactor in a recycle loop with a well-mixed reservoir was used to conduct the unsteady-state experiments. Fresh phenol feed and oxygen were added continuously to the reservoir. With the bioreactor at steady state, a pulse of phenol was added to perturb the system, and the phenol concentration was monitored continuously until steady state was again achieved. The biofilm reaction rate was then calculated using an unsteady-state phenol mass balance.

The experimental dynamics were compared to a dynamic mathematical model based upon diffusion and reaction within the biofilm, liquid mixing, and biofilm growth. Constant-pH experiments could be adequately described using an unstructured, double-Monod kinetic expression with substrate inhibition by phenol. Inclusion of biological structure to account for metabolic regulation phenomena was not necessary.

However, in experiments without pH control, the pH of the liquid phase dropped from 7.0 to 4.5, and damped oscillations were observed in the phenol concentration and reaction rate trajectories. Oscillatory solutions could not be induced in the model, and a linear stability analysis did not reveal any tendencies toward instability or oscillations. The addition of product (pH) inhibition to the reaction kinetics did not produce oscillations. The cause of the experimental oscillations remains unknown.

An active-cell assay technique for biofilms was developed. The method measures electron-transport activity using INT, an organic salt which is reduced to a red dye. The assay procedure involves incubating the biofilm sample with INT, extracting the red product with acetone, and then measuring the optical density of the extract at 490 nm.

The method was found to be quite specific for active biomass. Cells killed with $HgCl_2$ or heat did not react with INT. The assay is not overly sensitive to changes in such process variables as substrate and oxygen concentrations. In addition, it is inexpensive, quick to perform, and requires no highly specialized equipment. It should prove useful in future analyses of biofilm processes.

TABLE OF CONTENTS

LIST OF TABLES

LIST OF FIGURES

FIGURE PAGE

PART I

DYNAMICS OF A BIOLOGICAL FIXED FILM FOR PHENOL DEGRADATION

CHAPTER I

INTRODUCTION

Biological fixed films exhibit properties which make them preferable to suspended-cell systems for many continuous bioprocess applications. These properties include extremely high cell concentrations, enhanced cell retention due to cell immobilization, and an increased resistance to the detrimental effects of toxic shock loadings.

Applications of fixed films are becoming more numerous. The use of rotating biological contactors, trickling filters, fluidized beds, and activated biofilters for wastewater treatment has been recently reviewed.[1] In addition, microbial film fermenters have been used for animal cell culture, bacterial leaching of ores, and the production of vinegar, ethanol, citric acid, and beer.[2-6] Even cells which do not naturally form fixed films can be artifically packed into tissuelike masses by confining them within hollow-fiber bioreactors.[7]

While the pseudo-steady-state performance of fixed films has been extensively studied both experimentally and theoretically,[8-13] the unsteady-state behavior which results from sudden changes in environmental conditions has received little attention. This behavior is important from both a basic science and an engineering perspective. From the scientific point of view, dynamic experiments can help elucidate patterns of intracellular metabolic regulation. Such techniques have already been demonstrated in suspended-cell culture.[14-18] In mixed-culture biofilms, interactions between the various component

species may be explored using dynamic experiments. Unsteady-state biofilm performance data can also be used to evaluate the effects of transients on process stability and to develop mathematical models and control algorithms.

Some research effort has been devoted to unsteady-state biofilm phenomena. Nutt et. al.[19] used an empirical curve-fitting approach to correlate the influent and effluent stream compositions of a fluidized-bed bioreactor for treatment of municipal wastewater. Chi Tien et al.[20] have investigated the growth of microorganisms on the packing material of an expanded-bed adsorption column and the effect of this growth on the overall column performance. Their dynamic model described substrate uptake and growth by the microorganisms and predicted effluent breakthrough curves. Vanderborght et al.[21] have applied sudden pulses of high substrate concentration to a fluidized-bed bioreactor and monitored the overall reactor performance. They found that the amount of substrate consumed increased roughly in proportion to concentration of the shock loading; however, no mathematical model of the system was presented. Park et al.[22] have derived an unsteady-state model describing a fluidized-bed bioreactor for penicillin production and have predicted the effects of biofilm growth and feeding strategies on outlet product concentration. Benefield et al.[23,24] have modeled biofilm reactors in the unsteady state. In their model, the biofilm is assumed to be constantly in pseudo-steady state with respect to the bulk-liquid concentration. This assumption may not be appropriate under rapidly changing experimental conditions. Rittman et al.[25] have demonstrated that

for wastewater treatment, alternately feeding and starving a biofilm can achieve very low effluent concentrations during the starvation phase. Their unsteady-state model predicts biofilm growth and decay during the feeding cycles. Denac et al.[26] have modeled a biofilm for nitrification in the unsteady state for the purpose of describing batch nitrification processes.

None of the above studies has experimentally measured the short-term effects of sudden changes in substrate concentration on the biofilm reaction rate and then used these data to verify a dynamic biofilm model. Dynamic models of microbial processes are of questionable utility without experimental verification; dynamic chemostat models using kinetic expressions which accurately predict steady-state performance are often inadequate in unsteady-state applications.[27-29]

We have developed a technique for measuring the unsteady-state behavior of fluidized-bed bioparticles and have used it to study the effects of sudden changes in substrate concentration on the biofilm reaction rate. We have also constructed a dynamic mathematical model of the experimental system and used it to analyze and interpret the data.

This study has provided insight into basic biofilm phenomena as well as verification of the capabilities and limitations of the dynamic model.

CHAPTER II

EXPERIMENTAL APPROACH

Microbial Film

The biological fixed-film used in this study was a mixed culture of microorganisms attached to 30 to 60 mesh anthracite coal particles. This biofilm has been used at the Oak Ridge National Laboratory (ORNL) in the development of three-phase fluidized-bed reactors for biooxidation of phenolic wastewaters.[30] It has been used in the treatment of both synthetic and actual coal-gasification wastewaters over a period of several years. Microbial characterization studies have identified several of the component species, which are shown in Table 1.[30]

Medium

The composition of the medium, which consisted primarily of monohydric phenol plus mineral salts and micronutrients, is listed in Table 2. Phosphate provided some buffering capacity to reduce the natural acidification of the medium by biooxidation products such as carbon dioxide. In some experiments automatic pH control was also employed, using a titrant of 0.1 M KOH.

Bioreactor

The experimental bioreactor was designed to facilitate continuous measurement of the biofilm reaction rate following a perturbation from steady state. Figure 1 shows schematically the two key components: a

Table 1

Cultures Isolated From Phenol-Degrading Biofilm

Pseudomonas fluorescens
Pseudomonas mendocina
Pseudomonas stutzeri
Pseudomonas alcaligenes
Pseudomonas sp.
Alcaligenes sp. (two isolates)
Flavobacterium ferrugineum
Arthrobacter globiformis
Endomycopsis sp.
Four unidentified bacteria

Source: Donaldson, T. L., Strandberg, G. W., Hewitt, J. D., and Shields, G. S. (1984), "Biooxidation of Coal Gasification Wastewaters," *Environmental Progress*, *3*, p. 248.

Table 2

Composition of Experimental Medium

Component	Concentration (g/cm^3) × 10^6
Phenol	50 to 100 (varied between experiments)
Salts	
NH_4NO_3	200
K_2HPO_4	64
$MgSO_4 \cdot 7H_2O$	20
KI	2
Micronutrients	
H_3BO_3	0.02
$ZnSO_4 \cdot 7H_2O$	0.008
$(NH_4)_6Mo_7O_{24} \cdot 4H_2O$	0.004
$MnSO_4 \cdot 7H_2O$	0.008
$CuSO_4 \cdot 5H_2O$	0.009
$FeSO_4 \cdot 7H_2O$	0.005
Thiamine HCl	0.013

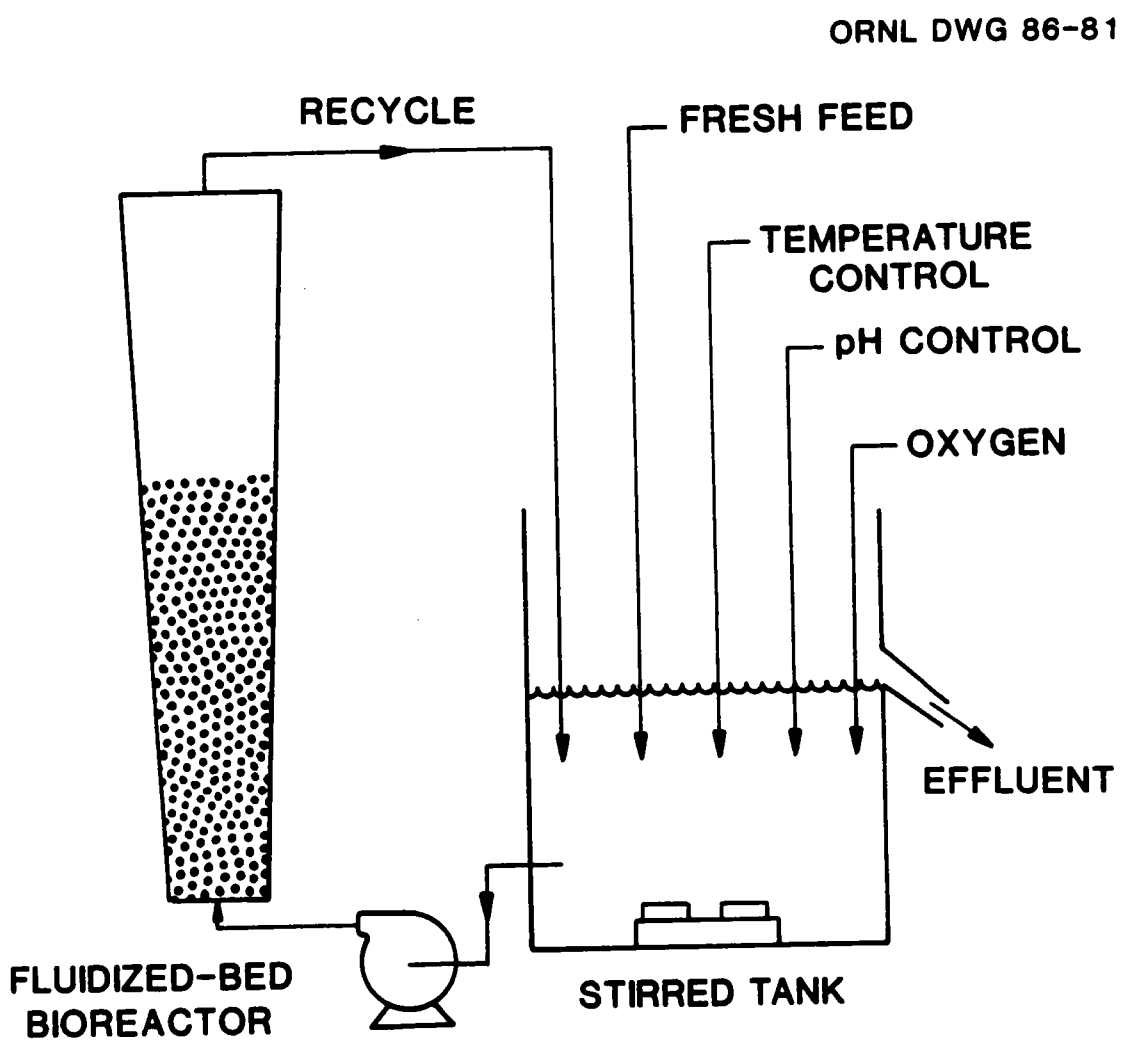

Figure 1. Experimental Bioreactor.

small fluidized bed of biofilm particles and a stirred tank. Biooxidation of phenol occurred within the fluidized-bed, while addition of fresh feed and oxygen, mixing of reagents, and automatic control of pH and temperature took place in the stirred tank. A liquid-recycle loop carried medium between the two components. The fluidized bed of biofilm particles was typically 40 mL in volume and was contained within a tapered glass column having an inner diameter of 1.25 cm at the bottom and 2.5 cm at the top. The total internal volume of the column and its headpiece was ~140 mL. The 210 mL stirred tank was a modified New Brunswick Model C-30 fermenter which had automatic temperature and pH control capabilities. Variable-speed Masterflex peristaltic pumps were used for medium delivery.

This reactor configuration has several advantageous features. By physically separating the reaction and mixing zones, the rate of transfer of oxygen from the gas to the liquid phase could be adjusted over a wide range without affecting the hydrodynamics and mass transfer within the fluidized bed.

By keeping the fluidized bed relatively small (~15 mL settled volume), a differential reactor could be approximated. That is, the change in medium concentration across the bed was sufficiently small that all biofilm particles were exposed to approximately identical conditions.

In addition, by using a high recycle flow rate relative to the fresh-feed flow rate, the entire liquid contents of the system could be assumed to be well mixed. The overall mean residence time of the medium (~20 min) was far greater than the residence time in the glass

column (~1 min). Residence time distribution studies using a black ink tracer confirmed that perfect mixing was a valid assumption.

Initially it was found that cells would slough off the biofilm, multiply in the rich medium, and cause significant free-cell concentrations. This problem was overcome by locating an Aquafine ultraviolet water sterilizer in-line between the fluidized bed and stirred tank. The sterilizer killed free cells, thus minimizing their contribution to the overall bioactivity.

Analytical Techniques

Phenol concentration was measured and recorded continuously by monitoring the optical density at 270 nm with a Beckman DB-G spectrophotometer and chart recorder. A slip-stream from the stirred tank was pumped through a Gelman 0.45 micron Acrodisc filter, into a quartz flow-through cuvette, and finally back to the stirred tank. The chart-recorder graphs were later processed using a digitizing tablet to create data tables within a DEC-10 computer at the University of Tennessee. The data were then converted from optical density to concentration units via a calibration curve. The accuracy of the optical density assay was tested periodically by comparison with the colorimetric 4-aminoantipyrine assay.[31] Below 10 mg/L the optical density assay was found to lose accuracy.

Biomass was quantified on a dry weight of biofilm basis. At the end of each experiment, the bed of biofilm particles was gently poured into a graduated cylinder, and the settled volume was measured. The bed was then rinsed with distilled water and transferred into a

preweighed aluminum pan, dried to a constant weight at 100°C, and then weighed again; this measurement provided the weight of coal plus dry biomass. The dried bed was then treated twice with 30-mL aliquots of 1 M NaOH for 15 min with occasional vigorous swirling to remove the biofilm. The coal was rinsed several times with distilled water to flush away biomass remnants, dried, and weighed again. Dry weight of biomass was then calculated by subtracting the weight of clean coal from the weight of coal plus biomass.

With the above data, an estimate could be made of the dry-weight concentration of the biofilm. The wet volume of the biofilm could be estimated by subtracting the volume of the clean coal and the void volume of the settled bed from the total volume of the settled bed. The void volume was assumed to be 10% of the total settled-bed volume. The clean-coal volume was calculated from the known density and mass of the clean coal in the bed. Dry-weight concentration was finally obtained by dividing the measured dry weight of the biofilm by its estimated wet volume.

Oxygen concentration was measured within the stirred tank using a YSI Model 53 oxygen monitor and Clark-type polarographic probe.

Procedure

The glass-column bioreactor was loaded with a 15 mL (settled volume) bed of biofilm particles taken from a larger fluidized-bed bioreactor which was maintained continuously on an identical medium. The stirred tank was then filled with medium, and continuous operation of the reactor was begun. The flow rate of fresh medium was typically

20 mL/min, and the recycle flow rate was ~140 mL/min. Pure oxygen gas was bubbled into the stirred tank at a rate of ~75 mL/min. The temperature and pH controllers were set to 30°C and 7.0, respectively. The concentration of phenol in the fresh medium varied from 50 to 100 mg/L, depending on the purposes of the experiments.

The reactor was operated continuously for a period of ~20 h to allow the biofilm to achieve a pseudo-steady state condition which was marked by a relatively constant phenol concentration in the reactor effluent.

To initiate a dynamic experiment, the system was perturbed by the injection of an aliquot (typically between 0.5 and 1.2 mL) of 50 g/L phenol solution into the stirred tank. The phenol concentration was then continuously monitored via absorbance at 270 nm until a steady reactor effluent concentration was again achieved.

Data Analysis

The instantaneous phenol degradation rate in the biofilm (R) was calculated from the effluent phenol concentration (P) data using an unsteady-state mass balance on phenol in the reactor,

$$V_L \frac{dP}{dt} = F(P_{in} - P) - R\, V_{bed} \qquad (1)$$

where V_L is the total liquid volume in the system, F and P_{in} are the volumetric flow rate and phenol concentration of the fresh feed, and V_{bed} is the settled volume of the bed of bioparticles. This equation was derived assuming that the liquid-mixing characteristics within the

reactor closely match those of a perfectly mixed, stirred-tank reactor. The validity of this assumption was tested by comparing the residence time distribution (RTD) curve of a pulse of black ink with the curve predicted using a continuous stirred tank model. These two curves are shown in Fig. 2. Agreement is excellent, confirming the validity of the perfect-mixing assumption.

All of the terms in Eq. (1) except R were determined from experimental measurements, and hence R can be calculated. The time derivative was determined from the slope of the phenol concentration versus time curve using a three-point numerical differentiation scheme for nonconstant step sizes.[32] Numerical differentiation tends to amplify random error in the data, and hence the calculated reaction-rate trajectories tended to be less smooth than the original phenol trajectory curves.

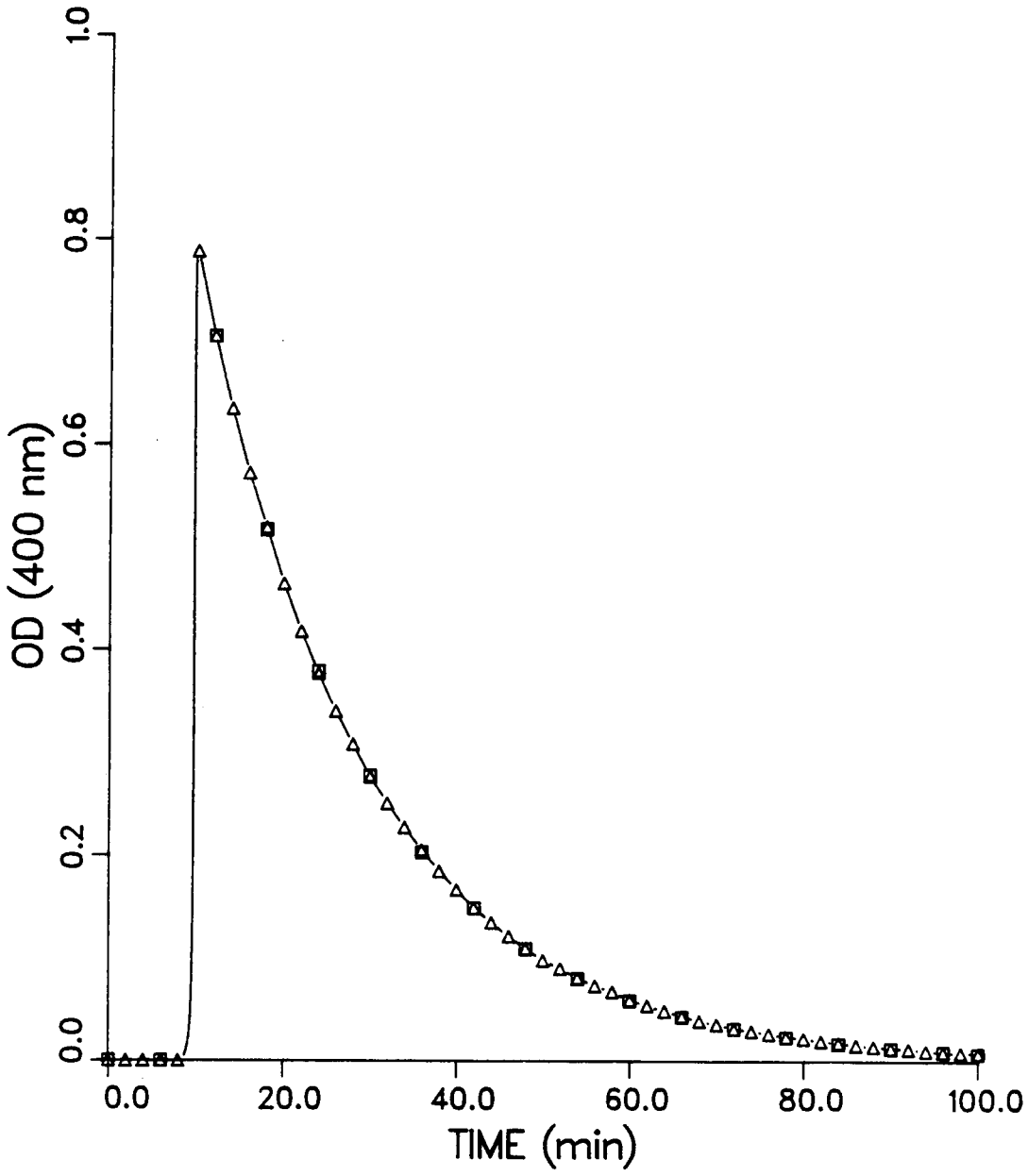

Figure 2. Predicted and experimental RTD curves.

Triangles: Predicted values; Squares: Experimental values.

CHAPTER III

EXPERIMENTAL RESULTS

Effect of Oxygen Concentration

Oxygen is required by this biofilm culture for the degradation of phenol; in an anaerobic environment, the degradation rate virtually ceases. To investigate the effect of oxygen concentration on the biofilm reaction rate, the stirred tank was sparged with a mixture of nitrogen and oxygen. The concentration of oxygen in the liquid phase was controlled by adjusting the proportions of the two gases via rotameters; the total gas flow rate was kept constant to prevent changes in the gas-phase volume fraction. Phenol and oxygen concentrations were monitored following each change in oxygen concentration until a new steady state was achieved (typically within one hour). In this way, several oxygen concentrations could be tested within a six-hour period, and the effects of biofilm growth could be neglected. The steady-state reaction rate corresponding to each oxygen concentration was calculated using Eq. (1) with the time derivative set equal to zero.

Figure 3 depicts the effect of oxygen concentration in the liquid phase on the observed steady-state biofilm reaction rate. The phenol concentration was held approximately constant at 75 mg/L during this experiment. The curve indicates that oxygen concentration is strongly rate-limiting below 20% saturation and weakly rate-limiting at 80% saturation. From a practical standpoint, these data indicate that if

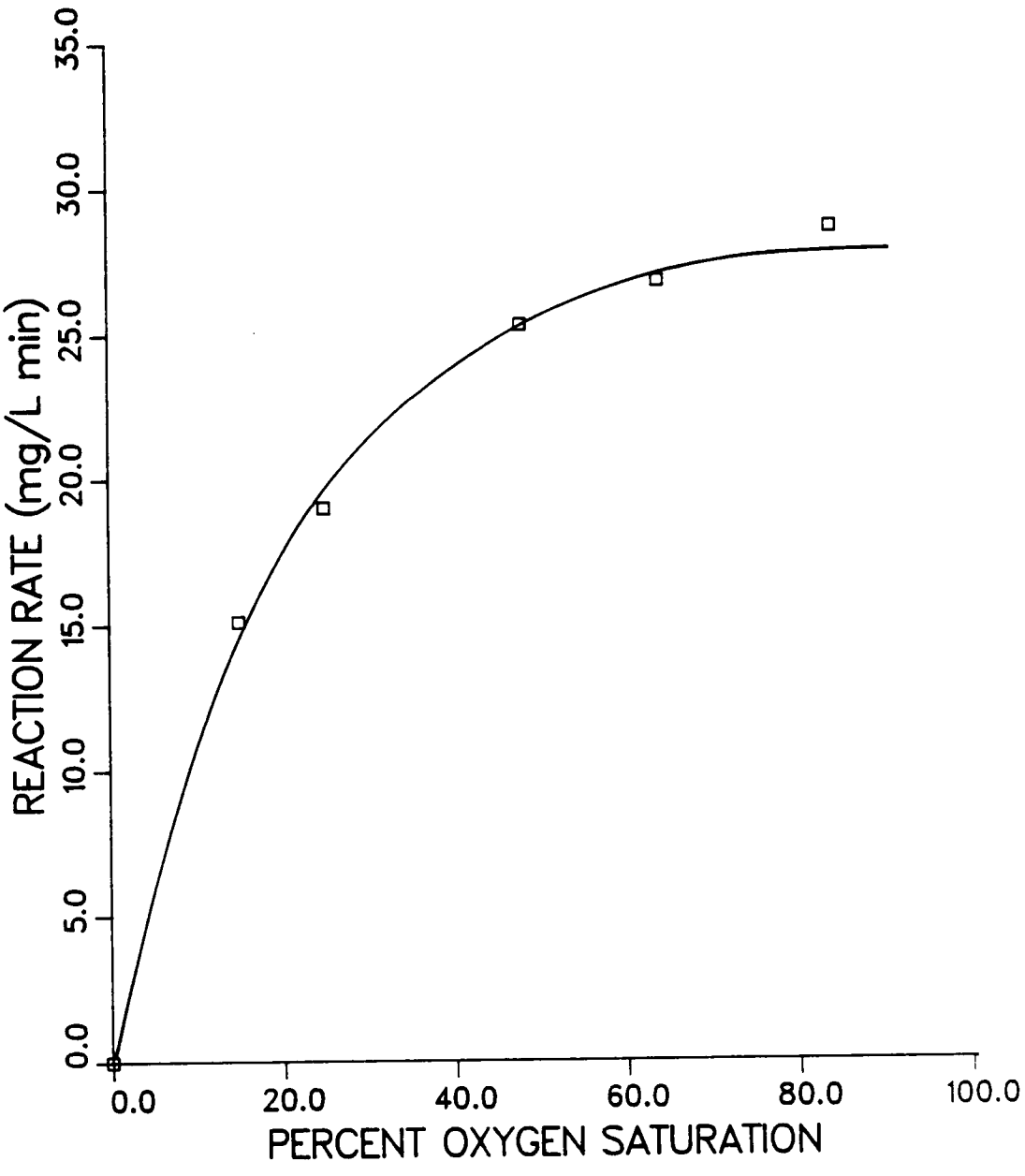

Figure 3. Effect of oxygen concentration on observed biofilm degradation rate.

air (21% oxygen) were used as a source of oxygen, the reaction rate would be limited to approximately half of the maximum rate.

The primary focus of the present study was on the effects of rapid changes in the phenol concentration on the biofilm reaction rate. In order to avoid masking the effects of phenol by oxygen limitation, the following experiments were conducted in the presence of relatively high oxygen concentrations, typically greater than 70% saturation.

Effect of Phenol Concentration

The trends observed in the biofilm's response to a sudden increase in phenol concentration depended upon the magnitude of increase. A typical response to relatively small increases is shown in Fig. 4, in which both phenol concentration and biofilm reaction rate are plotted as a function of time. At time zero, an aliquot of phenol was injected into the stirred tank, raising the concentration in the reactor from ~10 to 65 mg/L. As a result, the biofilm reaction rate rapidly increased. At the higher degradation rate, phenol was rapidly consumed, and its concentration returned to the original level. As the phenol concentration dropped, there was insufficient substrate to support the high reaction rate, and the rate also returned to its original value. This dynamic behavior is intuitively consistent with the concept that the biofilm was substrate-limited.

The pH of the medium was automatically controlled at 7.0 during this experiment. In a subsequent experiment, the same procedure was repeated without using pH control. These results are shown in Fig. 5.

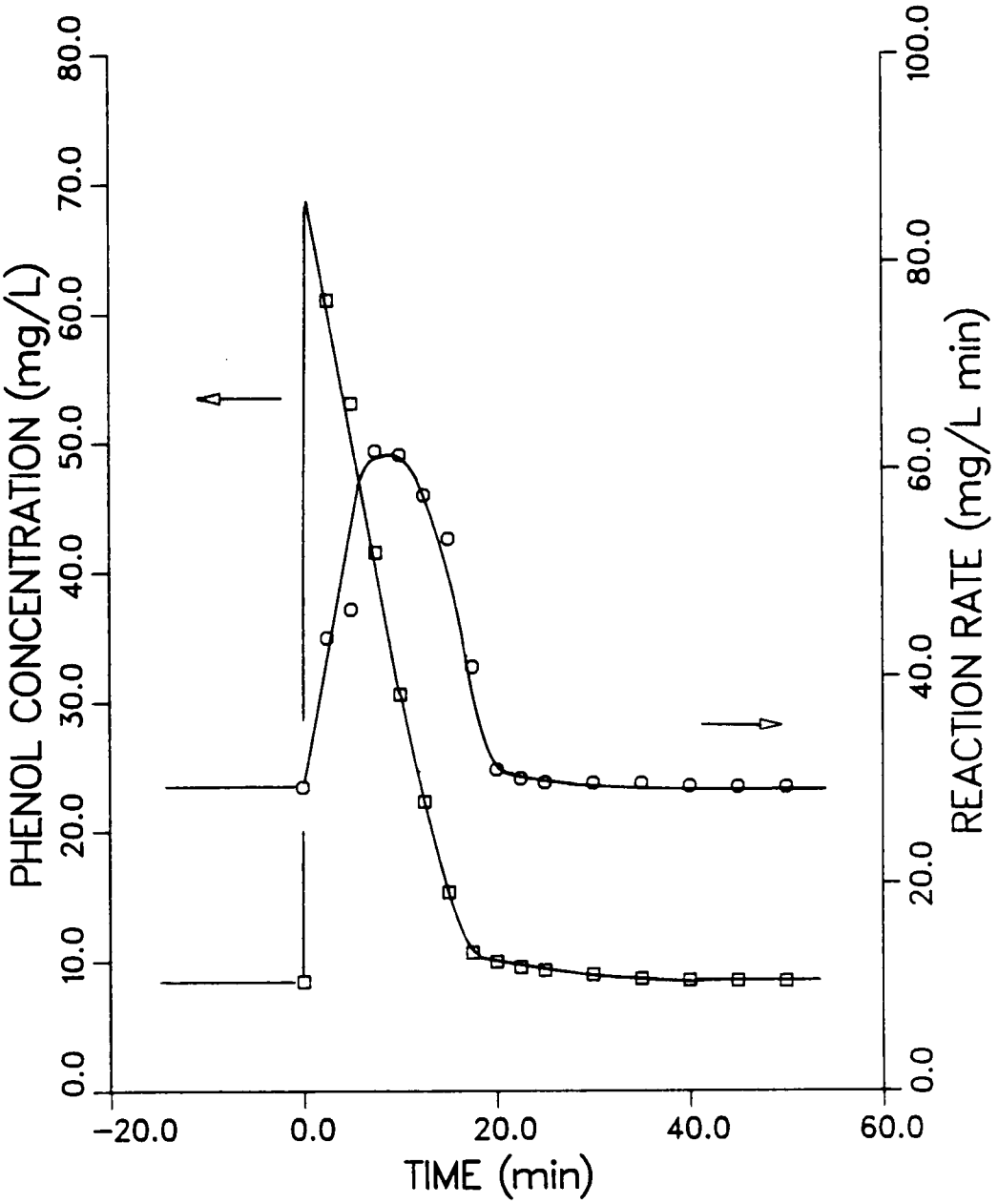

Figure 4. Biofilm response to a relatively small pulse of phenol.

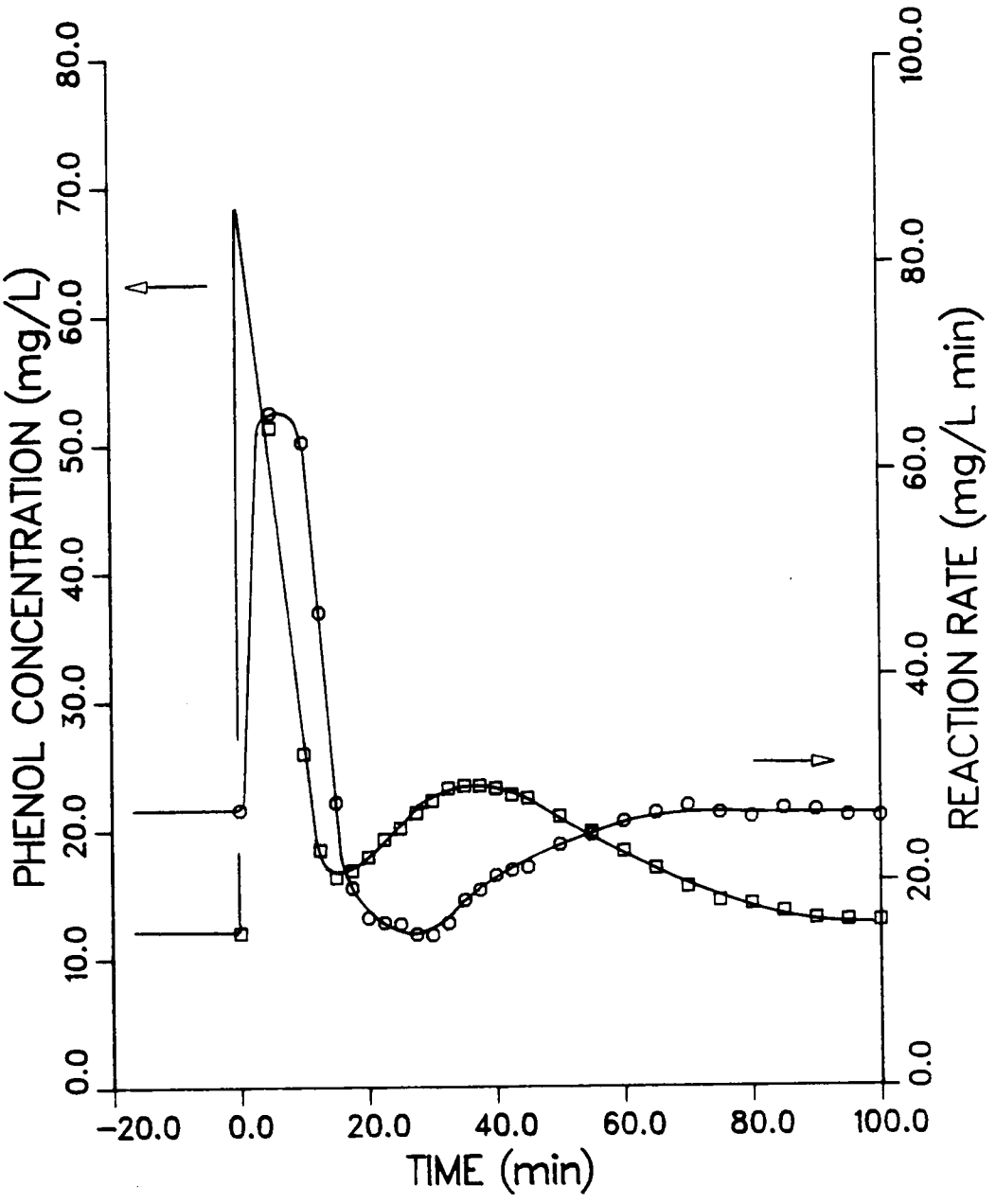

Figure 5. Biofilm response to a relatively small pulse of phenol without pH control.

Initial trends in the data are the same as in Fig. 4; an increase in the phenol concentration resulted in an increase in the reaction rate. However, there was an oscillatory return to the steady state which was not observed in Fig. 4. The pH within the reactor decreased from a value of 5.3 prior to the perturbation to 4.2 during the period of highest reaction rate. At the end of the experiment, it had returned to 5.5. The pH of the continuous phenol feed was 7.0. Carbon dioxide is produced by the biofilm in significant quantities[33] and was probably responsible for the acidification. An effluent sample was tested for the presence of volatile organic acids using a Varian Model 3700 Gas Chromatograph with a 60 to 80 Carbopack C/0.3% Carbowax 20 M/0.1% H_3PO_4 packing. The sensitivity of the instrument was ~0.5 mg/L. No organic acids were detected in the sample.

The interesting oscillatory behavior exhibited in Fig. 5 was only observed in experiments without pH control. In order to investigate the effects of phenol concentration independently of pH influences, automatic pH control at 7.0 was employed.

When larger pulses of phenol were used to perturb the biofilm, a different pattern of dynamic response was observed, as shown in Fig. 6. Immediately after the phenol concentration was increased from ~15 to 170 mg/L, the reaction rate dropped significantly. Then, as the phenol concentration was diminished by reaction and convection, the reaction rate increased until it peaked at a value slightly higher than the original steady-state value. It then returned to the steady-state reaction rate.

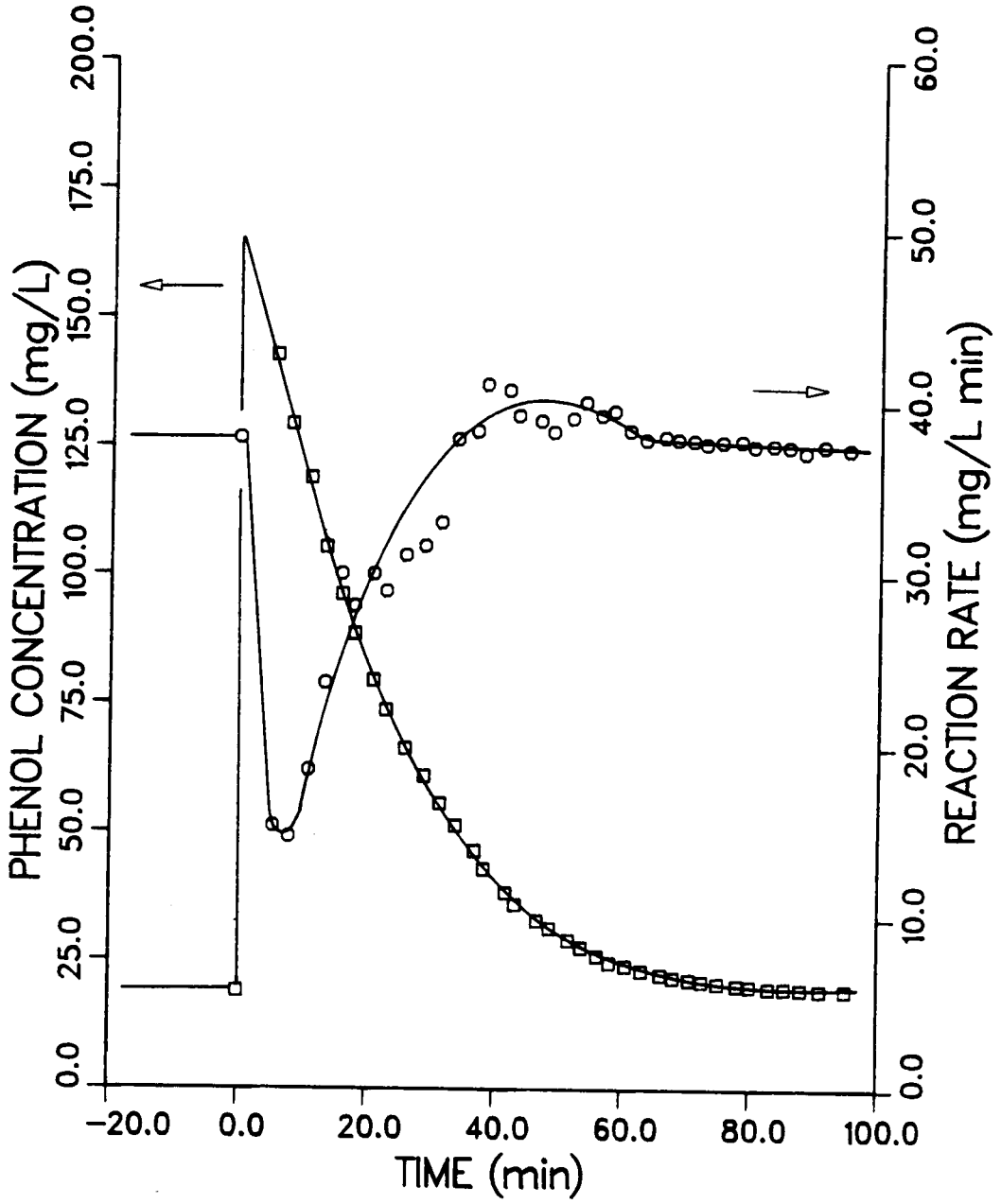

Figure 6. Biofilm response to a relatively large pulse of phenol.

A notable feature of Fig. 6 is the drop in reaction rate at the high phenol concentrations. Since phenol has been identified as an inhibitory substrate in other studies using pure and mixed cultures,[34-37] this drop may be due to phenol toxicity.

CHAPTER IV

MATHEMATICAL MODEL DEVELOPMENT

A mechanistic model of the experimental reactor has been developed to investigate the roles of hydrodynamics, mass transfer and reaction kinetics. The model is based upon unsteady-state mass balances on phenol and oxygen within the bulk-liquid and biofilm phases. Biofilm growth is also included.

The unsteady-state biofilm model is based upon the following assumptions:

1. The two rate-limiting substrates are phenol and oxygen.

2. Mass transfer within the biofilm obeys Fick's law.

3. The several microbial species within the biofilm can be adequately modeled as a single "average" species.

4. Consumption of oxygen is proportional to the consumption of phenol.

5. Production of new biomass is proportional to the consumption of phenol.

6. Biomass decay is negligible.

7. The resistance to substrate mass transfer between the liquid and solid phases is negligible. (The validity of this assumption is discussed in Appendix 1.)

8. The liquid-biofilm distribution coefficients of the substrates are unity.

9. The coal particles may be considered spherical in shape, of uniform size, and inert to the substrates.

10. The biofilm is uniform in thickness, composition, and reactivity.

11. There are no temperature gradients.

Biofilm Dynamics

The unsteady-state mass balance equation for phenol concentration (P) within the biofilm is

$$\frac{\partial P}{\partial t} = D_P \left[\frac{\partial^2 P}{\partial r^2} + \frac{2}{r} \frac{\partial P}{\partial r} \right] - R_P \ , \qquad (2)$$

where D_p is the effective diffusivity of phenol in the biofilm, R_p is the rate of phenol consumption by reaction, r is the radial position, and t is time. Since the oxygen concentration (0) may be reaction-rate limiting, a similar equation must be written for the oxygen concentration in the biofilm,

$$\frac{\partial O}{\partial t} = D_O \left[\frac{\partial^2 O}{\partial r^2} + \frac{2}{r} \frac{\partial O}{\partial r} \right] - R_O \ . \qquad (3)$$

The boundary conditions are obtained from assumptions 7 and 8:

$$r = r_i \ , \quad \frac{\partial P}{\partial r} = 0 \ , \quad \frac{\partial O}{\partial r} = 0$$

$$r = r_o \ , \quad P = P_b \ , \quad O = O_b$$

where r_i and r_o are the inner and outer radii of the biofilm, respectively, and P_b and O_b are the substrate concentrations in the bulk

liquid. The initial conditions are chosen to describe the experimental procedure. Since the experiments were begun by perturbing the steady-state biofilm, the initial conditions are:

$$t = 0 \quad , P = P\Big|_{ss} \quad , O = O\Big|_{ss} \quad ,$$

where the subscript ss denotes steady-state values.

R_p and R_o are kinetic expressions which represent an average of the collective contributions of several different species of microorganisms. Considerable research effort is currently being devoted to understanding the inter- and intracellular processes which regulate the rates of growth and reaction of single species and mixed populations in the unsteady state. Structured models being developed often incorporate such variables as intracellular concentrations of glucose, RNA, ATP, inorganic cations, etc.[38-40] As these models of cell behavior become more fully developed, their substitution into eqs. 2 and 3 should result in biofilm models of improved predictive capabilities. However, in the present study, it was found that a relatively simple, unstructured kinetic model which includes substrate inhibition by phenol[35] was sufficient to predict most of the trends observed in the data:

$$R_p = K_{max} X \left[\frac{O}{K_o + O}\right]\left[\frac{P}{K_p + P + P^2/K_I}\right], \qquad (4)$$

where K_{max} is a maximum specific reaction rate constant, X is the concentration of biomass in the biofilm, K_p and K_o are Monod

half-velocity constants for phenol and oxygen respectively, and K_I is an inhibition constant for phenol. The substrate inhibition functionality was suggested by the observed decline in reaction rate at high phenol concentrations (Fig. 6).

Oxygen consumption can be calculated using assumption 4:

$$R_o = Y_{o/p} R_p \ , \tag{5}$$

where $Y_{o/p}$ is the number of grams of oxygen consumed per gram of phenol consumed.

Equations 2, 3, and 4 can be rewritten in terms of the dimensionless variables defined below. Details of this procedure have been presented elsewhere.[22]

$$\overline{P} = \frac{P}{P^\circ}$$

$$\overline{O} = \frac{O}{O^\circ}$$

$$\overline{t} = \frac{t\ D_p}{r_i^2}$$

$$\overline{r} = \frac{r - r_i}{r_o - r_i}$$

$$h = \frac{r_o}{r_i} - 1$$

$$\overline{K}_p = \frac{K_p}{P^\circ}$$

$$\overline{K}_o = \frac{K_o}{0^\circ}$$

$$\overline{K}_I = \frac{K_I}{P^\circ}$$

$$\overline{D}_o = \frac{D_o}{D_p}$$

$$\overline{R}_p = \frac{K_{max} \times r_i^2}{P^\circ D_p} \left[\frac{\overline{0}}{\overline{K}_o + \overline{0}}\right] \left[\frac{\overline{P}}{\overline{K}_p + \overline{P} + \overline{P}^2/\overline{K}_I}\right]$$

P° and 0° are reference concentration values, arbitrarily chosen to be 200 mg/L and 36 mg/L, respectively. The dimensionless radial position variable ($\overline{r}$) varies from 0 to 1, regardless of changes in r_o due to biofilm growth. Thus the moving boundary conditions have been converted to fixed boundary conditions. This transformation introduces a new dependent variable, h, the dimensionless biofilm thickness. The dimensionless equations are

$$\frac{\partial \overline{P}}{\partial \overline{t}} = \frac{\partial \overline{P}}{\partial \overline{r}}\left[\frac{\overline{r}}{h}\frac{dh}{d\overline{t}} + \frac{2}{h(1 + h\overline{r})}\right] + \frac{1}{h^2}\frac{\partial^2 \overline{P}}{\partial \overline{r}^2} - \overline{R}_p \ , \qquad (2a)$$

$$\frac{\partial \overline{0}}{\partial \overline{t}} = \frac{\partial \overline{0}}{\partial \overline{r}}\left[\frac{\overline{r}}{h}\frac{dh}{d\overline{t}} + \frac{2\overline{D}_o}{h(1 + h\overline{r})}\right] + \frac{\overline{D}_o}{h^2}\frac{\partial^2 \overline{0}}{\partial \overline{r}^2} - Y_{o/p}\,\overline{R}_p \ . \qquad (3a)$$

The boundary and initial conditions expressed in dimensionless variables are

$$\bar{r} = 0 \quad , \quad \frac{\partial \bar{P}}{\partial \bar{r}} = 0 \quad , \quad \frac{\partial \bar{O}}{\partial \bar{r}} = 0$$

$$\bar{r} = 1 \quad , \quad \bar{P} = \bar{P}_b \quad , \quad \bar{O} = \bar{O}_b$$

$$\bar{t} = 0 \quad , \quad \bar{P} = \bar{P}\Big|_{ss} \qquad \bar{O} = \bar{O}\Big|_{ss} \quad .$$

Liquid-Phase Dynamics

Unsteady-state mass balances for phenol and oxygen in the liquid phase must also be written, since the concentrations of these species vary during the experiment. As discussed previously, the experimental reactor is well described by a perfect-mixing model. The appropriate mass balance equations are

$$V_T \, \varepsilon_\ell \, \frac{dP_b}{dt} = F(P_{in} - P_b) + N_p \, A_s \quad , \tag{6}$$

$$V_T \, \varepsilon_\ell \, \frac{dO_b}{dt} = F(O_{in} - O_b) + K_L a(V_T \alpha)(O^* - O_b) + N_o \, A_s \quad , \tag{7}$$

where V_T is the total wetted volume of the experimental reactor (column plus stirred tank), ε_ℓ is the liquid volume fraction, F is the volumetric flow rate of fresh feed, P_{in} and O_{in} are the phenol and oxygen concentrations in the feed, O^* is the liquid-phase concentration which would be in equilibrium with the gas-phase con-

centration, N_p and N_o are the mass fluxes of the substrates into the biofilm, A_s is the total surface area of the solid (bioparticle) phase, K_La is the average overall coefficient for oxygen transfer from the gas to the liquid phase, and $V_T\alpha$ is the wetted volume of the stirred tank. As before, the initial conditions are chosen to be consistent with the experimental procedure,

$$t = 0 \quad , \; P_b = P_b\Big|_{ss} \quad , \quad O = O_b\Big|_{ss} \; .$$

Equations (6) and (7) are coupled to the biofilm equations (eqs. 2a and 3a) through application of Fick's law at the outer surface of the biofilm to describe the fluxes of substrate from the bulk liquid into the biofilm:

$$N_p = -D_p \frac{\partial P}{\partial r}\Big|_{r = r_o} \; , \tag{8}$$

$$N_o = -D_o \frac{\partial O}{\partial r}\Big|_{r = r_o} \; . \tag{9}$$

The total biofilm surface area (A_s) may be expressed as

$$A_s = V_T \, \varepsilon_s \frac{3}{r_o} \; , \tag{10}$$

where ε_s is the volume fraction of the solid phase.

After incorporating equations 8-10 and nondimensionalizing, equations 6 and 7 become

$$\frac{d\bar{P}_b}{d\bar{t}} = \frac{1}{\bar{\tau}} (\bar{P}_{in} - \bar{P}_b) - \frac{3\varepsilon_s}{\varepsilon_\ell \, h(1 + h)} \frac{\partial \bar{P}}{\partial \bar{r}}\bigg|_{\bar{r} = 1} , \qquad (6a)$$

$$\frac{d\bar{O}_b}{dt} = \frac{1}{\bar{\tau}} (\bar{O}_{in} - \bar{O}_b) + \bar{K}_L a \frac{\alpha}{\varepsilon_\ell} (\bar{O}^* - O_b) - \frac{3\bar{D}_o \varepsilon_s}{\varepsilon_\ell h(1 + h)} \frac{\partial \bar{O}}{\partial \bar{r}}\bigg|_{\bar{r} = 1} , \qquad (7a)$$

where $\bar{\tau}$ (the dimensionless mean residence time) and $\bar{K}_L a$ are defined as:

$$\bar{\tau} = \frac{V_T \, \varepsilon_\ell \, D_p}{F \, r_i^2} ,$$

$$\bar{K}_L a = K_L a \, D_p / r_i^2 .$$

The dimensionless initial conditions are

$$\bar{t} = 0 \quad , \bar{P}_b = \bar{P}_b\Big|_{ss} \quad , \quad \bar{O}_b = \bar{O}_b\Big|_{ss} .$$

Bioparticle Growth

The amount of new biomass (m) produced due to growth of the microorganisms is assumed to be proportional to the amount of phenol consumed, with the proportionality constant being the yield coefficient ($Y_{x/p}$). Consequently, the rate of growth (dm/dt) may be calculated from the flux of phenol into the biofilm:

$$\frac{dm}{dt} = -Y_{x/p} \; D_p \frac{\partial P}{\partial r}\bigg|_{r = r_o} A_s . \qquad (11)$$

The rate of change in the biofilm volume (dV_f/dt) can then be calculated using the dry weight concentration of the biofilm (X),

$$\frac{dV_f}{dt} = \frac{1}{X}\frac{dm}{dt} . \qquad (12)$$

Since the volume of the inert coal particles remains constant,

$$\frac{dV_s}{dt} = \frac{dV_f}{dt} , \qquad (13)$$

where V_s is the total volume of the solid (bioparticle) phase.

Equations 11 through 13 are combined to give

$$\frac{dV_s}{dt} = \frac{1}{X} Y_{x/p} D_p A_s \left.\frac{\partial P}{\partial r}\right|_{r = r_o} , \qquad (14)$$

which expresses the rate of volumetric growth of the bioparticles.

The initial condition is

$$t = 0 \qquad V_s = V_{s,o} ,$$

where $V_{s,o}$ is the total solid-phase volume at the beginning of the experiment.

Equation 14 is made dimensionless using the following identities:

$$\frac{dV_s}{dt} = A_s r_i \frac{dh}{dt} ,$$

$$\frac{\partial P}{\partial r} = \frac{1}{r_i h}\frac{\partial P}{\partial \bar{r}} .$$

The result is

$$\frac{dh}{d\bar{t}} = \frac{\bar{Y}_{x/p}}{h} \left.\frac{\partial \bar{P}}{\partial \bar{r}}\right|_{\bar{r}=1} , \tag{14a}$$

where $\bar{Y}_{x/p}$, the dimensionless yield coefficient, is defined as

$$\bar{Y}_{x/p} = Y_{x/p}\ P^{\circ}/X \quad .$$

The dimensionless initial condition is

$$\bar{t} = 0 \qquad h = h_o \ ,$$

where h_o is the initial biofilm thickness.

The volume fraction of the gas phase (ε_g) should remain constant, since the gas flow rate into the stirred tank does not vary. However, the solid-phase volume fraction (ε_s) increases due to biofilm growth. Since the total wetted volume of the system (V_T) is constant, any increase in ε_s must result in a corresponding decrease in the liquid-phase volume fraction (ε_ℓ). This effect is included in the model as shown below.

The volume fraction of the solid phase (ε_s) is related to the total volume of the solid phase (V_s) by

$$\varepsilon_s = \frac{V_s}{V_T} \ , \tag{15}$$

where ε_s is thus related to the initial void fraction ($\varepsilon_{s,o}$) as follows:

$$\frac{\varepsilon_s}{\varepsilon_{s,o}} = \frac{V_s}{V_{s,o}} \ . \tag{16}$$

Equation 16 can be combined with the definition of h to obtain

$$\varepsilon_s = \varepsilon_{s,o}\left[\frac{1 + h}{1 + h_o}\right]^3 \quad . \tag{16a}$$

The liquid volume fraction may then be calculated from the known gas-phase volume fraction (ε_g) using

$$\varepsilon_\ell = 1 - \varepsilon_s - \varepsilon_g \quad . \tag{17}$$

Equations 2a, 3a, 6a, 7a, 14a, 16a, 17 and their associated initial and boundary conditions compose the dynamic biofilm model.

CHAPTER V

EVALUATION OF MODEL PARAMETERS

Independent a priori values for the parameters were obtained insofar as possible. It should be noted, however, that no single set of parameters for this model will accurately describe the biofilm system over an extended period of time because of naturally occurring changes in the biofilm. The phenol-degrading biofilm has exhibited changes in physical appearance, density, growth rate, relative concentrations of the various component species, and other properties over several years in our laboratory.

Accurate measurement of fixed-film kinetic parameters is difficult. Diffusional resistance within films has been shown to mask the true reaction kinetics.[41,42] Parameters measured in suspended-cell culture have been successfully applied to biofilm modeling in some studies,[13,34] while in other cases, suspended and immobilized cells have been known to exhibit different kinetic behavior.[43,44] Further research effort is needed in the area of biofilm parameter estimation.

In the present study, all of the parameters in the kinetic model were experimentally determined except the half-velocity constants (K_p and K_o). These were estimated using literature values. Chi and Howell[35] found an average K_p value of 6 mg/L for phenol degradation by a Pseudomonas isolate. Sokol and Howell[36] reported an average K_p of 1 mg/L phenol using Pseudomonas putida. Using the same Pseudomonas species, Yang and Humphrey[37] also found a K_p of 1 mg/L.

Tang and Fan,[34] using a mixed culture, estimated K_p to be 10 mg/L phenol. In the present study, a value of 1 mg/L phenol was used.

Oxygen half-velocity constants specifically measured for phenol-biooxidation reactions were not found in the literature, but values for other reaction systems can provide a rough estimate of K_O. Johnson[45] measured K_O to be 0.04 mg/L for Candida utilis. A value of 1.3 mg/L oxygen was reported for mixed-culture nitrification.[46] Atkinson and Mavituna[47] have tabulated K_O values for several micro-organisms; these values are typically less than 0.1 mg/L. K_O was taken to be 0.1 mg/L in this study.

The value of X, the concentration of active cells within the biofilm was obtained from experimental measurements of the dry-weight concentration of the biofilm. Figure 7 depicts the relationship between biofilm dry-weight concentration and the observed phenol-degradation rate.

The intercept of this plot at zero reaction rate suggests that a certain portion of the biofilm (~0.007 mg/L) is unreactive. This fraction may be composed of the glycocalyx (i.e., the extracellular polysaccharide matrix which is often associated with fixed films)[48,49] or perhaps dead or inactive cells. To obtain the concentration of "active-cell" biomass, the inactive portion (0.007 mg/L) was subtracted from the total biomass concentration.

The remaining two kinetic parameters, K_{max}, the maximum reaction rate constant, and K_I, the phenol inhibition constant, were chosen to provide agreement between the modeling predictions and experimental results. K_I was estimated to be 60 mg/L phenol, a value which

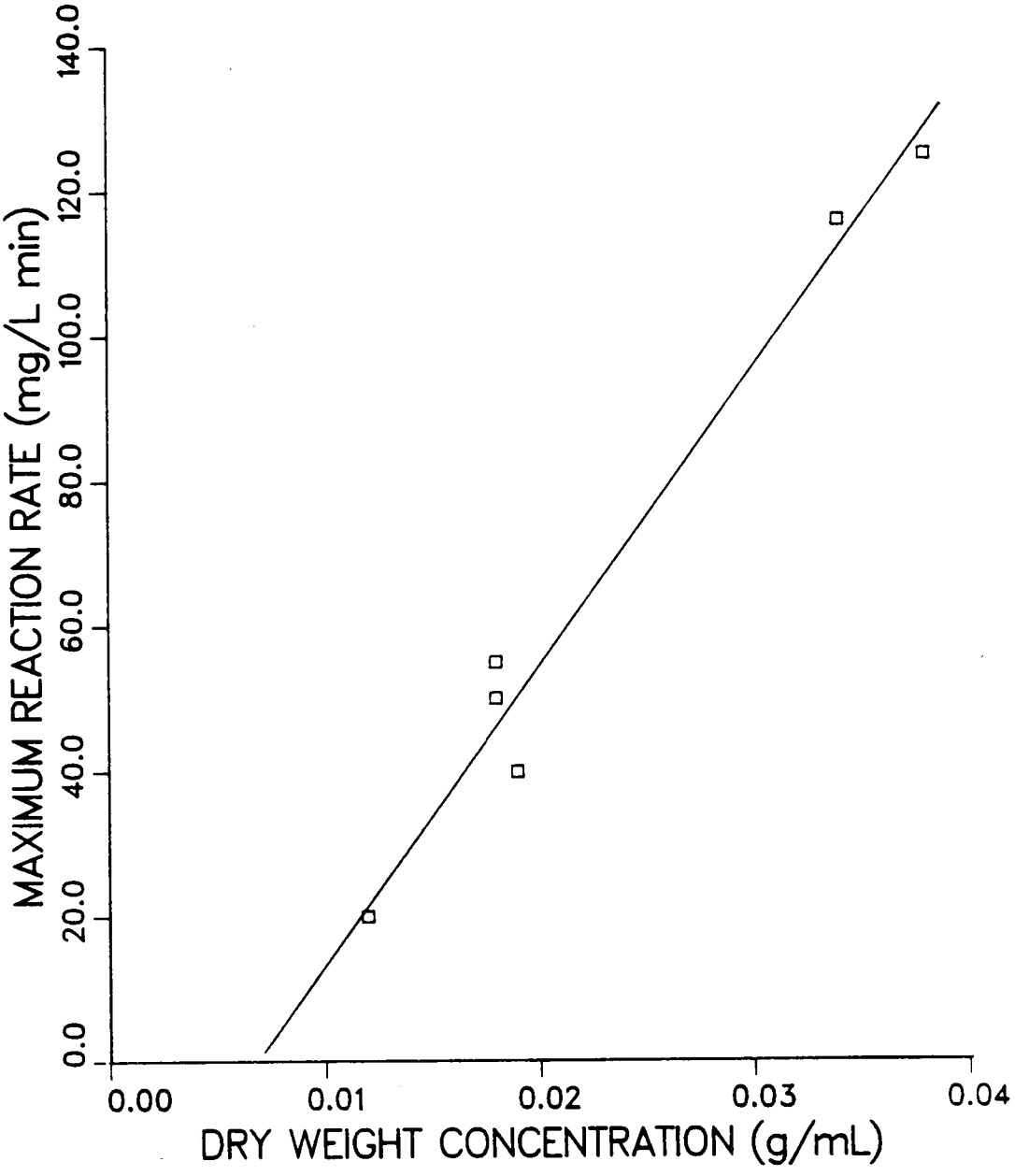

Figure 7. Effect of biofilm dry-weight concentration on the biofilm reaction rate.

compares favorably with other values in the literature. Yang and Humphrey[37] measured K_I to be 15 mg/L phenol for Pseudomonas putida. Sokol and Howell[36] obtained an average value of 16 mg/L phenol for the same organism, and Tang and Fan[34] reported a value of 113 mg/L for a mixed culture.

The chosen value of K_{max}, 1.6×10^{-4} g phenol/g cells•s, is also consistent with other reported values. For instance, Tang and Fan[34] determined K_{max} to be 2.0×10^{-4} for their phenol-degrading mixed culture.

The stoichiometric coefficient ($Y_{o/p}$), the grams of oxygen consumed per gram of phenol consumed, was directly measured to be 1.4 g/g. Preoxygenated medium was pumped through a fluidized bed of biofilm particles in a one-pass mode. The $Y_{o/p}$ was calculated from the differences in oxygen and phenol concentrations in the influent and effluent streams.

The cell yield ($Y_{x/p}$), the grams of biomass produced per gram of phenol consumed, was a less critical parameter, since the effects of film growth were minimal during the brief experiments. A reasonable value of 0.4 g cells/g phenol was assumed. For comparison, Hill and Robinson[50] reported $Y_{x/p}$ to be 0.52 g cells/ g phenol for Pseudomonas putida.

The coal support particles were somewhat irregular in shape, but were modeled as spheres. To estimate an average coal-particle radius (r_1), the average volume of the particles was first determined by dividing the mass of 1000 coal particles by the known density of the

coal. The radius of a sphere having this same volume was determined to be 0.022 cm.

Diffusivities of phenol and oxygen in water at 30°C water were calculated to be 1.1×10^{-5} cm^2/s and 2.7×10^{-5} cm^2/s, respectively, using the Wilke-Chang correlation.[51] The effective diffusivities within the biofilm were then taken to be 25% of these values. Bailey and Ollis[52] list a range of effective diffusivities for oxygen in microbial films from 2 to 70% of the water value. Smith and Coackley[53] reported 35%, and other values summarized by Matson and Characklis[54] are between 8 and 100%. Tang and Fan[34] estimated the intrafilm effective diffusivities of phenol and oxygen to range from 9 to 25% of their values in water.

The coefficient of oxygen transfer from the gas to the liquid phase (K_La) was directly measured. Distilled water was deoxygenated by autoclaving at 121°C for 45 min and then cooling under nitrogen-gas pressure. An experiment was then conducted to measure the amount of oxygen transferred to the water in the absence of reaction. Under these conditions, eq. 7 can be simplified and rearranged to yield

$$K_La = \frac{\varepsilon_\ell}{\alpha\ \tau} \frac{(O_{in} - O_b)}{(O^* - O_b)} .$$

This equation was used to calculate K_La. For the experimental conditions of interest, K_La ranged from 0.005 to 0.01 s^{-1}.

CHAPTER VI

MODEL SOLUTION AND RESULTS

Two of the equations in the dynamic model (eqs. 2a and 3a) are parabolic partial differential equations. The IMSL routine DPDES[55] (version 9.1), which can solve a system of two-dimensional partial differential equations having boundary conditions of the Robin form, was used to solve the model. DPDES uses cubic Hermite polynomials for discretization in the spatial dimension, and a variable-order Adams Predictor-Corrector method for the time integration. The calculations were carried out in double precision on an IBM 3081-D computer located at the University of Tennessee.

Initial values for the bulk concentrations and concentration profiles within the biofilm must be supplied to DPDES. These values were obtained by solving the steady-state versions of eqs. 2a, 3a, 6a and 7a (i.e., with all time derivatives set to zero). In the iterative procedure, values of the bulk liquid concentrations were assumed and equations 2a, and 3a solved to evaluate

$$\left.\frac{\partial P}{\partial r}\right|_{r = r_o} \quad \text{and} \quad \left.\frac{\partial O}{\partial r}\right|_{r = r_o}$$

via the shooting method. These two values were then inserted into eqs. 6a and 7a to calculate a better approximation of the bulk concentrations. The procedure was repeated until convergence was achieved. These calculations of the initial conditions were done in double precision using a DEC system-10 computer at the University of Tennessee.

In the experimental procedure, the bulk-liquid phenol concentration was suddenly increased by the addition of a pulse of phenol to the stirred tank. This procedure was modeled by increasing the inlet phenol concentration (P_{in}) from ~60 to 2.6×10^5 mg/L for a duration of ~0.2 s. The phenol concentrations in the biofilm and bulk liquid, as well as the reaction rate and growth rate were then computed as a function of time following the pulse until steady state was again achieved.

The time trajectory of the phenol concentration profile through the biofilm is shown in Fig. 8 for a typical simulation. All of the variables are dimensionless as described earlier. Initially, the concentration of phenol is relatively low or zero in the biofilm. After the pulse of phenol is added, the intrafilm concentration rises to relatively high levels throughout. As a result, the innermost regions of the biofilm, which were initially starved for substrate, now contribute to the overall rate of substrate consumption. The overall rate may either rise or fall, however, depending upon the degree of substrate inhibition.

Small Phenol Pulse

Modeling simulations were conducted to describe both relatively small-pulse and large-pulse experiments. A comparison of the modeling and experimental curves for a small-pulse experiment is shown graphically in Fig. 9, in which phenol concentration in the bulk liquid and observed biofilm reaction rate are both plotted as a function of time. Values of the parameters used in the simulation are listed in Table 3,

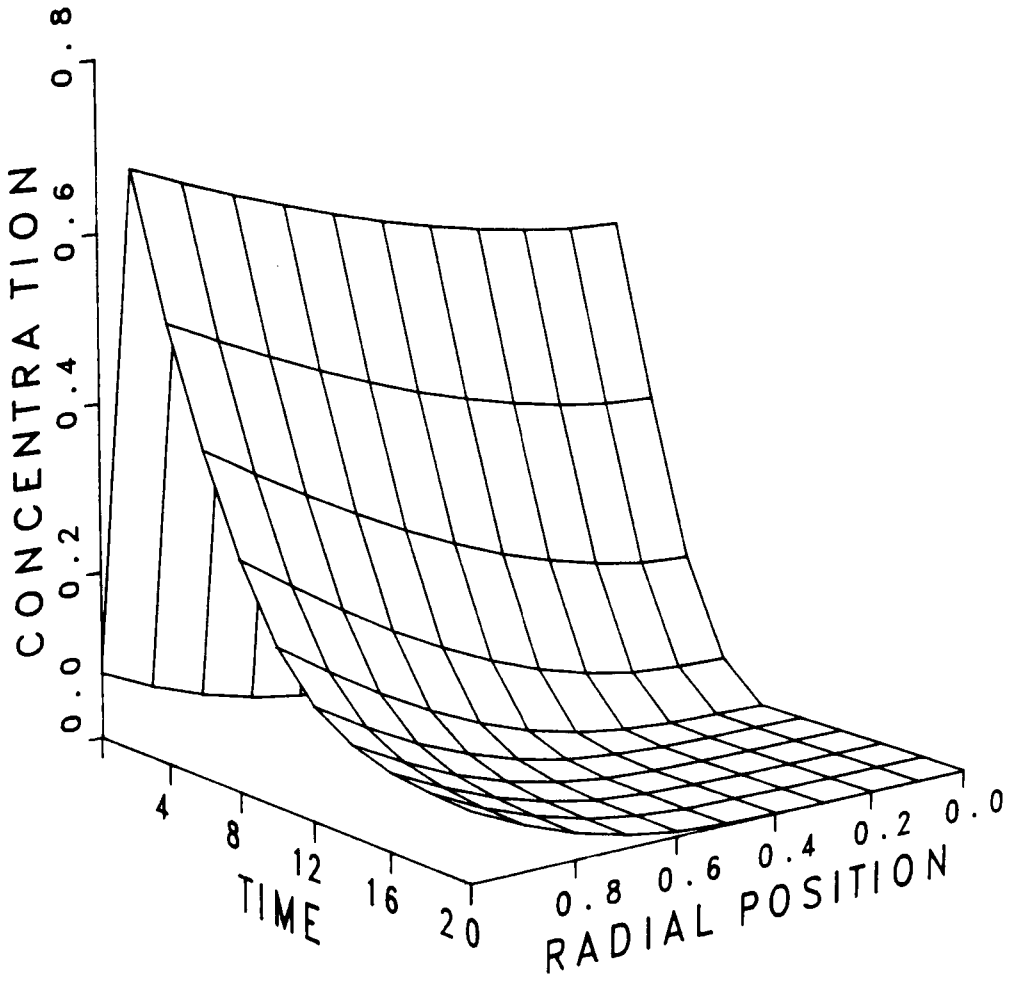

Figure 8. Predicted phenol-concentration profiles in the biofilm following a pulse of phenol.

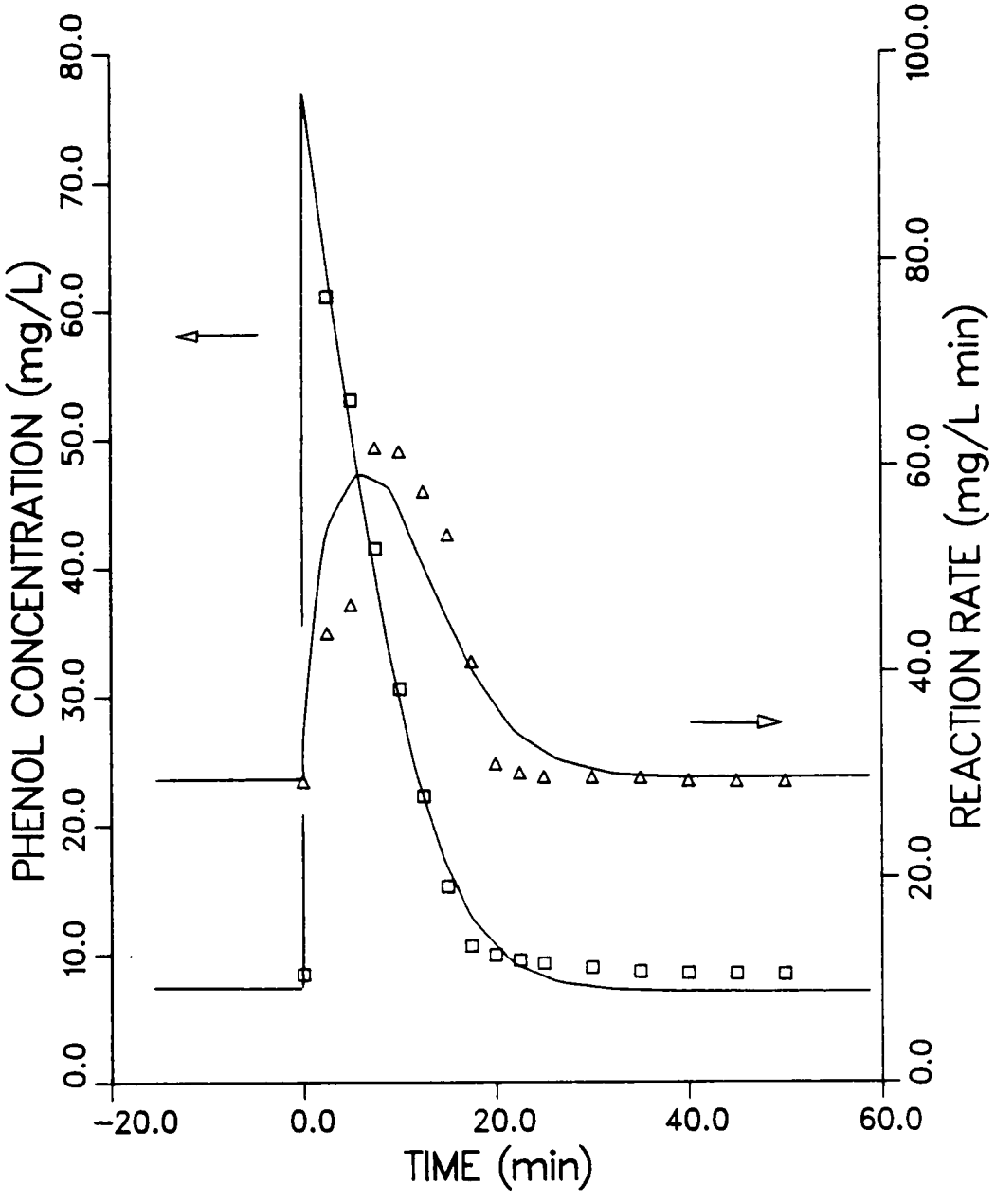

Figure 9. Comparison of predicted and experimental biofilm dynamics following a relatively small pulse of phenol.

Solid curves: Model prediction; Data points: Experimental values.

Table 3

Values of Parameters for Figure 9

Parameter	Value
K_{max}	1.6×10^{-4} g phenol/g cells•s
X	0.015 g cells/cm^3
K_p	1.0×10^{-6} g/cm^3
K_I	60×10^{-6} g/cm^3
K_o	0.1×10^{-6} g/cm^3
$Y_{o/p}$	1.4 g oxygen/g phenol
$Y_{x/p}$	0.4 g cells/g phenol
D_p	2.75×10^{-6} cm^2/s
D_o	6.50×10^{-6} cm^2/s
r_i	0.022 cm
r_o	0.040 cm
K_La	1×10^{-2} s^{-1}
P_{in}	50×10^{-6} g/cm^3
F	0.317 cm^3/s
V_T	362 cm^3
α	0.62
$\varepsilon_{s,o}$	0.07
ε_g	0.01

and a tabulation of the computed results is included in Appendix 2. The trends in the modeling curves duplicate those observed in the pH-controlled experiments (e.g., Fig. 4, page 18). The initial increase in phenol concentration is accompanied by a substantial increase in the biofilm reaction rate. At the higher reaction rates, phenol is rapidly consumed. Its concentration declines to the original level, and the reaction rate also returns to its initial value.

Large Phenol Pulse

When a relatively large pulse of phenol is used, somewhat different dynamic behavior is predicted, as shown in Fig. 10. In this case, the initial increase in phenol concentration drives the reaction rate down. As the phenol concentration falls due to biofilm reaction and convection, substrate inhibition is reduced, and the reaction rate rises and eventually exceeds its initial value before returning to the original steady-state.

Values for the parameters used in this simulation are listed in Table 4, and the computed results are tabulated in Appendix 3. To enhance agreement between the model and experimental data, the inhibition constant (K_I) was adjusted from 60 to 50 mg/L and the coal-particle radius was increased from 0.22 to 0.28 cm. This latter change effectively decreased the biofilm thickness while leaving all other geometric parameters unchanged. The experimentally measured film thickness resulted in too pronounced a peak in the predicted reaction-rate curve. A likely interpretation of this discrepancy is that the innermost regions of the biofilm had lost biological activity

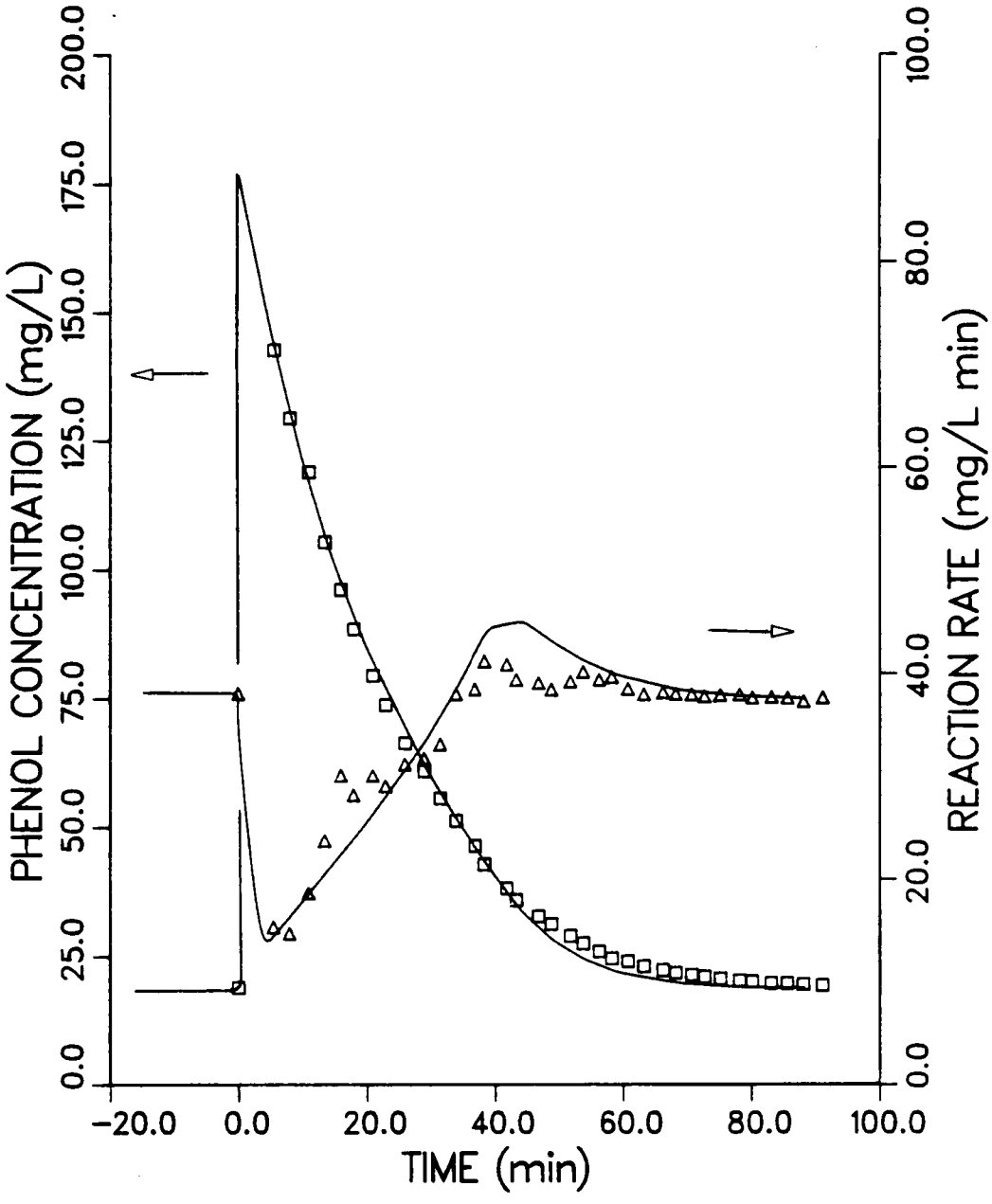

Figure 10. Comparison of predicted and experimental biofilm dynamics following a relatively large pulse of phenol.

Solid curves: Model predictions; Data points: Experimental values.

Table 4

Values of Parameters for Figure 10

Parameter	Value
K_{max}	1.6×10^{-4} g phenol/g cells•s
X	0.012 g cells/cm^3
K_p	1.0×10^{-6} g/cm^3
K_I	50×10^{-6} g/cm^3
K_o	0.10×10^{-6} g/cm^3
$Y_{o/p}$	1.4 g oxygen/g phenol
$Y_{x/p}$	0.40 g cells/g phenol
D_p	2.75×10^{-6} cm^2/s
D_o	6.50×10^{-6} cm^2/s
r_i	0.028 cm
r_o	0.043 cm
K_La	0.5×10^{-2} s^{-1}
P_{in}	65×10^{-6} g/cm^3
F	0.325 cm^3/s
V_T	362 cm^3
α	0.62
$\varepsilon_{s,o}$	0.06
ε_g	0.01

due to long periods of oxygen deprivation. Hence their contribution to the overall reaction rate would be overestimated by the model. Decreasing the biofilm thickness forces the model to account for only the outer, biologically active fraction.

Although the innermost portions of the biofilm were not experimentally confirmed to be inactive, it is reasonable to assume that they were. While the biofilm particles were being established and maintained prior to the dynamic experiment, they were exposed to a bulk oxygen concentration of ~10 mg/L, which corresponds to a model-predicted oxygen penetration depth of ~0.012 cm. However, since the average biofilm thickness was determined to be 0.043 cm, the innermost regions were probably without oxygen for extended periods of time.

The degree of quantitative agreement achieved between the predicted and experimental curves in both the small- and large-pulse experiments seems quite satisfactory considering the inherent complexity of the biofilm and the several assumptions and simplifications that were made in the model development. Of particular interest is that unsteady-state biofilm behavior was predicted relatively well using a "steady-state" or unstructured kinetic model. With other types of experimental perturbations or other biofilms, however, such agreement may not be possible, and more sophisticated kinetic models may be required.

Oscillatory Dynamics

One example of dynamic behavior which is not readily described with the present model is the oscillations in the phenol concentration

trajectory in the absence of pH control (Fig. 5, page 19). Modeling simulations were conducted using a wide range of parameter values, but no oscillations were obtained.

Linear analysis was employed to determine whether the model was of a form likely to produce oscillatory solutions. The order of the model was reduced by assuming that the oxygen concentration within the biofilm is not rate-limiting and that the effects of growth are negligible during the course of an experiment. The first assumption is supported by the modeling simulations (Appendixes 2 and 3) and experimental evidence (Fig. 3, page 16), both of which indicate that the effect of oxygen concentration is relatively small under the experimental conditions. The second assumption is quite good; growth accounts for less than a 1% change in the biofilm thickness during an experiment.

The above assumptions reduce the model to two equations:

$$\frac{\partial \bar{P}}{\partial \bar{t}} = \frac{\partial \bar{P}}{\partial \bar{r}}\left[\frac{2}{h(1 + h\bar{r})}\right] + \frac{1}{h^2}\frac{\partial^2 \bar{P}}{\partial \bar{r}^2} - \frac{K_{max} \; X \; r_i^2}{P^\circ \; D_p}\left[\frac{\bar{P}}{\bar{K}_p + \bar{P} + \bar{P}^2/\bar{K}_I}\right] , \quad (18)$$

$$\frac{d\bar{P}_b}{d\bar{t}} = \frac{1}{\tau}(\bar{P}_{in} - \bar{P}_b) - \frac{3\varepsilon_s}{\varepsilon_\ell h \; (1 + h)}\frac{\partial \bar{P}}{\partial \bar{r}}\bigg|_{\bar{r} = 1} . \quad (6a)$$

Equation 18 can then be further simplified to an ordinary differential equation using the method of orthogonal collocation, as described by Villadsen.[56] A single-point, interior-collocation approach was used to eliminate the derivatives with respect to the radial position. The resulting ordinary differential equations were then linearized about

their steady-state values, and characteristics of the eigenvalues were determined over a range of the parameters. Details of the above procedure are included in Appendix 4.

The linear analysis revealed that over the range of parameters shown in Table 5, no unstable or oscillatory solutions are predicted. While this analysis is strictly valid only for small perturbations of the linearized model from steady state, it implies that the oscillatory behavior observed experimentally in the absence of pH control is not likely to be reproduced by the dynamic model.

Product-inhibition kinetics were also investigated in an attempt to explain the oscillatory behavior. It was hypothesized that in the absence of pH control, a metabolic product accumulates and inhibits the phenol degradation rate. The oscillations were observed to be coincident with a decrease in the pH of the medium from 7.0 to ~4.5. Whether acidic conditions induce the production of a particularly toxic substance or the acidity itself is inhibitory (pH inhibition) need not be specified, since the analysis applies to either case. The product was assumed to inhibit the phenol degradation rate in a linear fashion:

$$R_p = K_{max} X \left[1 - \frac{A}{K_A}\right] \left[\frac{P}{K_p + P + P^2/K_I}\right] ,$$

where A is the concentration of the inhibitor and K_A is the product-inhibition constant.

To test the hypothesis, dynamic simulations were conducted using the above kinetic expression. Unsteady-state mass balance equations

Table 5

Range of Parameters Tested for Unstable or Oscillatory Behavior of Linearized Biofilm Model

Variable	Minimum value	Typical value	Maximum value
K_p	0.1×10^{-6} g/cm^3	1×10^{-6} g/cm^3	10×10^{-6} g/cm^3
K_I	8×10^{-6} g/cm^3	80×10^{-6} g/cm^3	800×10^{-6} g/cm^3
K_{max} X	1×10^{-6} g/cm^{3}s	2×10^{-6} g/cm^{3}s	4×10^{-6} g/cm^{3}s
τ	600 s	1200 s	2400 s
P_{in}	50×10^{-6} g/cm^3	100×10^{-6} g/cm^3	200×10^{-6} g/cm^3
ε_s	0.01	0.05	0.10
h	0.34	0.68	1.36

for the inhibitor within the biofilm and the liquid phases (analogous to equations 3a and 6a) were written, nondimensionalized, and solved simultaneously with equations 2a and 6a. Effects of growth and oxygen concentration were taken to be negligible in these studies. Assuming a yield coefficient of 0.1 g product/g phenol, an effective biofilm diffusivity of 6.5×10^{-6} cm^2/s, a product-inhibition constant of 10×10^{-6} g/cm^3, and the parameter values listed in Table 3, page 43, simulations were conducted for P_{in} values of 25×10^{-6} and 100×10^{-6} g/cm^3 phenol. In both cases, the reaction rate was substantially reduced by the presence of the inhibitor, yet in neither case was there an oscillatory return to steady state.

Since the experimentally observed oscillations were not able to be reproduced with either the original dynamic model or the modified model which incorporates product inhibition, it is likely that some phenomena other than those included in the models are involved and need to be identified to adequately describe the system. These phenomena may include intracellular metabolic regulation processes which can occur gradually, imparting time lags into the process dynamics. Such time lags have been known to induce oscillatory tendencies in chemostat models.[57]

Further research is needed to ascertain the cause(s) of this interesting dynamic behavior seen in the absence of pH control.

CHAPTER VII

CONCLUSIONS

The differential fluidized-bed bioreactor has several characteristics which make it a useful research tool for studying the unsteady-state behavior of fixed-film bioparticles. It facilitates control of important process variables, eliminates hydrodynamic effects due to three-phase operation, and has the liquid-mixing characteristics of a stirred-tank reactor.

Observed trends in the dynamic response of the biofilm to sudden increases in the phenol concentration depended upon the size of the increase. Following small increases (e.g., from 10×10^{-6} to 70×10^{-6} g/cm^3 phenol), the reaction rate rose; following larger increases (e.g., from 15×10^{-6} to 170×10^{-6} g/cm^3 phenol), the rate initially fell, suggesting substrate-inhibition by phenol, and then recovered as the phenol concentration declined. No time lags were observed in these experiments.

The dynamic model of the biofilm reactor, which included an unstructured kinetic expression for substrate inhibition by phenol, was able to predict most of the trends in the data. A comparison of the experimental and modeling curves supports the hypothesis that the innermost regions of thick biofilms are relatively unreactive.

Without automatic pH control, the pH of the medium dropped from 7.0 to below 4.5. Under these acidic conditions, oscillatory dynamic behavior occurred. Attempts to model the oscillations using substrate-inhibition and product-inhibition kinetic expressions were

unsuccessful. Kinetic models which incorporate biological structure may be necessary to adequately describe this behavior; further study is needed.

Gradual, naturally occurring variations in several biofilm properties including the appearance, density and growth rate have been observed. Changes in the dry-weight concentration in the biofilm exerted a strong effect on the overall reactor performance. Further study of these spontaneous changes is needed for bioreactor optimization.

LIST OF REFERENCES

LIST OF REFERENCES

1. Kinner, N. E., and Eighmy, T. T. (1985), "Biological Fixed Film Systems," J. Water Pollut. Cont. Fed., 57, p. 526.

2. Atkinson, B., and Knights, A. J. (1975), "Microbial Film Fermenters: Their Present and Future Applications," Biotech. and Bioeng., 17, p. 1245.

3. Smith, E. L., and Greenshields, R. N. (1974), "Tower Fermentation Systems and Their Application to Aerobic Processes," The Chemical Engineer, 284, p. 28.

4. Greenshields, R. N., and Smith, E. L. (1971), "Tower Fermenters and Their Applications," The Chemical Engineer, 249, p. 182.

5. Arcuri, E. J., Worden, R. M., and Shumate, S. E. (1980), "Ethanol Production by Immobilized Cells of Zymomonas mobilis," Biotech. Letters, 2, p. 499.

6. Anderson, J. G., Blain, J. A., Divers, M., and Todd, J. R. (1980), "Use of the Disk Fermenter to Examine Production of Citric Acid by Aspergillus niger," Biotech. Letters, 2, p. 99.

7. Robertson, C. R., and Kim, I. H. (1985), "Dual Aerobic Hollow-Fiber Bioreactor for Cultivation of Streptomyces aureofaciens," Biotech. and Bioeng., 27, p. 1012.

8. Atkinson, B. (1974), Biochemical Reactors, Pion Limited, London, p. 76.

9. Andrews, G. F. (1983), "Fluidized-Bed Fermenters: A Steady-State Analysis," Biotech. and Bioeng., 24, p. 2013.

10. Hancher, C. W., and Perona, J. J. (1982), "Kinetic Model for a Fluidized-Bed Bioreactor for Denitrification of Wastewaters," Biotech. and Bioeng. Symp. No. 12, p. 317.

11. Shieh, W. K., Mulcahy, L. T., and La Motta, E. J. (1982), "Mathematical Model for the Fluidized-Bed Biofilm Reactor," Enzyme Microb. Technol., 4, p. 269.

12. Rittman, B. E., and McCarty, P. L. (1980), "Model of Steady-State Biofilm Kinetics," Biotech. and Bioeng., 22, p. 2343.

13. Rittman, B. E., and McCarty, P. L. (1980), "Evaluation of Steady-State-Biofilm Kinetics," Biotech. and Bioeng., 22, p. 2359.

14. Daigger, G. T., and Grady, C. P. L. (1982), "An Assessment of the Role of Physiological Adaptation in the Transient Response of Bacterial Cultures," Biotech. and Bioeng., 24, p. 1427.

15. Sundstrom, D. W., Klei, H. E., and Quinlan, J. (1983), "Response of Composition in Biological Reactors to Changes in Inlet Concentration," Biotech. and Bioeng., 25, p. 857.

16. Cooney, C. L., and Wang, D. I. C. (1976), "Transient Response of Enterobacter aerogenes Under a Dual Nutrient Limitation in a Chemostat," Biotech. and Bioeng., 18, p. 189.

17. Lievense, J. C., and Lim, H. C. (1985), "A Mathematical Model for the Asymmetric Dynamic Response in Microbial Systems," paper presented at 190th ACS National Meeting, Chicago, Ill., September 8-14, 1985.

18. Young, T. B., and Bungay, H. R. (1973), "Dynamic Analysis of a Microbial Process: A Systems Engineering Approach," Biotech. and Bioeng., 15, p. 377.

19. Nutt, S. G., Stephenson, J. P., and Pries, J. H. (1981), "Steady- and Non-Steady-State Performance of the Aerobic (Oxygenic) Biological Fluidized Bed," Biological Fluidized Bed Treatment of Water and Wastewater, ed. by P. F. Cooper and B. Atkinson, Ellis Horwood Limited, Chichester, p. 145.

20. Tien, C., and Wang, S. C. (1982), "Dynamics of Adsorption Columns with Bacterial Growth Outside Adsorbents," Can. J. Chem. Eng., 60, p. 363.

21. Vanderborght, J. P., and Gilliard, C. (1974), "BOD Removal in Fluidized Beds: High Biomass Concentration or High Oxygen Transfer?" Biological Fluidized Bed Treatment of Water and Wastewater, ed. by P. F. Cooper and B. Atkinson, Ellis Horwood Limited, Chichester, p. 383.

22. Park, Y., Davis, M. E., and Wallis, D. A. (1984), "Analysis of a Continuous, Aerobic, Fixed-Film Bioreactor. II. Dynamic Behavior," Biotech. and Bioeng., 26, p. 468.

23. Benefield, L., and Molz, F. (1983), "A Kinetic Model for the Activated Sludge Process which Considers Diffusion and Reaction in the Microbial Floc," Biotech. and Bioeng., 25, p. 2591.

24. Benefield, L., and Molz, F. (1985), "Mathematical Simulation of a Biofilm Process," Biotech. and Bioeng., 27, p. 921.

25. Rittman, B. E., and Brunner, C. W. (1984), "The Nonsteady-State Biofilm Process for Advanced Organics Removal," J. Water Pollut. Cont. Fed., 56, p. 874.

26. Denac, M., Uzman, S., Tanaka, H., and Dunn, I. J. (1983), "Modeling of Experiments on Biofilm Penetration Effects in a Fluidized-Bed Nitrification Reactor," Biotech. and Bioeng., 25, p. 1841.

27. Young, T. B., Bruley, D. F., and Bungay, H. R. (1970) "A Dynamic Model of the Chemostat," Biotech. and Bioeng., 12, p. 747.

28. Regan, D. L., and Roper, G. H. (1971), "Response of Continuous Cultures to Stimuli in Glucose Feed Rate and Dilution Rate," Biotech. and Bioeng., 13, p. 815.

29. Sundstrom, D. W., Klei, H. E., and Brookman, G. T. (1976), "Response of Biological Reactors to Sinusoidal Variations of Substrate Concentration," Biotech. and Bioeng., 18, p. 1.

30. Donaldson, T. L., Strandberg, G. W., Hewitt, J. D., and Shields, G. S. (1984), "Biooxidation of Coal Gasification Wastewaters," Environmental Progress, 3, p. 248.

31. Standard Methods for the Examination of Water and Wastewater, 14th Ed., (1975), Amer. Public Health Assoc., Washington, D. C., p. 580.

32. Burden, R. L., Faires, J. D., and Reynolds, A. C. (1981), Numerical Analysis, Second Ed., Prindle, Weber and Schmidt, Boston, p. 127.

33. Strandberg, G. W. (1985), personal communication, Oak Ridge National Laboratory.

34. Tang, W. T., and Fan, L. S. (1985), "Steady State Phenol Biodegradation in a Draft Tube Gas-Liquid-Solid Fluidized Bed Bioreactor," paper presented at 190th ACS National Meeting, Chicago, Ill., September 8-14, 1985.

35. Chi, C. T., and Howell, J. A. (1976), "Transient Behavior of a Continuous Stirred Tank Biological Reactor Utilizing Phenol as an Inhibitory Substrate," Biotech. and Bioeng., 18, p. 63.

36. Sokol, W., and Howell, J. A. (1981), "Kinetics of Phenol Oxidation by Washed Cells," Biotech. and Bioeng., 23, p. 2039.

37. Yang, R. D., and Humphrey, A. E. (1975), "Dynamic and Steady State Studies of Phenol Biodegradation in Pure and Mixed Cultures," Biotech. and Bioeng., 17, p. 1211.

38. Moreira, A. R., Van Dedem, G., and Moo-Young, M. (1979), "Process Modeling Based on Biochemical Mechanisms of Microbial Growth," Biotech. and Bioeng. Symp. No. 9, p. 179.

39. Esener, A. A., Veerman, T., Roels, J. A., and Kossen, N. W. F. (1982), "Modeling of Bacterial Growth; Formulation and Evaluation of a Structured Model," Biotech. and Bioeng., 24, p. 1749.

40. Bremer, H. (1981), "Simulated Bacterial Growth," J. Theor. Biol., 92, p. 23.

41. Webster, I. A. (1982), "The Lineweaver-Burk Plot Intercept: Influence of Diffusion," Biotech. and Bioeng., 24, p. 981.

42. Lee, S. B., and Ryu, D. D. Y. (1980), "External Diffusion Effects on the Kinetic Constants of Immobilized Enzyme Systems," J. Theor. Biol., 84, 259.

43. Wardell, J. N., Brown, C. M., and Flannigan, B. (1983), "Microbes and Surfaces," Soc. for Gen. Micro. Symp. 34, p. 352.

44. Messing, R. A. (1981), "Support-Bound Microbial Cells," App. Biochem. and Biotech., 6, p. 167.

45. Johnson, M. J. (1967), "Aerobic Microbial Growth at Low Oxygen Concentrations," J. Bacteriology, 94, p. 101.

46. Process Design Manual for Nitrogen Control (1975), U.S. EPA Office of Technology Transfer, Washington, D.C.

47. Atkinson, B., and Mavituna, F. (1983), Biochemical Engineering and Biotechnology Handbook, Nature Press, New York, p. 265.

48. Costerton, J. W., Geesey, G. G., and Cheng, K. J. (1978), "How Bacteria Stick," Sci. Amer., 238, p. 86.

49. Eighmy, T. T., Maratea, D., and Bishop, P. L. (1983), "Electron Microscopic Examination of Wastewater Biofilm Formation and Structural Components," App. and Env. Micro., 45, p. 1921.

50. Hill, G. A., and Robinson, C. W. (1975), "Substrate Inhibition Kinetics: Phenol Degradation by Psuedomonas putida," Biotech. and Bioeng., 17, p. 1599.

51. Wilke, C. R., and Chang, P. (1955), "Correlation of Diffusion Coefficients in Dilute Solutions," AIChE J., 1, p. 264.

52. Bailey, J. E., and Ollis, D. F. (1977), Biochemical Engineering Fundamentals, McGraw-Hill, New York, p. 452.

53. Smith, P. G., and Coackley, P. (1984), "Diffusivity, Tortuosity, and Pore Structure of Activated Sludge," Water Research, 18, p. 117.

54. Matson, J. V., and Characklis, W. G. (1976), "Diffusion into Microbial Aggregates," Water Research, 10, p. 877.

55. IMSL Library Users Manual, Vol. 1 (1984), IMSL, Houston.

56. Villadsen, J. V., and Stewart, W. E. (1967), "Solution of Boundary-Value Problems by Orthogonal Collocation," Chem. Eng. Science, 22, p. 1483.

57. MacDonald, N. (1976), "Time Delay in Simple Chemostat Models," Biotech. and Bioeng., 18, p. 805.

58. Bailey, J. E., and Ollis, D. F. (1977), Biochemical Engineering Fundamentals, McGraw Hill, New York, p. 435.

59. Bailey, J. E., and Ollis, D. F. (1977), Biochemical Engineering Fundamentals, McGraw Hill, New York, p. 646.

APPENDICES

APPENDIX 1

INTERPHASE MASS-TRANSFER RESISTANCE

The assumption of negligible resistance to mass transfer from the liquid to solid phase can be examined by estimating the drop in the concentrations of phenol and oxygen across the stagnant liquid film. In a fluidized bed, the velocity of the upflowing medium equals the particles' natural settling velocity, and the particles are held suspended. Thus a correlation for small, settling particles may be used to estimate the interphase mass-transfer coefficient:[58]

$$Sh = 2.0 + 0.31[Gr\ Sc]^{0.33} \quad , \tag{19}$$

where Sh is the Sherwood number (a dimensionless mass-transfer coefficient), Gr is the Grashof number, and Sc is the Schmidt number. Experimental measurements of settling velocities as a function of biofilm thickness were used to estimate that the Sherwood number was ~33 for phenol and 25 for oxygen. For a typical dimensionless film thickness (h) of 0.8, these Sherwood numbers translate into mass transfer coefficients (k_L) of 4.5×10^{-3} cm/s for phenol and 8.0×10^{-3} cm/s for oxygen.

The fluxes (N) of phenol and oxygen into the biofilm were computed in the dynamic model. By combining these fluxes with the above k_L values and a simple stagnant liquid-film model:

$$N = k_L(C_b - C) \quad ,$$

the change in concentration between the bulk liquid (C_b) and biofilm surface (C) were calculated for both substrates. For typical values of the parameters, the maximum concentration decreases were 3.5 mg/L phenol and 2.9 mg/L oxygen. These decreases were less than 10% of the

bulk-liquid concentrations. At lower bulk concentrations, the substrate fluxes and the concentration drops both decline, keeping the percentage error moderate under all conditions tested. Since the mass-transfer correlation (eq. 19) does not account for the turbulence and particle interaction which occur in fluidized beds, it probably underestimates k_L and hence overestimates the concentration changes. In view of the inherent uncertainties in the values of several other modeling parameters, the degree of error due to the assumption of negligible interphase mass-transfer resistance is not considered excessive.

APPENDIX 2

TABULATED RESULTS OF SMALL PHENOL-PULSE SIMULATION

The computed results corresponding to Fig. 9, page 42 and Table 3, page 43 are listed below. Included are the dimensionless radial position (R), phenol concentration (P), oxygen concentration (O), film thickness (h), time, and concentration gradients at the outer surface of the biofilm (GRADP and GRADO). PFRAC is defined by

$$PFRAC = \frac{P}{K_p + P + P^2/K_I} ,$$

and indicates the degree to which the phenol concentration is limiting the overall rate of reaction at a given point in the biofilm. The analogous variable for oxygen is

$$OFRAC = \frac{O}{K_o + O} .$$

PBULK and OBULK are the bulk-liquid concentrations of phenol and oxygen in units of mg/L. DEG RATE is the bioreactor's phenol degradation rate normalized by the volume of the settled bed of bioparticles. Its units are mg phenol/L settled bed•min.

INITIAL CONDITIONS

R	P	O	h
0.0	0.000057	0.530069	0.800000
0.100000	0.000136	0.530303	0.800000
0.200000	0.000257	0.530662	0.800000
0.300000	0.000485	0.531338	0.800000
0.400000	0.000970	0.532773	0.800000
0.500000	0.002182	0.536364	0.800000
0.600000	0.005661	0.546667	0.800000
0.700000	0.013950	0.571216	0.800000
0.800000	0.028659	0.614775	0.800000
0.900000	0.050104	0.678286	0.800000
1.000000	0.077917	0.760657	0.800000

TIME= 0.100000

PBULK	OBULK
76.7646569531014435	30.2723755294770847

DEG. RATE 78.469990
FILM THICKNESS 0.800011
GRADP 0.613822
GRADO 1.163922

R	P	O	PFRAC	OFRAC
0.0	0.003050	0.143114	0.377423	0.982831
0.100000	0.006130	0.145223	0.544644	0.983076
0.200000	0.016484	0.155681	0.736228	0.984195
0.300000	0.036150	0.181187	0.794399	0.986390
0.400000	0.065671	0.223906	0.772177	0.988958
0.500000	0.104422	0.283040	0.716355	0.991245
0.600000	0.151138	0.356658	0.650671	0.993039
0.700000	0.204208	0.442618	0.586449	0.994384
0.800000	0.261861	0.538974	0.528551	0.995383
0.900000	0.322298	0.644120	0.478505	0.996134
1.000000	0.383823	0.756809	0.436217	0.996708

TIME= 0.500000

PBULK	OBULK
69.1286825607559017	28.5926705266586438

DEG. RATE 55.147336
FILM THICKNESS 0.800030
GRADP 0.431398
GRADO 1.311986

R	P	O	PFRAC	OFRAC
0.0	0.103816	0.000015	0.717250	0.005937
0.100000	0.104485	0.001720	0.716262	0.407597
0.200000	0.108938	0.014160	0.709710	0.849943
0.300000	0.120231	0.046551	0.693310	0.949033
0.400000	0.138410	0.099227	0.667783	0.975424
0.500000	0.162673	0.170012	0.635736	0.985508
0.600000	0.192112	0.256423	0.600097	0.990345
0.700000	0.225861	0.356099	0.563378	0.993028
0.800000	0.263140	0.466917	0.527389	0.994674
0.900000	0.303264	0.587019	0.493251	0.995759
1.000000	0.345643	0.714817	0.461550	0.996515

TIME= 1.000000

PBULK	OBULK
61.2740850453161201	27.6185415315770513

DEG. RATE 54.729935
FILM THICKNESS 0.800052
GRADP 0.428150
GRADO 1.349395

R	P	O	PFRAC	OFRAC
0.0	0.087862	-0.000229	0.740861	-0.100849
0.100000	0.087928	0.000491	0.740763	0.164035
0.200000	0.089584	0.006879	0.738320	0.733460
0.300000	0.097068	0.031418	0.727236	0.926292
0.400000	0.111574	0.077613	0.705853	0.968794
0.500000	0.132554	0.143822	0.675873	0.982914
0.600000	0.159173	0.227542	0.640210	0.989132
0.700000	0.190591	0.326259	0.601852	0.992396
0.800000	0.226038	0.437651	0.563197	0.994320
0.900000	0.264828	0.559650	0.525862	0.995553
1.000000	0.306370	0.690464	0 490784	0.996392

TIME= 2.000000

PBULK	OBULK
46.8549630793611058	26.5467057691402992

DEG. RATE 59.205697
FILM THICKNESS 0.800096
GRADP 0.463201
GRADO 1.450809

R	P	O	PFRAC	OFRAC
0.0	0.024867	-0.000491	0.778841	-0.244271
0.100000	0.024829	-0.000032	0.778732	-0.013137
0.200000	0.024683	0.001141	0.778304	0.313289
0.300000	0.027510	0.012037	0.785267	0.828027
0.400000	0.037447	0.044835	0.794694	0.947185
0.500000	0.055227	0.101664	0.784544	0.975999
0.600000	0.080277	0.180800	0.751950	0.986361
0.700000	0.111676	0.279483	0.705703	0.991134
0.800000	0.148425	0.394712	0.654263	0.993706
0.900000	0.189572	0.523623	0.603034	0.995248
1.000000	0.234275	0.663668	0.554859	0.996247

TIME= 3.000000

PBULK	OBULK
34.0328628314966473	26.2676302554334207

DEG. RATE 57.895062
FILM THICKNESS 0.800143
GRADP 0.452985
GRADO 1.392114

R	P	O	PFRAC	OFRAC
0.0	-0.000117	0.129724	-0.023951	0.981093
0.100000	0.000039	0.130429	0.007825	0.981193
0.200000	0.000308	0.131905	0.057990	0.981400
0.300000	0.001367	0.136117	0.214507	0.981965
0.400000	0.005100	0.148623	0.500662	0.983457
0.500000	0.014507	0.178331	0.717862	0.986175
0.600000	0.031594	0.231248	0.791408	0.989305
0.700000	0.056596	0.308133	0.783086	0.991952
0.800000	0.088754	0.406804	0.739545	0.993892
0.900000	0.126981	0.524080	0.683692	0.995252
1.000000	0.170164	0.656691	0.626332	0.996207

TIME= 4.000000

PBULK OBULK
24.1995334073367694 27.1025298666026089
DEG. RATE 51.912147
FILM THICKNESS 0.800186
GRADP 0.406205
GRADO 1.240104

R	P	O	PFRAC	OFRAC
0.0	-0.00026	0.30131	-0.05667	0.99177
0.100000	-0.000114	0.301970	-0.023300	0.991789
0.200000	0.000018	0.302928	0.003642	0.991815
0.300000	0.000217	0.304406	0.041670	0.991854
0.400000	0.001004	0.307917	0.167149	0.991946
0.500000	0.003968	0.318155	0.439915	0.992203
0.600000	0.012093	0.343974	0.687871	0.992784
0.700000	0.027814	0.392634	0.785868	0.993673
0.800000	0.051697	0.465876	0.787997	0.994662
0.900000	0.083115	0.561893	0.747828	0.995570
1.000000	0.120998	0.677563	0.692210	0.996324

TIME= 5.000000

PBULK OBULK
17.2798267907302687 28.2563544667909916
DEG. RATE 45.658366
FILM THICKNESS 0.800224
GRADP 0.357294
GRADO 1.084074

R	P	O	PFRAC	OFRAC
0.0	-0.000374	0.437199	-0.080856	0.994314
0.100000	-0.000219	0.437808	-0.045907	0.994322
0.200000	-0.000087	0.438629	-0.017619	0.994333
0.300000	0.000031	0.439645	0.006066	0.994346
0.400000	0.000240	0.441152	0.045791	0.994365
0.500000	0.001101	0.444789	0.180350	0.994411
0.600000	0.004317	0.455596	0.460257	0.994543
0.700000	0.012955	0.482678	0.699730	0.994847
0.800000	0.029385	0.533089	0.788578	0.995332
0.900000	0.054089	0.608310	0.785709	0.995907
1.000000	0.086399	0.706409	0.743015	0.996473

TIME= 6.000000

PBULK OBULK
12.7896755411476879 29.4036481748929184
DEG. RATE 40.001103
FILM THICKNESS 0.800258
GRADP 0.313043
GRADO 0.944027

R	P	O	PFRAC	OFRAC
0.0	-0.000444	0.536132	-0.097326	0.995359
0.100000	-0.000289	0.536696	-0.061332	0.995363
0.200000	-0.000156	0.537388	-0.032234	0.995369
0.300000	-0.000041	0.538197	-0.008246	0.995376
0.400000	0.000072	0.539150	0.014147	0.995384
0.500000	0.000391	0.540852	0.072486	0.995399
0.600000	0.001729	0.545700	0.256517	0.995440
0.700000	0.006315	0.560303	0.551632	0.995558
0.800000	0.017309	0.594033	0.742630	0.995809
0.900000	0.036508	0.652249	0.794502	0.996182
1.000000	0.063948	0.735091	0.774384	0.996611

TIME= 7.500000

PBULK OBULK
9.25830038603370276 30.7232492234026147
DEG. RATE 34.150693
FILM THICKNESS 0.800301
GRADP 0.267279
GRADO 0.799453

R	P	O	PFRAC	OFRAC
0.0	-0.000502	0.625498	-0.111473	0.996019
0.100000	-0.000347	0.626009	-0.074533	0.996022
0.200000	-0.000214	0.626552	-0.044636	0.996026
0.300000	-0.000098	0.627127	-0.019954	0.996029
0.400000	0.000004	0.627735	0.000761	0.996033
0.500000	0.000145	0.628529	0.028179	0.996038
0.600000	0.000696	0.630600	0.122204	0.996051
0.700000	0.002916	0.637674	0.367072	0.996095
0.800000	0.009627	0.658113	0.644550	0.996216
0.90000	0.02372	0.70051	0.77530	0.99644
1.000000	0.046292	0.768081	0.792195	0.996756

TIME= 9.000000

PBULK 7.85908357225294130

OBULK 31.4483622812527344

DEG. RATE 31.355179

FILM THICKNESS 0.800339

GRADP 0.245417

GRADO 0.730024

R	P	O	PFRAC	OFRAC
0.0	-0.000524	0.666616	-0.117099	0.996264
0.100000	-0.000369	0.667097	-0.079777	0.996266
0.200000	-0.000236	0.667554	-0.049553	0.996269
0.300000	-0.000120	0.667996	-0.024582	0.996271
0.400000	-0.000018	0.668427	-0.003607	0.996274
0.500000	0.000090	0.668905	0.017671	0.996276
0.600000	0.000456	0.670172	0.083527	0.996283
0.700000	0.001995	0.674942	0.284714	0.996310
0.800000	0.007128	0.690376	0.579628	0.996392
0.900000	0.019016	0.725849	0.753965	0.996568
1.000000	0.039295	0.786209	0.794770	0.996830

TIME= 11.000000

PBULK 7.27394802595907075

OBULK 31.8167620162275924

DEG. RATE 30.037083

FILM THICKNESS 0.800387

GRADP 0.235121

GRADO 0.697123

R	P	O	PFRAC	OFRAC
0.0	-0.000539	0.685665	-0.120695	0.996367
0.100000	-0.000384	0.686129	-0.083135	0.996370
0.200000	-0.000250	0.686541	-0.052719	0.996372
0.300000	-0.000134	0.686912	-0.027590	0.996374
0.400000	-0.000032	0.687249	-0.006481	0.996375
0.500000	0.000070	0.687594	0.013818	0.996377
0.600000	0.000376	0.688550	0.069928	0.996382
0.700000	0.001676	0.692455	0.250645	0.996403
0.800000	0.006186	0.705875	0.546762	0.996471
0.900000	0.017120	0.738329	0.741223	0.996625
1.000000	0.036370	0.795419	0.794465	0.996867

TIME= 13.000000

PBULK	OBULK
7.13438806617788090	31.9169024450067553

DEG. RATE 29.748450
FILM THICKNESS 0.800434
GRADP 0.232881
GRADO 0.689870

R	P	O	PFRAC	OFRAC
0.0	-0.000542	0.690560	-0.121603	0.996393
0.100000	-0.000387	0.691020	-0.083981	0.996395
0.200000	-0.000254	0.691419	-0.053514	0.996397
0.300000	-0.000138	0.691770	-0.028339	0.996399
0.400000	-0.000036	0.692081	-0.007190	0.996401
0.500000	0.000066	0.692392	0.012951	0.996402
0.600000	0.000358	0.693272	0.066885	0.996407
0.700000	0.001604	0.696975	0.242591	0.996426
0.800000	0.005969	0.709919	0.538356	0.996491
0.900000	0.016674	0.741639	0.737764	0.996640
1.000000	0.035672	0.797923	0.794235	0.996877

TIME= 16.000000

PBULK	OBULK
7.10036217670211522	31.9415037006127527

DEG. RATE 29.680867
FILM THICKNESS 0.800504
GRADP 0.232381
GRADO 0.688229

R	P	O	PFRAC	OFRAC
0.0	-0.000543	0.691776	-0.121827	0.996399
0.100000	-0.000388	0.692235	-0.084190	0.996402
0.200000	-0.000255	0.692630	-0.053710	0.996404
0.300000	-0.000139	0.692975	-0.028525	0.996405
0.400000	-0.000037	0.693279	-0.007366	0.996407
0.500000	0.000064	0.693579	0.012735	0.996408
0.600000	0.000354	0.694438	0.066128	0.996413
0.700000	0.001587	0.698090	0.240577	0.996432
0.800000	0.005916	0.710914	0.536232	0.996496
0.900000	0.016565	0.742452	0.736885	0.996644
1.000000	0.035502	0.798538	0.794169	0.996879

TIME= 20.000000

PBULK 7.09441270605404162

OBULK 31.9456674587336167

DEG. RATE 29.667615

FILM THICKNESS 0.800596

GRADP 0.232317

GRADO R 0.688015 P

		O	PFRAC	OFRAC
0.0	-0.000543	0.691981	-0.121875	0.996400
0.100000	-0.000388	0.692439	-0.084235	0.996403
0.200000	-0.000255	0.692834	-0.053753	0.996405
0.300000	-0.000139	0.693178	-0.028567	0.996406
0.400000	-0.000037	0.693481	-0.007407	0.996408
0.500000	0.000064	0.693780	0.012684	0.996409
0.600000	0.000353	0.694635	0.065957	0.996414
0.700000	0.001583	0.698277	0.240145	0.996433
0.800000	0.005905	0.711079	0.535802	0.996497
0.900000	0.016544	0.742585	0.736718	0.996645
1.000000	0.035472	0.798642	0.794157	0.996879

APPENDIX 3

TABULATED RESULTS OF LARGE PHENOL-PULSE SIMULATION

The computed results corresponding to Fig. 10, page 45 and Table 4, page 46 are listed below. Included are the dimensionless radial position (R), phenol concentration (P), oxygen concentration (O), film thickness (h), time, and concentration gradients at the outer surface of the biofilm (GRADP and GRADO). PFRAC is defined by

$$PFRAC = \frac{P}{K_p + P + P^2/K_I} ,$$

and indicates the degree to which the phenol concentration is limiting the overall rate of reaction at a given point in the biofilm. The analogous variable for oxygen is

$$OFRAC = \frac{O}{K_o + O} .$$

PBULK and OBULK are the bulk-liquid concentrations of phenol and oxygen in units of mg/L. DEG RATE is the bioreactor's phenol degradation rate normalized by the volume of the settled bed of bioparticles. Its units are mg phenol/L settled bed•min.

INITIAL CONDITIONS

R	P	O	h
0.0	0.000057	0.530069	0.500000
0.100000	0.000136	0.530303	0.500000
0.200000	0.000257	0.530662	0.500000
0.300000	0.000485	0.531338	0.500000
0.400000	0.000970	0.532773	0.500000
0.500000	0.002182	0.536364	0.500000
0.600000	0.005661	0.546667	0.500000
0.700000	0.013950	0.571216	0.500000
0.800000	0.028659	0.614775	0.500000
0.900000	0.050104	0.678286	0.500000
1.000000	0.077917	0.760657	0.500000

TIME= 0.100000

PBULK	OBULK
177.261996068748594	30.0109398355627413

DEG. RATE 69.415943M

FILM THICKNESS 0.500022

GRADP 0.473069

GRADO 0.420838

R	P	O	PFRAC	OFRAC
0.0	0.507103	0.479661	0.329134	0.994815
0.100000	0.513326	0.483854	0.326472	0.994860
0.200000	0.530807	0.495107	0.319219	0.994976
0.300000	0.558064	0.512628	0.308526	0.995147
0.400000	0.593515	0.535637	0.295641	0.995354
0.500000	0.635508	0.563380	0.281698	0.995582
0.600000	0.682368	0.595145	0.267609	0.995817
0.700000	0.732436	0.630275	0.254028	0.996049
0.800000	0.784107	0.668179	0.241382	0.996272
0.900000	0.835864	0.708331	0.229915	0.996483
1.000000	0.886310	0.750273	0.219738	0.996679

TIME= 1.000000

PBULK 147.104198158039793

OBULK 30.0708846779985812

DEG. RATE 14.096918

FILM THICKNESS 0.500040

GRADP 0.096075

GRADO 0.360055

R	P	O	PFRAC	OFRAC
0.0	0.681478	0.549310	0.267863	0.995469
0.100000	0.682274	0.552203	0.267636	0.995493
0.200000	0.684313	0.559784	0.267054	0.995554
0.300000	0.687491	0.571656	0.266153	0.995646
0.400000	0.691719	0.587484	0.264963	0.995763
0.500000	0.696922	0.606982	0.263514	0.995898
0.600000	0.703033	0.629899	0.261832	0.996047
0.700000	0.709996	0.656019	0.259941	0.996204
0.800000	0.717760	0.685148	0.257864	0.996364
0.900000	0.726282	0.717117	0.255623	0.996526
1.000000	0.735521	0.751772	0.253236	0.996686

TIME= 2.000000

PBULK 122.058733981743742

OBULK 29.5179139477962309

DEG. RATE 17.720793

FILM THICKNESS 0.500057

GRADP 0.120778

GRADO 0.417185

R	P	O	PFRAC	OFRAC
0.0	0.542003	0.502179	0.314739	0.995046
0.100000	0.542984	0.505507	0.314352	0.995079
0.200000	0.545553	0.514338	0.313344	0.995163
0.300000	0.549575	0.528200	0.311779	0.995289
0.400000	0.554934	0.546691	0.309718	0.995448
0.500000	0.561530	0.569462	0.307217	0.995629
0.600000	0.569273	0.596208	0.304333	0.995824
0.700000	0.578087	0.626658	0.301114	0.996026
0.800000	0.587902	0.660573	0.297609	0.996230
0.900000	0.598657	0.697735	0.293860	0.996430
1.000000	0.610294	0.737948	0.289908	0.996624

TIME= 3.000000

PBULK OBULK
102.075967338731513 28.7319920558444934
DEG. RATE 21.429030
FILM THICKNESS 0.500079
GRADP 0.146061
GRADO 0.480382

R	P	O	PFRAC	OFRAC
0.0	0.427389	0.445419	0.367477	0.994419
0.100000	0.428563	0.449240	0.366849	0.994466
0.200000	0.431688	0.459484	0.365186	0.994589
0.300000	0.436594	0.475595	0.362604	0.994771
0.400000	0.443134	0.497088	0.359219	0.994996
0.500000	0.451179	0.523540	0.355139	0.995248
0.600000	0.460616	0.554575	0.350469	0.995512
0.700000	0.471342	0.589857	0.345307	0.995780
0.800000	0.483266	0.629084	0.339742	0.996042
0.900000	0.496304	0.671982	0.333858	0.996293
1.000000	0.510380	0.718300	0.327727	0.996532

TIME= 4.000000

PBULK OBULK
85.8826072788974955 27.8431822659149404
DEG. RATE 25.216961
FILM THICKNESS 0.500104
GRADP 0.171891
GRADO 0.548428

R	P	O	PFRAC	OFRAC
0.0	0.330862	0.381810	0.427613	0.993495
0.100000	0.332245	0.386191	0.426616	0.993568
0.200000	0.335969	0.398044	0.423952	0.993758
0.300000	0.341827	0.416707	0.419827	0.994036
0.400000	0.349636	0.441598	0.414449	0.994371
0.500000	0.359234	0.472199	0.408021	0.994734
0.600000	0.370475	0.508048	0.400738	0.995103
0.700000	0.383228	0.548725	0.392779	0.995465
0.800000	0.397373	0.593850	0.384309	0.995808
0.900000	0.412801	0.643074	0.375471	0.996127
1.000000	0.429413	0.696080	0.366395	0.996421

TIME= 5.000000

PBULK 72.4863883143829284

OBULK 26.8602145992030685

DEG. RATE 29.291767

FILM THICKNESS 0.500134

GRADP 0.199682

GRADO 0.624532

R	P	O	PFRAC	OFRAC
0.0	0.246873	0.310205	0.498072	0.992005
0.100000	0.248490	0.315239	0.496505	0.992132
0.200000	0.252885	0.328964	0.492293	0.992458
0.300000	0.259807	0.350588	0.485797	0.992920
0.400000	0.269028	0.379407	0.477396	0.993454
0.500000	0.280346	0.414785	0.467460	0.994009
0.600000	0.293575	0.456145	0.456344	0.994549
0.700000	0.308546	0.502960	0.444367	0.995054
0.800000	0.325105	0.554747	0.431816	0.995514
0.900000	0.343110	0.611064	0.418933	0.995925
1.000000	0.362432	0.671505	0.405923	0.996291

TIME= 6.000000

PBULK 61.0955962108211494

OBULK 25.7545291199282609

DEG. RATE 33.755631

FILM THICKNESS 0.500168

GRADP 0.230134

GRADO 0.710724

R	P	O	PFRAC	OFRAC
0.0	0.170488	0.227210	0.584357	0.989117
0.100000	0.172381	0.233034	0.581893	0.989386
0.200000	0.177565	0.249018	0.575236	0.990060
0.300000	0.185732	0.274211	0.565020	0.990965
0.400000	0.196601	0.307747	0.551926	0.991942
0.500000	0.209914	0.348832	0.536631	0.992884
0.600000	0.225435	0.396734	0.519773	0.993738
0.700000	0.242944	0.450782	0.501918	0.994485
0.800000	0.262241	0.510356	0.483552	0.995125
0.900000	0.283141	0.574889	0.465068	0.995670
1.000000	0.305478	0.643863	0.446772	0.996132

TIME= 7.000000

PBULK 51.0404760308337551

OBULK 24.4659970738943997

DEG. RATE 38.954376

FILM THICKNESS 0.500207

GRADP 0.265605

GRADO 0.813155

R	P	O	PFRAC	OFRAC
0.0	0.097013	0.127490	0.694642	0.980768
0.100000	0.099238	0.134286	0.690925	0.981723
0.200000	0.105376	0.153057	0.680758	0.983929
0.300000	0.115052	0.182658	0.665041	0.986498
0.400000	0.127918	0.222024	0.644845	0.988865
0.500000	0.143647	0.270155	0.621351	0.990831
0.600000	0.161930	0.326109	0.595735	0.992392
0.700000	0.182481	0.389011	0.569047	0.993614
0.800000	0.205034	0.458050	0.542146	0.994572
0.900000	0.229348	0.532486	0.515679	0.995327
1.000000	0.255202	0.611650	0.490100	0.995929

TIME= 8.000000

PBULK 41.7971697212829874

OBULK 23.0026052128943412

DEG. RATE 44.383351

FILM THICKNESS 0.500253

GRADP 0.302658

GRADO 0.919068

R	P	O	PFRAC	OFRAC
0.0	0.029604	0.030838	0.776812	0.925010
0.100000	0.031983	0.038047	0.778656	0.938342
0.200000	0.038648	0.058249	0.778838	0.958847
0.300000	0.049334	0.090645	0.770009	0.973160
0.400000	0.063753	0.134357	0.749941	0.981733
0.500000	0.081567	0.188370	0.720686	0.986902
0.600000	0.102410	0.251582	0.685653	0.990161
0.700000	0.125914	0.322881	0.647935	0.992317
0.800000	0.151723	0.401202	0.609813	0.993807
0.900000	0.179512	0.485559	0.572770	0.994878
1.000000	0.208986	0.575065	0.537672	0.995671

TIME= 9.000000

PBULK	OBULK
33.8118256409966484	22.2048854673022369

DEG. RATE 45.027421
FILM THICKNESS 0.500302
GRADP 0.307091
GRADO 0.923977

R	P	O	PFRAC	OFRAC
0.0	0.003632	0.058250	0.418227	0.958848
0.100000	0.005091	0.062635	0.499366	0.961618
0.200000	0.009474	0.075810	0.638708	0.968076
0.300000	0.017356	0.099477	0.736643	0.975485
0.400000	0.029085	0.134673	0.776247	0.981775
0.500000	0.044661	0.181405	0.774834	0.986406
0.600000	0.063844	0.238968	0.749798	0.989647
0.700000	0.086274	0.306299	0.712733	0.991904
0.800000	0.111548	0.382209	0.670684	0.993502
0.900000	0.139267	0.465517	0.627759	0.994658
1.000000	0.169059	0.555122	0.586231	0.995517

TIME= 10.000000

PBULK	OBULK
28.1616117115266462	22.4577577936484296

DEG. RATE 43.043438
FILM THICKNESS 0.500350
GRADP 0.293597
GRADO 0.879463

R	P	O	PFRAC	OFRAC
0.0	0.000922	0.142502	0.155666	0.982759
0.100000	0.001598	0.144546	0.241771	0.982999
0.200000	0.003772	0.151115	0.427237	0.983726
0.300000	0.008426	0.165113	0.614594	0.985085
0.400000	0.016496	0.189312	0.730411	0.986966
0.500000	0.028455	0.225127	0.775473	0.989017
0.600000	0.044335	0.272651	0.775123	0.990914
0.700000	0.063895	0.331181	0.749718	0.992508
0.800000	0.086767	0.399630	0.711899	0.993783
0.900000	0.112540	0.476785	0.669080	0.994784
1.000000	0.140808	0.561444	0.625492	0.995567

TIME= 11.000000

PBULK 24.4683679498940343

OBULK 22.9748584100938551

DEG. RATE 41.217521

FILM THICKNESS 0.500396

GRADP 0.281177

GRADO 0.839130

R	P	O	PFRAC	OFRAC
0.0	0.000357	0.210067	0.066577	0.988239
0.100000	0.000741	0.211236	0.129093	0.988303
0.200000	0.001950	0.214902	0.279942	0.988501
0.300000	0.004847	0.223624	0.487557	0.988944
0.400000	0.010551	0.240715	0.659583	0.989721
0.500000	0.019908	0.268685	0.751436	0.990781
0.600000	0.033249	0.308515	0.779194	0.991962
0.700000	0.050498	0.359990	0.768636	0.993103
0.800000	0.071362	0.422242	0.737728	0.994114
0.900000	0.095449	0.494112	0.697263	0.994966
1.000000	0.122342	0.574371	0.653494	0.995666

TIME= 12.000000

PBULK 22.1616704834034621

OBULK 23.4441506685688594

DEG. RATE 39.913244

FILM THICKNESS 0.500441

GRADP 0.272312

GRADO 0.810553

R	P	O	PFRAC	OFRAC
0.0	0.00017	0.25651	0.03337	0.99034
0.100000	0.000446	0.257340	0.081845	0.990379
0.200000	0.001247	0.259770	0.199398	0.990468
0.300000	0.003280	0.265886	0.394122	0.990685
0.400000	0.007637	0.278915	0.593369	0.991116
0.500000	0.015353	0.301932	0.720936	0.991788
0.600000	0.026992	0.336608	0.773271	0.992628
0.700000	0.042638	0.383190	0.776507	0.993518
0.800000	0.062072	0.441037	0.752537	0.994363
0.900000	0.084933	0.509082	0.715000	0.995113
1.000000	0.110808	0.586104	0.671882	0.995753

TIME= 14.000000

PBULK OBULK
19.9176125311168022 24.0235481502535748
DEG. RATE 38.417699
FILM THICKNESS 0.500526
GRADP 0.262168
GRADO 0.777923

R	P	O	PFRAC	OFRAC
0.0	0.000061	0.305113	0.012097	0.991873
0.100000	0.000262	0.305714	0.049726	0.991889
0.200000	0.000784	0.307283	0.135463	0.991930
0.300000	0.002162	0.311401	0.301124	0.992036
0.400000	0.005360	0.320918	0.511684	0.992270
0.500000	0.011517	0.339215	0.675580	0.992684
0.600000	0.021439	0.368676	0.758164	0.993265
0.700000	0.035405	0.410128	0.779519	0.993941
0.800000	0.053308	0.463257	0.765095	0.994632
0.900000	0.074835	0.527138	0.731981	0.995280
1.000000	0.099588	0.600589	0.690341	0.995855

TIME= 16.000000

PBULK OBULK
19.1330390179131662 24.2635273576456640
DEG. RATE 37.848344
FILM THICKNESS 0.500609
GRADP 0.258340
GRADO 0.765566

R	P	O	PFRAC	OFRAC
0.0	0.000033	0.323116	0.006539	0.992322
0.100000	0.000214	0.323656	0.041079	0.992335
0.200000	0.000661	0.324986	0.116716	0.992366
0.300000	0.001851	0.328524	0.269641	0.992448
0.400000	0.004685	0.336933	0.479385	0.992635
0.500000	0.010314	0.353627	0.655296	0.992980
0.600000	0.019625	0.381228	0.750031	0.993485
0.700000	0.032976	0.420801	0.779102	0.994094
0.800000	0.050310	0.472174	0.768862	0.994733
0.900000	0.071337	0.534489	0.737769	0.995344
1.000000	0.095665	0.606588	0.696900	0.995896

TIME= 18.000000

PBULK	OBULK
18.8662350888876240	24.3513179749516304

DEG. RATE 37.645043
FILM THICKNESS 0.500692
GRADP 0.257009
GRADO 0.761319

R	P	O	PFRAC	OFRAC
0.0	0.000024	0.329399	0.004811	0.992468
0.100000	0.000200	0.329919	0.038370	0.992479
0.200000	0.000623	0.331175	0.110701	0.992508
0.300000	0.001753	0.334526	0.259073	0.992582
0.400000	0.004467	0.342572	0.467926	0.992755
0.500000	0.009919	0.358725	0.647769	0.993079
0.600000	0.019021	0.385689	0.746851	0.993560
0.700000	0.032160	0.424613	0.778748	0.994147
0.800000	0.049296	0.475377	0.770052	0.994769
0.900000	0.070150	0.537150	0.739713	0.995367
1.000000	0.094331	0.608783	0.699140	0.995910

APPENDIX 4

ORTHOGONAL COLLOCATION AND LINEAR ANALYSIS

Using a one-point interior-collocation approach,[56] the derivatives with respect to the spatial dimension (r) are approximated in terms of polynomials,

$$\frac{d\overline{P}_l}{d\overline{r}} = 2.29(\overline{P}_b - \overline{P}_l)$$

$$\frac{d\overline{P}_b}{d\overline{r}} = 3.50(\overline{P}_b - \overline{P}_l)$$

$$\frac{d^2\overline{P}_l}{d\overline{r}^2} = 3.50(\overline{P}_b - \overline{P}_l)$$

$$\frac{d^2\overline{P}_b}{d\overline{r}^2} = 3.50(\overline{P}_b - \overline{P}_l)$$

where $\overline{P}_l$ and $\overline{P}_b$ are the dimensionless concentrations of phenol at the internal collocation point ($\overline{r}_l = 0.655$) and at the external surface of the biofilm ($\overline{r} = 1$), respectively. Substituting these identities into equation 18 and 6a yields:

$$\frac{d\overline{P}_l}{d\overline{t}} = 2.29(\overline{P}_b - \overline{P}_l)\left[\frac{2}{h(1 + h\overline{r}_l)}\right] + \frac{3.50}{h^2}(\overline{P}_b - \overline{P}_l) - \frac{K_{max} \text{ X } r_i^2}{P^\circ \, D_p}\left[\frac{\overline{P}_l}{\overline{K}_p + \overline{P}_l + \overline{P}_l^2/\overline{K}_I}\right],$$

and

$$\frac{d\overline{P}_b}{d\overline{t}} = \frac{1}{\overline{\tau}}(\overline{P}_{in} - \overline{P}_b) - \frac{3\varepsilon_s}{\varepsilon_\ell \, h(1 + h)}[3.50(\overline{P}_b - \overline{P}_l)] .$$

The reduced model can now be linearized about the steady-state values using Taylor's theorum,

$$\frac{d\bar{P}_1}{dt} = F_1 = \frac{\partial F_1}{\partial \bar{P}_1}\bigg|_{ss}(\bar{P}_1 - \bar{P}_1 \mid_{ss}) + \frac{\partial F_1}{\partial \bar{P}_b}\bigg|_{ss}(\bar{P}_b - \bar{P}_b \mid_{ss}) +$$

$$\frac{\partial F_1}{\partial \bar{P}_{in}}\bigg|_{ss}(\bar{P}_{in} - \bar{P}_{in} \mid_{ss}) ,$$

$$\frac{d\bar{P}_b}{dt} = F_2 = \frac{\partial F_2}{\partial \bar{P}_1}\bigg|_{ss}(\bar{P}_1 - \bar{P}_1 \mid_{ss}) + \frac{\partial F_2}{\partial \bar{P}_b}\bigg|_{ss}(\bar{P}_b - \bar{P}_b \mid_{ss}) +$$

$$\frac{\partial F_2}{\partial \bar{P}_{in}}\bigg|_{ss}(\bar{P}_{in} - \bar{P}_{in} \mid_{ss}) ,$$

where the subscript ss stands for steady state. Writing the above equations in state-space notation,

$$\dot{P}(t) = \underline{A}P(t) + \underline{B}U(t)$$

where P(t) and U(t) are vectors of deviation variables,

$$P(t) = \begin{bmatrix} \bar{P}_1 - \bar{P}_1 \mid_{ss} \\ \bar{P}_b - \bar{P}_b \mid_{ss} \end{bmatrix}$$

$$U(t) = \left[\bar{P}_{in} - \bar{P}_{in} \mid_{ss}\right] .$$

The coefficients of the $\underline{A}$ and $\underline{B}$ matrices are,

$$a_{11} = -2.29\left[\frac{2}{h(1 + h\bar{r}_1)}\right] - \frac{3.50}{h^2} + \left[\frac{\bar{K}_m}{\bar{P}_1 \mid_{ss}} + 1 + \frac{\bar{P}_1 \mid_{ss}}{\bar{K}_I}\right]^{-2}\left[\frac{1}{\bar{K}_I} - \frac{\bar{K}_m}{\bar{P}_1{}^2 \mid_{ss}}\right]$$

$$a_{12} = 2.29\left[\frac{2}{h(1 + h\bar{r}_1)}\right] + \frac{3.50}{h^2}$$

$$a_{21} = 3.50\left[\frac{3\varepsilon_s}{\varepsilon_\ell\, h(1 + h)}\right]$$

$$a_{22} = -\frac{1}{\bar{\tau}} - 3.50\left[\frac{3\varepsilon_s}{\varepsilon_\ell\, h(1 + h)}\right]$$

$$b_{11} = 0$$

$$b_{12} = \frac{1}{\bar{\tau}} \ .$$

Certain characteristics of the solution to the model can be inferred by examining the $\underline{A}$ matrix.[59] For instance, the linearized system is asymptotically stable if and only if

$$\det \underline{A} > 0 \quad \text{and}$$

$$\text{tr } \underline{A} < 0 \ ,$$

where the determinant and trace are defined below.

$$\det \underline{A} = a_{11}a_{22} - a_{12}a_{21}$$

$$\text{tr } \underline{A} = a_{11} + a_{22} \ .$$

In addition, the eigenvalues of the system will both be real and have the same sign if the following criteria are met.

$$\left[\frac{\text{tr } \underline{A}}{2}\right]^2 > \det \underline{A} > 0 \ .$$

Real eigenvalues are indicative of nonoscillatory (overdamped) responses of the system to perturbations from steady state. The above criteria were used to test the range of parameters shown in Table 5, page 50, changing one variable at a time. Over this range, no unstable or oscillatory solutions were predicted by the criteria.

APPENDIX 5

COMPUTER PROGRAMS

PMFBR1.FOR

```
*SIMULATION OF THE RESIDENCE TIME DISTRIBUTION OF THE
*PERFECTLY MIXED FLUIDIZED-BED BIOREACTOR
*
CONSTANT VB=.030,VT=.530,F=0.010,K1=20.,K2=10.
INCON IC=14.495
TRIG=IMPULS(10.,10000.)
SPIKE=PULSE(1.0,TRIG)
PULS=2.5E3*SPIKE
CI=50.+PULS
U=(CI-CO)*F/VT + R*VB/VT
R=-K1*CO/(K2+CO)
CO=INTGRL(IC,U)
TIMER FINTIM=200.,OUTDEL=10.,PRDEL=5.
PRINT CI,CO
END
STOP
ENDJOB
```

DATA.FOR

```
C           THIS FILE IS A SIMULATION FILE WHICH READS
C       IN INPUT AND OUTPUT DATA, CALCULATES A SET OF SIMU-
C       LATED OUTPUT AND THEN PRINTS OUT BOTH THE ACTUAL AND
C       CALCULATED OUTPUT DATA.  THE SIMULATION IS A DISCRETE
C       LINEAR DIFFERENCE MODEL DERIVED FROM Z TRANSFORMS.
C       THE FILE IS SET UP TO SIMULATE A PERFECTLY MIXED TANK
C       WITH DEAD TIME.
C
C
C
        DIMENSION X(100),U(100),XCALC(100)
        REAL KP
        DO 100 I=1,92
        READ (58,*) U(I),X(I)
 100    CONTINUE
C       DO 200 I = 1,92
C       WRITE (5,*) I,U(I),X(I)
C 200   CONTINUE
C
C       PERFORM SIMULATION
C
        KP = 0.173
        TAU = 27.1
        N = 0
        DELT = 1.
        SAMPLE = 0.2
C
C       NOTE THAT "SAMPLE" IS THE NUMBER OF SAMPLES TAKEN
C       PER MINUTE OF OPERATION.  THUS THE OUTPUT VALUES
C       OF THE TIME CONSTANT AND DEAD TIME ARE IN UNITS
C       OF MINUTES.
C
        N2 = N + 2
        DO 300 I=1,N2
        XCALC(I) = X(I)
 300    CONTINUE
C
        A1 = -(EXP(-DELT/TAU))
        A2 = 0.
        B1 = KP*(1+A1)
        B2 = 0.
C
        COST = 0.
        DO 400 I=1,92
        IF (I .LE. N2) GO TO 350
        XCALC(I) = B1*U(I-1-N) - A1*XCALC(I-1)
        1       + B2*U(I-2-N) - A2*XCALC(I-2)
        COST = COST + (X(I)-XCALC(I))**2
 350    WRITE (5,*) I,X(I),XCALC(I)
 400    CONTINUE
        TAU = TAU/SAMPLE
        N = N/SAMPLE
        WRITE (5,500) KP,TAU,N,COST
        WRITE (5,500) KP,TAU,N,COST
 500    FORMAT (//1X, 5HGAIN=, E15.6, 10X, 4HTAU=, E15.6, 10X,
        1       2HN=, I6, //, 20X, 5HCOST=, E15.6)
        STOP
        END
```

```
    D.FOR
C       THIS FILE CONVERTS PERCENT TRANSMITTANCE VERSUS TIME
C       (ARBITRARY UNITS) TO PHENOL CONCENTRATION (mg/L) VERSUS
C       TIME (min).  IT USES A LINEAR CALIBRATION CURVE FOR THE
C       CONCENTRATION CONVERSION.
C
C
        DIMENSION TIN(46),PT(46),OD(46),TMIN(46),P(46)
        REAL MCALIB
        MCALIB=0.00613
        BCALIB=-0.0062
        N=37
C
        DO 100 I=1,N
C               READ (3,*)TIN(I),PT(I)
                READ (3,50)TIN(I),PT(I)
 50             FORMAT(2G15.7)
                TMIN(I)=TIN(I)/0.02
                PT(I)=PT(I)/100.
                OD(I)=-(ALOG10(PT(I)))
                P(I)=(OD(I)-BCALIB)/MCALIB
                WRITE (23,*)TMIN(I),P(I)
 100    CONTINUE
C
        WRITE (23,150)MCALIB
 150    FORMAT (8H MCALIB= ,F15.7)
        WRITE (23,160)BCALIB
 160    FORMAT (8H BCALIB= ,F15.7)
        STOP
        END
```

```
    RATE4.FOR
C       THIS FILE CALCULATES VOLUMETRIC DEGRADATION RATES FROM
C       PHENOL CONCENTRATION(P) VERSUS TIME(T) PMFBR DATA.  THE
C       DATA ARE READ IN THROUGH THE DATA FILE FOR33.DAT UN-
C       FORMATTED.  THE NUMERICAL DIFFERENTIATION IS DONE USING
C       A THREE-POINT ALGORITHM (P127, BURDEN) DERIVED FROM
C       LAGRANGE INTERPOLATING POLYNOMIALS.
C
C
        DIMENSION P(100),PDOT(100),R(100),T(100),TMIN(100)
        N=37
        VBED=0.022
        FEED=.0264
        PIN=60.
        M=2
        VTOTAL=0.360-VBED
        TAU=VTOTAL/FEED
C
        DO 50 I=1,N
                READ (3,*)TMIN(I),P(I)
                T(I)=TMIN(I)
 50     CONTINUE
        DO 100 I=(M+1),(N-M)
                F1=(T(I)-T(I+M))/((T(I-M)-T(I))*(T(I-M)-T(I+M)))
                F2=(2.*T(I)-T(I-M)-T(I+M))/((T(I)-T(I-M))*(T(I)-T(I+M)))
                F3=(T(I)-T(I-M))/((T(I+M)-T(I-M))*(T(I+M)-T(I)))
                PDOT(I)=P(I-M)*F1+P(I)*F2+P(I+M)*F3
                R(I)=-(PDOT(I)-(PIN-P(I))/TAU)*VTOTAL/VBED
                WRITE (24,*)TMIN(I),P(I),PDOT(I),R(I)
 100    CONTINUE
C
        WRITE (24,150)VBED
 150    FORMAT(/,7H VBED= ,G15.7)
        WRITE (24,200) PIN
 200    FORMAT(6H PIN= ,G15.7)
        WRITE (24,250)FEED
 250    FORMAT(11H FEED RATE= ,G15.7)
        STOP
        END
```

```
TANKI2.FOR

C       THIS FILE IS A STEADY-STATE SIMULATION OF A SERIES OF
C       STIRRED TANK REACTORS.  THE EFFLUENT OF THE FIRST
C       REACTOR IS THE INFLUENT TO THE SECOND AND SO FORTH.
C       THE REACTION TAKES PLACE IN FIXED-FILM BIOLOGICAL
C       PARTICLES WHICH ARE SUSPENDED IN THE LIQUID PHASE.  OXYGEN,
C       ONE OF THE TWO SUBSTRATES, IS ASSUMED TO BE BUBBLED INTO
C       THE REACTORS WITH A MASS-TRANSFER COEFFICIENT BEING DENOTED
C       "XKLA".  THE REACTION RATE IS EVALUATED BY LETTING THE
C       SUBROUTINE "FLOC" (USE EITHER FLOC.FOR OR FLOC2.FOR)
C       DETERMINE THE CONCENTRATION GRADIENT AT THE PARTICLE
C       SURFACE.  THE BISECTION METHOD IS USED TO ITERATE TO THE
C       CORRECT EFFLUENT CONCENTRATION FOR EACH TANK.  IMPORTANT
C       VARIABLE NAMES ARE LISTED BELOW.
C
C       VARIABLE NAME                   MEANING
C
C       PIC,XIC         ASSUMED EFFLUENT SUBSTRATE CONCENTRATIONS FOR
C                       A GIVEN TANK
C       RO              OUTER FILM RADIUS
C       RI,RIN          INNER FILM RADIUS
C       PGRAD,XGRAD     SUBSTRATE GRADIENTS AT THE FILM SURFACE--
C                       CALCULATED BY SUBROUTINE "FLOC"
C       XSTAR           SAT'N CONCENTRATION OF OXYGEN IN THE LIQUID
C       CP,CX           SUBSTRATE MONOD CONSTANTS
C       CI              SUBSTRATE INHIBITION CONSTANT
C       C1,C2           LUMPED KINETIC PARAMETERS (DEFINED IN THE
C                       MODELING EQUATIONS BELOW)
C       XN              NUMBER OF PARTICLES PER UNIT VOLUME
C                       (PARTICLE DENSITY)
C       TAU             RESIDENCE TIME FOR EACH REACTOR
C       GAMMA           STOICHIOMETRIC COEFFICENT (GRAM X/GRAM P)
C       DP,DX           SUBSTRATE DIFFUSIVITIES IN THE FILM
C       PINLET,XINLET   SUBSTRATE CONCENTRATIONS GOING INTO THE
C                       FIRST TANK
C       NTANKS          THE NUMBER OF TANKS IN SERIES
C       FRAC            THE FRACTION BY WHICH THE SUBSTRATE DIF-
C                       FUSIVITIES ARE REDUCED IN THE FILM
C                       RELATIVE TO THOSE IN PURE WATER (DPW,DXW)
C       INTRVL          NUMBER OF DISCRETE INTERVALS INTO WHICH
C                       THE FILM IS DIVIDED FOR COMPUTATIONS
C       XKMAX           MAX REACTION RATE (GRAM P/GRAM DRY CELLS*
C                       SEC)
C       RHO             BIOFILM DENSITY (GRAM DRY CELLS/ML)
C       h               DIMENSIONLESS BIOFILM THICKNESS [(RO/RI)-1]
C
C
C

      IMPLICIT DOUBLE PRECISION (A-H,O-Z)
      DIMENSION PO(50),XO(50),PINLET(50),XINLET(50),
```

```
     1       PGUESS(50),XGUESS(50),DELTAP(50),DELTAX(50),
     1       R(50),P(50),PDOT(50),X(50),XDOT(50)
      COMMON CP,CX,CI,C1,C2,R,P,PDOT,X,XDOT,INTRVL
C
C     INITIALIZE THE PROCESS
C
      NTANKS=1
      XINLET(1)=1.D-6
C     PINLET(1)=100.D-6
      PINLET(1)=65.D-6
      EPS=0.95D0
      h=.682D0
C     h=.941D0
      RI=0.022D0
      RO=RI*(1.D0+h)
      XKLA=.01D0
C     XKLA=0.1D-6
      XSTAR=40.D-6
      DPW=1.1D-5
      DXW=2.6D-5
      FRAC=0.25D0
      DP=DPW*FRAC
      DX=DXW*FRAC
      CP=1.D-6
C     CX=5.D-7
      CX=1.D-7
C     CI=80.D-6
      CI=80.D-6
      GAMMA=1.4D0
C     XKMAX=1.5833D-4
      XKMAX=1.333D-4
      XPI=3.141592654D0
      XN=3.D0*(1.D0-EPS)/(4.D0*EPS*XPI*RO**3)
C     RESTIM=1.2D3
      RESTIM=1.03D3
C     RHO=0.015D0
      RHO=0.019D0
      TAU=RESTIM/NTANKS
      INTRVL=10
      C1=XKMAX*RHO/DP
      C2=GAMMA*XKMAX*RHO/DX
C
C     CONVERGENCE CRITERIA:
C
      FACTR1=.0005D0
      FACTR2=.01D0
      FACTR3=.01D0
C
C     THE OUTER LOOP:
C     THE INDEX J CORRESPONDS TO WHICH STIRRED TANK
C     IS BEING CONSIDERED
```

```
C
      DO 100 J=1,NTANKS
      PGUESS(1)=PINLET(J)*.5D0
      PI=PINLET(J)
      XI=XINLET(J)
      I=0
      PMAX=0.D0
      PMIN=0.D0
C
C     THE INNER LOOP CALCULATES THE CONCENTRATIONS OF
C     SUBSTRATE AND OXYGEN LEAVING EACH TANK.  THE
C     BISECTION METHOD IS USED TO ITERATE TO THE PROPER
C     EFFLUENT CONCENTRATIONS (PO AND XO).
C
10    I=I+1
      PIC=PGUESS(I)
      XIC=((PGUESS(I)-PI)*GAMMA+(XI+XKLA*XSTAR*TAU))
     1       /(1.D0+TAU*XKLA)
C     WRITE (5,10050)PIC,XIC
      IF (XIC .LT. 0.D0 .OR. PIC .LT. 0.D0)      GO TO 20
      GO TO 30
20    PMIN=PGUESS(I)
      IF (PMAX .EQ. 0.D0)PGUESS(I)=PGUESS(I)*2.D0
      IF (PMAX .NE. 0.D0)PGUESS(I)=(PMIN+PMAX)/2.D0
      I=I-1
      GO TO 10
C
C     THE SUBSTRATE AND OXYGEN GRADIENTS AT THE PELLET
C     SURFACE (PGRAD AND XGRAD) ARE CALCULATED BY
C     SUBROUTINE "FLOC".
C
C30   RIN=RI
30    CALL FLOC(PIC,XIC,RO,RI,PGRAD,XGRAD)
C     WRITE (5,10060)PGRAD,XGRAD
C
C     THE EFFLUENT CONCENTRATIONS ARE CALCULATED BELOW
C     USING REACTOR MASS BALANCES.
C
      PO(I)=PI-(DP*PGRAD*4.D0*XPI*(RO**2)*XN*TAU)
      XO(I)=(XI-DX*XGRAD*4.D0*XPI*(RO**2)*XN*TAU+
     1       XKLA*XSTAR*TAU)/(1.D0+TAU*XKLA)
C     WRITE (5,10020)PO(I),XO(I)
C     WRITE(5,10030)PO(I),PGUESS(I)
      WRITE (5,10010)RI
C
C     THE MIDPOINT METHOD ITERATES TOWARD THE PROPER
C     SOLUTION BY COMPARING THE PREDICTED AND CALCULATED
C     REACTOR EFFLUENT CONCENTRATIONS.
C
      IF (XO(I) .LT. 0.D0 .OR. PO(I) .LT. 0.D0)GO TO 40
      GO TO 50
```

```
40      PMAX=PGUESS(I)
        IF (PMIN .EQ. 0.D0)PGUESS(I)=PGUESS(I)/2.D0
        IF (PMIN .NE. 0.D0)PGUESS(I)=(PMIN+PMAX)/2.D0
        I=I-1
        GO TO 10
C
C       CHECK THE RESULTS OF THIS ITERATION AGAINST THE
C       CONVERGENCE CRITERIA.
C
50      DELTAP(I)=PO(I)-PIC
        DELTAX(I)=XO(I)-XIC
        PAV=(PO(I)+PIC)/2.D0
        XAV=(XO(I)+XIC)/2.D0
        IF (ABS(DELTAP(I)) .LT. FACTR1*PAV .AND. ABS(DELTAX(I))
        1       .LT. FACTR1*XAV)GO TO 90
        IF (DELTAP(I) .LT. 0.D0)GO TO 60
        GO TO 70
60      PMAX=PGUESS(I)
        IF (PMIN .EQ. 0.D0)PGUESS(I+1)=PGUESS(I)/2.D0
        IF (PMIN .NE. 0.D0)PGUESS(I+1)=(PMIN+PMAX)/2.D0
        GO TO 80
70      PMIN=PGUESS(I)
        IF (PMAX .EQ. 0.D0)PGUESS(I+1)=PGUESS(I)*2.D0
        IF (PMAX .NE. 0.D0)PGUESS(I+1)=(PMIN+PMAX)/2.D0
80      WRITE (5,10040)J,I,PGUESS(I+1)
        IF (I .GT. 40)GO TO 120
        GO TO 10
C
C       OUTPUT THE RESULTS FOR THIS TANK
C
90      WRITE (5,10070)
        PINLET(J+1)=PO(I)
        XINLET(J+1)=XO(I)
100     CONTINUE
C
C       OUTPUT THE FINAL RESULTS FOR ALL TANKS
C
        DO 110 J=1,(NTANKS+1)
        WRITE (5,*) J,PINLET(J),XINLET(J)
C       WRITE (22,*) J,PINLET(J),XINLET(J)
110     CONTINUE
        DO 115 I=1,(INTRVL+1)
        K=(-I+INTRVL+2)
C       WRITE (5,*)R(K),P(K),X(K)
        WRITE (41,*)PDOT(K),XDOT(K)
        WRITE (40,*)P(K),X(K)
 115    CONTINUE
        WRITE (49,*)PINLET(NTANKS+1),XINLET(NTANKS+1)
        GO TO 130
120     WRITE (5,10080)
130     STOP
```

```
10010   FORMAT(4H RI:,D15.9)
10020   FORMAT(7H PO,XO:,2D15.9)
10030   FORMAT(17H PO(I),PGUESS(I):,2D15.9)
10040   FORMAT(17H J,I,PGUESS(I+1):,2I4,D15.9)
10050   FORMAT(/,13H PIC AND XIC:,2D15.9)
10060   FORMAT(13H PGRAD,XGRAD:,2D15.9)
10070   FORMAT(39H THE METHOD HAS CONVERGED FOR THIS TANK)
10080   FORMAT(38H THE BISECTION METHOD DID NOT CONVERGE)
        END
```

FLOCI.FOR

```
C       THIS FILE CALCULATES THE OXYGEN AND SUBSTRATE CONCENTRA-
C       TION PROFILES IN A BIOFILM PARTICLE.  THE PROFILES REP-
C       RESENT THE STEADY-STATE BALANCE BETWEEN MASS TRANSFER
C       AND REACTION WITHIN THE FILM.  KEY VARIABLES ARE THE
C       SUBSTRATE CONCENTRATION AND CONCENTRATION GRADIENT
C       (P AND PDOT), AND THOSE FOR OXYGEN (X AND XDOT); THE
C       ASSUMED INITIAL CONCENTRATION GRADIENTS AT THE PARTICLE
C       SURFACE (PDOTIC AND XDOTIC); THE INNER AND OUTER RADII
C       OF THE FILM (RIN AND RO), THE NUMBER OF STEPS PER ITERATION
C       (N); THE DERIVATIVE OF THE GRADIENTS (P2DOT AND X2DOT); THE
C       MONOD CONSTANTS FOR SUBSTRATE AND OXYGEN(CP AND CO); AND
C       THE LUMPED KINETIC PARAMETERS (C1 AND C2).  THE PROFILE
C       DATA (R(I), P(I), AND X(I)) ARE WRITTEN UNFORMATTED INTO
C       FILE FOR21.DAT.  CI IS THE SUBSTRATE INHIBITION CONSTNT.
C
C
C
        SUBROUTINE FLOC(PIC,XIC,RO,RIN,PGRAD,XGRAD)
        IMPLICIT DOUBLE PRECISION (A-H,O-Z)
        DIMENSION XDOTIC(50),PDOTIC(50),X(50),P(50),XDOT(50),PDOT(50),
        1       XFC(50),PFC(50),R(50),P2DOT(50),X2DOT(50)
        COMMON CP,CX,CI,C1,C2,R,P,PDOT,X,XDOT,INTRVL
C
C       CALCULATE THE INITIAL ESTIMATE OF PDOT
C
        FILM=RO-RIN
        PDOTMX=(C1/3.D0)*(RO-(RIN**3/RO**2))
        XDOTMX=(C2/3.D0)*(RO-(RIN**3/RO**2))
        IF (XIC .GT. CX/2.D0 .AND. PIC .GT. CP/2.D0)GO TO 30
        CLUMP1=SQRT(C1*(FILM**2)/CP)
        CLUMP2=SQRT(C2*(FILM**2)/CX)
        PDOTMN=PIC*(CLUMP1)*DTANH(CLUMP1)/FILM
        XDOTMN=XIC*(CLUMP2)*DTANH(CLUMP2)/FILM
        IF (XIC .LE. CX/2.D0 .AND. PIC .LE. CP/2.D0)  GO TO 20
        IF (XIC .LE. CX/2.D0)  GO TO 10
        PDOTIC(1)=PDOTMN/2.D0
        GO TO 40
10      PDOTIC(1)=(XDOTMN*C1/C2)/2.D0
        GO TO 40
20      PDOTIC(1)=PDOTMN*XDOTMN/XDOTMX
        GO TO 40
30      PDOTIC(1)=PDOTMX/4.D0
C
C       CALCULATE THE CONCENTRATION PROFILES IN THE PELLET
C
40      XDOTIC(1)=PDOTIC(1)*C2/C1
C
C       BELOW ARE THE CONVERGENCE CRITERIA AND OTHER SPECIFICATIONS
C
```

```
C       N=20
        N=INTRVL
        TOL1=1.D-3
        TOL2=1.D-5
        TOL3=1.D-6
        FACTOR=2.D0
C
C       INITIALIZATION OF THE PROCESS FOR EACH ITERATION
C
        M=0
        LOOP = 0
        K1LOOP=0
C
C       THE OUTER LOOP ADJUSTS THE "ACTIVE" FILM THICKNESS BY
C       INCREASING THE INNER RADIUS OF THE PELLET (RIN).
C
50      DELR=-(RO-RIN)/N
        X(1)=XIC
        P(1)=PIC
        R(1)=RO
        PPOS=0.D0
        PNEG=0.D0
        XPOS=0.D0
        XNEG=0.D0
        J=0
        IF (LOOP .EQ. 1)FACTOR=1.05D0
C
C       THE MIDDLE LOOP DETERMINES THE INITAL SLOPE (PDOTIC)
C       WHICH BEST MEETS THE BOUNDARY CONDITION PDOT=0 AT RIN.
C
60      J=J+1
        K1=0
        K2=0
        K1A=0
        K1B=0
        K2A=0
        K2B=0
        XDOT(1)=XDOTIC(J)
        PDOT(1)=PDOTIC(J)
C
C       THE MIDPOINT METHOD IS USED TO CALCULATE THE CONCENTRATION
C       PROFILES IN THE PELLET.  THE INITIAL CONDITIONS PDOTIC
C       AND XDOTIC ARE OBTAINED FROM THE MIDDLE LOOP ABOVE.
C
        DO 70 I=1,(N+1)
                P2DOT(I)=C1*((P(I)/(P(I)+CP+P(I)**2/CI))*(X(I)/(X(I)+CX)))-
     1          2.D0*PDOT(I)/R(I)
                X2DOT(I)=C2*((P(I)/(P(I)+CP+P(I)**2/CI))*(X(I)/(X(I)+CX)))-
     1          2.D0*XDOT(I)/R(I)
                RM=R(I)+DELR/2.D0
                PM=P(I)+(DELR/2.D0)*PDOT(I)
```

```
                XM=X(I)+(DELR/2.D0)*XDOT(I)
                PDOTM=PDOT(I)+(DELR/2.D0)*P2DOT(I)
                XDOTM=XDOT(I)+(DELR/2.D0)*X2DOT(I)
                R(I+1)=R(I)+DELR
                P(I+1)=P(I)+DELR*PDOTM
                X(I+1)=X(I)+DELR*XDOTM
                PDOT(I+1)=PDOT(I)+DELR*(C1*(PM/(PM+CP+PM**2/CI))*
          1     (XM/(XM+CX))-2.D0*PDOTM/RM)
                XDOT(I+1)=PDOT(I+1)*C2/C1
C               XDOT(I+1)=XDOT(I)+DELR*(C2*(PM/(PM+CP+PM**2/CI))*
C         1     (XM/(XM+CX))-2.D0*XDOTM/RM)
                IF (P(I) .LT. 0.D0 .OR. X(I) .LT. 0.D0)K1=K1-1
                IF (PDOT(I) .LT. 0.D0 .OR. XDOT(I) .LT. 0.D0)K2=K2-1
                IF (PDOT(I) .LT. -(TOL2*PIC/(RO-RIN)))K2A=-1
                IF (XDOT(I) .LT. -(TOL2*XIC/(RO-RIN)))K2B=-1
                IF (P(I) .LT. -(TOL1*PIC))K1A=-1
                IF (X(I) .LT. -(TOL1*XIC))K1B=-1
                IF (K1A .LT. K1B)    K1LOOP=-1
                IF (K2 .EQ. -1 .OR. K1 .EQ. -1)RINEW=RIN+0.8*(R(I)-RIN)
C               WRITE (5,*)I,P(I),X(I),PDOT(I),R(I)
70        CONTINUE
          IF (K1LOOP .EQ. -1)    GO TO 110
C
C         COMPARE THE PREDICTED FINAL CONDITIONS WITH THE DESIRED
C         ONES TO EVALUATE THE ACCURACY OF THE ASSUMED INITIAL CONDI-
C         TIONS.
C
          XFC(J)=ABS(XDOT(N+1))
          PFC(J)=ABS(PDOT(N+1))
          IF (K1 .LT. 0)PNEG=PDOTIC(J)
          IF (K1 .EQ. 0 .AND. K2 .LT. 0)PPOS=PDOTIC(J)
          IF (K1 .EQ. 0 .AND. K2 .EQ. 0)PNEG=PDOTIC(J)
          IF (PPOS .EQ. 0.D0)PDOTIC(J+1)=PDOTIC(J)/FACTOR
          IF (PNEG .EQ. 0.D0)PDOTIC(J+1)=PDOTIC(J)*FACTOR
          IF (PNEG .NE. 0.D0 .AND. PPOS .NE. 0.D0)PDOTIC(J+1)=(PPOS+
          1       PNEG)/2.D0
          XDOTIC(J+1)=PDOTIC(J+1)*C2/C1
C         WRITE (5,*)PPOS,PNEG
          IF (ABS(PDOTIC(J+1)-PDOTIC(J)) .LT. TOL3*PDOTIC(J))
          1       GO TO 80
          IF (J .GT. 40)    GO TO 170
          GO TO 60
80        IF (K2A .LT. 0)    LOOP=1
          IF (LOOP .EQ. 0)    GO TO 150
          M=M+1
C         IF (M .GT. 10)GO TO 170
          IF (K2A .EQ. -1)GO TO 90
          GO TO 150
90        RIOLD=RIN
          RIN=RINEW
C 1000    WRITE (5,*)M,RIOLD,RIN
```

```
      XDOTIC(1)=XDOT(1)
C     IF (ABS(RIHIGH-RILOW) .LT. 0.00001D0*RO)GO TO 3000
100   GO TO 50
C
C     THE SECTION BELOW IS IDENTICAL TO THE ONE ABOVE EXCEPT
C     THAT THE CALCULATIONS ARE DONE IN TERMS OF THE OXYGEN
C     CONCENTRATION RATHER THAN SUBSTRATE CONCENTRATION.
C     THIS ALLOWS THE ROUTINE TO COPE WITH CASES IN WHICH THE
C     SUBSTRATE MAY BE DEPLETED BEFORE COMPLETELY PENETRATING
C     THE FILM.
C
C     COMPARE THE PREDICTED FINAL CONDITIONS WITH THE DESIRED
C     ONES TO EVALUATE THE ACCURACY OF THE ASSUMED INITIAL CONDI-
C     TIONS.
C
110   XFC(J)=ABS(XDOT(N+1))
      PFC(J)=ABS(PDOT(N+1))
      IF (K1 .LT. 0)XNEG=XDOTIC(J)
      IF (K1 .EQ. 0 .AND. K2 .LT. 0)XPOS=XDOTIC(J)
      IF (K1 .EQ. 0 .AND. K2 .EQ. 0)XNEG=XDOTIC(J)
      IF (XPOS .EQ. 0.D0)XDOTIC(J+1)=XDOTIC(J)/FACTOR
      IF (XNEG .EQ. 0.D0)XDOTIC(J+1)=XDOTIC(J)*FACTOR
      IF (XNEG .NE. 0.D0 .AND. XPOS .NE. 0.D0)XDOTIC(J+1)=(XPOS+
     1       XNEG)/2.D0
      PDOTIC(J+1)=XDOTIC(J+1)*C1/C2
C     WRITE (5,*)XPOS,XNEG
      IF (ABS(XDOTIC(J+1)-XDOTIC(J)) .LT. TOL3*XDOTIC(J))
     1       GO TO 120
      IF (J .GT. 40)    GO TO 170
      GO TO 60
120   WRITE (5,10010)
      IF (K2B .LT. 0)    LOOP=1
      IF (LOOP .EQ. 0)    GO TO 150
      M=M+1
      IF (M .GT. 10)GO TO 170
      IF (K2B .EQ. -1)GO TO 130
      GO TO 150
130   RIOLD=RIN
      RIN=RINEW
C     WRITE (5,*)M,RIOLD,RIN
      PDOTIC(1)=PDOT(1)
      XDOTIC(1)=XDOT(1)
C     IF (ABS(RIHIGH-RILOW) .LT. 0.001D0*RO)GO TO 150
140   GO TO 50
C150  WRITE (5,10020)
C     DO 160 I=1,(N+1)
C     WRITE (21,*) R(I),P(I),X(I)
C160  CONTINUE
 150  PGRAD=PDOTIC(J)
      XGRAD=XDOTIC(J)
```

```
C       WRITE (5,*)PGRAD,XGRAD
        GO TO 190
170     WRITE (5,10030)
        DO 180 I=1,N+1
C       WRITE (21,*)R(I),P(I),X(I)
180     CONTINUE
190     RETURN
10010   FORMAT(22H SUBSTRATE IS LIMITING)
10020   FORMAT(25H THE METHOD HAS CONVERGED)
10030   FORMAT(28H THE METHOD DID NOT CONVERGE)
        END
```

FILM5I JCL

```
//IMSLJOB JOB ,WORDEN,GROUP=J52011,USER=P83638,
// MSGLEVEL=(0,0),MSGCLASS=H,TIME=(3,00),PASSWORD=?
/*ROUTE CMSRJO USERID=PA83638
/*JOBPARM ROOM=GRAD,LINES=9
/*ROUTE PRINT RMT1
//STEP1 EXEC FORTQCLG,GOREG=500K
//FORT.SYSIN DD *
C       THIS FILE IS A DYNAMIC SIMULATOR OF A PERFECTLY MIXED
C       FLUIDIZED BED BIOREACTOR.  IT COMPRISES THE FOLLOWING
C       DIFFERENTIAL EQUATIONS:
C
C         1)  MASS BALANCE ON SUBSTRATE (P) WITHIN EACH SPHERICAL
C             BIOFILM PARTICLE
C         2)  PARTICLE MASS BALANCE ON OXYGEN (O)
C         3)  MASS BALANCE ON SUBSTRATE IN LIQUID PHASE (PB)
C         4)  MASS BALANCE ON OXYGEN IN LIQUID PHASE (OB)
C         5)  EQUATION DESCRIBING GROWTH OF BIOFILM
C
C       THE FIRST TWO OF THESE EQUATIONS ARE PDE'S, AND THE OTHER
C       THREE ARE ODE'S.  THE SYSTEM IS SOLVED BY THE IMSL ROUTINE
C       'DPDES'.  A DESCRIPTION OF THE OPERATION OF THIS ROUTINE
C       CAN BE OBTAINED BY TYPING 'PRINT FOR:IMSLD.DOC'.
C       THE INITIAL P AND O CONCENTRATION PROFILES ARE READ IN FROM
C       FOR40.DAT, AND THE CONCENTRATION GRADIENTS ARE READ IN
C       FROM FOR41.DAT.  THESE DATA CORRESPOND TO STEADY-STATE
C       VALUES CALCULATED FOR THE CONDITIONS OF INTEREST BY
C       TANKS2.FOR AND FLOC2.FOR.  ALL CONCENTRATION DATA ARE
C       NORMALIZED AFTER BEING READ IN, SINCE THE EQUATIONS BELOW WERE
C       DERIVED DIMENSIONLESS.  THE COEFFICIENTS OF THE BOUNDARY
C       CONDITION EQUATIONS ARE READ IN FROM FOR42.DAT AND FOR43.DAT.
C
C       THE MAIN VARIABLES ARE:
C               U(1):  P (DIMENSIONLESS SUBSTRATE CONC IN THE BIOFILM)
C               U(2):  O (DIMENSIONLESS OXYGEN CONC IN THE FILM)
C               U(3):  PB (DIMENSIONLESS SUBSTRATE CONC IN THE LIQUID)
C               U(4):  OB (DIMENSIONLESS OXYGEN CONC IN THE LIQUID)
C               U(5):  H (DIMENSIONLESS FILM THICKNESS)
C               UT??:  TIME DERIVATIVE OF VARIABLE ??
C               GRAD?:  GRADIENT OF VARIABLE ? AT THE FILM SURFACE
C               ?NORM:  VALUE OF VARIABLE USED TO NORMALIZE (G/CM**3)
C               XK?MAX:  REACTION RATE CONSTANT (G/CM**3 SEC)
C               RI:  RADIUS OF INERT BIOFILM SUPPORT (CM)
C               D?:  DIFFUSIVITY OF ? IN THE BIOFILM (CM**2/SEC)
C               EPS:  VOLUME FRACTION OF THE LIQUID PHASE
C               YXP:  VOL OF FILM PRODUCED PER UNIT OF SUBSTRATE
C                     CONSUMED (CM**3/G)
C               YOP:  MG O CONSUMED PER MG P CONSUMED
C               XK?:  MONOD CONSTANT (G/CM**3)
C               XKI:  SUBSTRATE INHIBITION CONSTANT (G/CM**3)
```

```
C               RESTIM:  RESIDENCE TIME OF FEED IN THE REACTOR (SEC)
C               XKLA:  MASS TRANS COEFF FOR GAS-LIQUID O TRANSFER (1/SEC)
C               ?IN:  CONCENTRATION OF ? IN FEED (G/CM**3)
C               R?:  REACTION RATE OF ? IN FILM (G/CM**3 SEC)
C               EPS0:  INITIAL LIQUID VOLUME FRACTION
C               H0:  INITIAL DIMENSIONLESS FILM THICKNESS
C               T0:  THE TIME AT WHICH THE DESIRED PERTURBATION IN
C                    OPERATING CONDITIONS IS ENACTED
C               DELT:  THE DURATION OF THE PERTURBATION
C
C         OTHER VARIABLES ARE USED AS DESCRIBED IN THE IMSL DOCUMENT
C         MENTIONED ABOVE.
C
C       THE MAIN PROGRAM CONTAINS VALUES OF SOFTWARE PARAMETERS, LISTS
C       THE INITIAL CONDITIONS FOR THE DIFFERENTIAL EQUATIONS, CALLS
C       'DPDES' AND OUTPUTS RESULTS.
C
        IMPLICIT REAL*8(A-H,O-Z)
        REAL*8 Y(5,2,21),X(21),WK(52117),A0(5),A1(5),B0(5),B1(5),
     1  G0(5),G1(5)
        DOUBLE PRECISION PB,OB,P(21),PDOT(21),O(21),ODOT(21)
        EXTERNAL FCN,BNDRY
        COMMON UTPB,UTOB,UTH,GRADP,GRADO,H0,A0,A1,B0,B1,G0,G1,
     1  PNORM,ONORM,RI,DP,DO,XKIBAR,XKPBAR,XKOBAR
        T=0.0D0
        IY=5
        NX=11
        NPDES=5
        PNORM=200.D-6
        ONORM=40.D-6
        RI=0.022D0
C       RI=.02814D0
C
C       NOTE THAT RI IS SPECIFIED BOTH HERE AND IN SBR. FCN
C       IT MUST BE CHANGED IN BOTH PLACES.
C
C       H0=0.4D0
        H0=.682D0
        FACTR=1.D0/(NX-1.D0)
                WRITE (6,5)
 5              FORMAT (/,19H INITIAL CONDITIONS)
                WRITE (6,35)
        DO 7 I=1,NX
                X(I)=(FACTR*I)-FACTR
C               READ (54,*)P(I),O(I)
        READ (40,*)P(I),O(I)
C               READ (53,*)PDOT(I),ODOT(I)
        READ (41,*)PDOT(I),ODOT(I)
C       WRITE (6,*)P(I),O(I)
                Y(1,1,I)=P(I)/PNORM
                Y(2,1,I)=O(I)/ONORM
```

```
C       WRITE (6,*)Y(1,1,I),Y(2,1,I)
                Y(1,2,I)=PDOT(I)*RI*H0/PNORM
                Y(2,2,I)=ODOT(I)*RI*H0/ONORM
C       READ (41,*)Y(1,2,I),Y(2,2,I)
C       READ (40,*)Y(1,1,I),Y(2,1,I)
 7      CONTINUE
        DO 10 I=1,NX
                Y(3,1,I)=Y(1,1,NX)
                Y(4,1,I)=Y(2,1,NX)
                Y(5,1,I)=H0
                Y(3,2,I)=0.D0
                Y(4,2,I)=0.D0
                Y(5,2,I)=0.D0
        WRITE (6,37)X(I),Y(1,1,I),Y(2,1,I),
     1  Y(5,1,I)
 10     CONTINUE
        DO 12 I=1,5
                READ (42,*)A0(I),B0(I),G0(I)
                READ (43,*)A1(I),B1(I),G1(I)
 12     CONTINUE
        H=0.0001D0
        TOL=1.D-4
        INDEX=1
        GRADP=Y(1,2,NX)
        GRADO=Y(2,2,NX)
        UTPB=0.D0
        UTOB=0.D0
 15     DO 20 I=1,14
                IF (I .EQ. 1)TEND=5.D-1
                IF (I .EQ. 2)TEND=1.D0
                IF (I .EQ. 3)TEND=2.D0
                IF (I .EQ. 4)TEND=4.D0
                IF (I .EQ. 5)TEND=8.D0
                IF (I .EQ. 6)TEND=12.D0
                IF (I .EQ. 7)TEND=16.D0
                IF (I .EQ. 8)TEND=20.D0
                IF (I .EQ. 9)TEND=25.D0
                IF (I .EQ. 10)TEND=30.D0
               IF (I .EQ. 11)TEND=35.D0
               IF (I .EQ. 12)TEND=40.D0
               IF (I .EQ. 13)TEND=50.D0
               IF (I .EQ. 14)TEND=60.D0
                CALL DPDES(NPDES,FCN,BNDRY,T,H,TEND,X,Y,IY,NX,TOL,
     1           INDEX,WK,IER)
                H=Y(5,1,NX)
                RATE=.9D0*PNORM*1.D6*DP*3.D0*GRADP*60.D0/(RI**2*H*
     1  (1.D0+H))
                PBULK=Y(3,1,NX)*PNORM*1.D6
                OBULK=Y(4,1,NX)*ONORM*1.D6
                WRITE (6,30)TEND
 30             FORMAT (/,/,7H TIME= ,F10.6)
```

```
                WRITE (6,18)
 18             FORMAT (/,9X,6H PBULK,20X,6H OBULK)
                WRITE (6,*) PBULK,OBULK
                WRITE (6,25)RATE
 25             FORMAT (10H DEG. RATE,F12.6)
               WRITE (6,32)Y(5,1,NX)
 32            FORMAT (15H FILM THICKNESS,F12.6)
               WRITE (6,33)GRADP
               WRITE (6,34)GRADO
 33            FORMAT (6H GRADP,F12.6)
 34            FORMAT (6H GRADO,F12.6)
               WRITE (6,36)
 35             FORMAT(6X,2H X,9X,2H P,8X,2H O,
     1  8X,2H H)
 36           FORMAT (6X,2H X,9X,2H P,9X,2H O,
     1  7X,6H PFRAC,5X,6H OFRAC)
                DO 40 K=1,NX
                PFRAC=Y(1,1,K)/(XKPBAR+Y(1,1,K)+Y(1,1,K)**2/XKIBAR)
                OFRAC=Y(2,1,K)/(XKOBAR+Y(2,1,K))
C                       WRITE (6,37)X(K),Y(1,1,K),Y(2,1,K),Y(3,1,K),
C    1  Y(4,1,K),Y(5,1,K)
                 WRITE (6,37)X(K),Y(1,1,K),Y(2,1,K),PFRAC,OFRAC
 37             FORMAT (6F11.6)
 40             CONTINUE
 20     CONTINUE
 50     STOP
        END
C
C       SUBROUTINE FCN EVALUATES THE TIME DERIVATIVES FOR EACH
C       DEPENDENT VARIABLE.  IT ALSO CONTAINS ALL VALUES OF THE
C       MODEL PARAMETERS.
C
        SUBROUTINE FCN(NPDES,X,T,U,UX,UXX,UT)
        IMPLICIT REAL*8 (A-H,O-Z)
        REAL*8 U(5),UX(5),UXX(5),UT(5),A0(5),A1(5),B0(5),B1(5),
     1  G0(5),G1(5)
        COMMON UTPB,UTOB,UTH,GRADP,GRADO,H0,A0,A1,B0,B1,G0,G1,
     1  PNORM,ONORM,RI,DP,DO,XKIBAR,XKPBAR,XKOBAR
        T0=0.0D0
C       DELT=5.D-4
C       DELT=2.8D-4
        DELT=8.6D-4
C       DELT=8.6D-4
C       XKPM=1.58D-4
C       RI=0.02814D0
        RI=0.022D0
        XKPM=1.333D-4
        RHO=0.019D0
        XKPMAX=XKPM*RHO
        XKP=1.D-6
C       XKO=5.D-7
```

```
      XKO=1.D-7
      XKI=80.D-6
C     XKI=1.D6
      DPW=1.1D-5
      DOW=2.6D-5
      FRAC=0.25D0
      DP=DPW*FRAC
      DO=DOW*FRAC
      EPS0=0.95D0
      YOP=1.4D0
      YXP=.4D0
C     YXP=0.D0
      GAM=DO/DP
      RESTIM=1.03D3
      SIG=RI**2/(RESTIM*DP)
      XKLA=1.D-2
      XKPBAR=XKP/PNORM
      XKOBAR=XKO/ONORM
      XKIBAR=XKI/PNORM
      XKLBAR=XKLA*RI**2/DP
      YXPBAR=YXP*PNORM
      PIN=65.D-6
      OIN=8.D-6
      PINBAR=PIN/PNORM
      OINBAR=OIN/ONORM
      IF (T .GT. T0 .AND. T .LE. (T0+DELT))PINBAR=1.D3/SIG
 55   EPS=1.D0-(1.D0-EPS0)*(((1.D0+U(5))/(1.D0+H0))**3)
      RP=XKPMAX*(U(1)/(XKPBAR+U(1)+U(1)**2/XKIBAR))*(U(2)/(XKOBAR
     1 +U(2)))
      IF (U(1) .LE. 0.D0 .OR. U(2) .LE. 0.D0)RP=0.D0
      RO=RP*YOP
      RPBAR=RP*(RI**2)/(PNORM*DP)
      ROBAR=RO*(RI**2)/(ONORM*DP)
 57   UT(1)=UXX(1)/U(5)**2+UX(1)*(UTH*X/U(5)+
     1 2.D0/(U(5)*(1.D0+X*U(5))))-RPBAR
      UT(2)=UXX(2)*GAM/U(5)**2+UX(2)*(UTH*X/U(5)+
     1 2.D0*GAM/(U(5)*(1.D0+X*U(5))))-ROBAR
      UT(3)=SIG*(PINBAR-U(3))-3.D0*(1.D0-EPS)*GRADP/
     1 ((1.D0+U(5))*EPS*U(5))
      UT(4)=SIG*(OINBAR-U(4))+XKLBAR*(1.D0-U(4))-3.D0*GAM*
     1 (1.D0-EPS)*GRADO/(EPS*U(5)*(1.D0+U(5)))
      UT(5)=YXPBAR*GRADP/U(5)
      UTPB=UT(3)
      UTOB=UT(4)
      UTH=UT(5)
      IF (X .GT. .99D0)GRADP=UX(1)
      IF (X .GT. .99D0)GRADO=UX(2)
C     IF (X .GT. .99D0)WRITE (6,*)X,GRADP,GRADO
      RETURN
      END
C
```

```
C
      SUBROUTINE BNDRY(NPDES,X,T,ALPHA,BETA,GAMMAP)
      IMPLICIT REAL*8 (A-H,O-Z)
      REAL*8 ALPHA(5),BETA(5),GAMMAP(5),A0(5),A1(5),B0(5),B1(5),
     1 G0(5),G1(5)
      COMMON UTPB,UTOB,UTH,GRADP,GRADO,H0,A0,A1,B0,B1,G0,G1,
     1 PNORM,ONORM,RI,DP,DO,XKIBAR,XKPBAR,XKOBAR
      IF (X .GT. 0.5)CALL BNDRY1(NPDES,X,T,ALPHA,BETA,GAMMAP)
      IF (X .LT. 0.5)CALL BNDRY0(NPDES,X,T,ALPHA,BETA,GAMMAP)
      RETURN
      END
      SUBROUTINE BNDRY0(NPDES,X,T,ALPHA,BETA,GAMMAP)
      IMPLICIT REAL*8(A-H,O-Z)
      REAL*8 ALPHA(5),BETA(5),GAMMAP(5),A0(5),A1(5),B0(5),B1(5),
     1 G0(5),G1(5)
      COMMON UTPB,UTOB,UTH,GRADP,GRADO,H0,A0,A1,B0,B1,G0,G1,
     1 PNORM,ONORM,RI,DP,DO,XKIBAR,XKPBAR,XKOBAR
      DO 280 I=1,5
              ALPHA(I)=A0(I)
              BETA(I)=B0(I)
              GAMMAP(I)=G0(I)
280   CONTINUE
      GAMMAP(3)=UTPB
      GAMMAP(4)=UTOB
      GAMMAP(5)=UTH
      RETURN
      END
      SUBROUTINE BNDRY1(NPDES,X,T,ALPHA,BETA,GAMMAP)
      IMPLICIT REAL*8 (A-H,O-Z)
      REAL*8 ALPHA(5),BETA(5),GAMMAP(5),A0(5),A1(5),B0(5),B1(5),
     1 G0(5),G1(5)
      COMMON UTPB,UTOB,UTH,GRADP,GRADO,H0,A0,A1,B0,B1,G0,G1,
     1 PNORM,ONORM,RI,DP,DO,XKIBAR,XKPBAR,XKOBAR
      DO 290 I=1,5
              ALPHA(I)=A1(I)
              BETA(I)=B1(I)
              GAMMAP(I)=G1(I)
290   CONTINUE
      GAMMAP(1)=UTPB
      GAMMAP(2)=UTOB
      GAMMAP(3)=UTPB
      GAMMAP(4)=UTOB
      GAMMAP(5)=UTH
      RETURN
      END
//LKED.SYSIN DD *
```

FOR40 DATA

```
//GO.FT40F001 DD *
 1.13206423902744179E-08, 2.12027545465176329E-05
 2.71647064728390506E-08, 2.12121391075511520E-05
 5.13692984716447474E-08, 2.12264756735812138E-05
 9.69998682938092753E-08, 2.12535030110912651E-05
 1.93920616764503737E-07, 2.13109099159546764E-05
 4.36445093956535220E-07, 2.14545590293684182E-05
 1.13221289233872028E-06, 2.18666676484101739E-05
 2.79008549782257324E-06, 2.28486383455044561E-05
 5.73175073888185197E-06, 2.45910092959780289E-05
 1.00207624013272371E-05, 2.71314238960418339E-05
 1.55834960937500000E-05, 3.04262738523230088E-05
```

FOR41 DATA

```
//GO.FT41F001 DD *
 1.89979272387948054E-05, 1.12526184414400001E-05
 2.70211043792642143E-05, 1.60048079784872654E-05
 4.69151579146443959E-05, 2.77882089186739883E-05
 8.63253962495423524E-05, 5.11311962401135472E-05
 1.67286508568752348E-04, 9.90850858445686985E-05
 3.52328768547164963E-04, 2.08687039831782324E-04
 7.88069007560567000E-04, 4.66779335247412761E-04
 1.52814260747242760E-03, 9.05130621349053270E-04
 2.40660977289816226E-03, 1.42545348087044996E-03
 3.28180947893713020E-03, 1.94384099906276173E-03
 4.08871835147736137E-03, 2.42177933125966789E-03
```

FOR42.DATA

```
//GO.FT42F001 DD *
 0.00000000000000000E+00, 1.0000000000000000, 0.00000000000000000E+00
 0.00000000000000000E+00, 1.0000000000000000, 0.00000000000000000E+00
 1.0000000000000000, 0.00000000000000000E+00, 0.00000000000000000E+00
 1.0000000000000000, 0.00000000000000000E+00, 0.00000000000000000E+00
 1.0000000000000000, 0.00000000000000000E+00, 0.00000000000000000E+00
```

FOR43 DATA

```
//GO.FT43F001 DD *
 1.0000000000000000, 0.00000000000000000E+00, 0.00000000000000000E+00
 1.0000000000000000, 0.00000000000000000E+00, 0.00000000000000000E+00
 1.0000000000000000, 0.00000000000000000E+00, 0.00000000000000000E+00
 1.0000000000000000, 0.00000000000000000E+00, 0.00000000000000000E+00
 1.0000000000000000, 0.00000000000000000E+00, 0.00000000000000000E+00
```

ORTIN5.FOR

```
*       1-COLLOCATION POINT, TWO EQUATION MODEL OF THE PMFBBR
*       WITH INHIBITION KINETICS
*
INITIAL
CONSTANT h=.682,X1=0.654654,XKMAX=1.76,SIG=0.14666,...
XK=5.E-3,CBIN=0.5,A12=2.29129,A22=3.5,EPS=0.95,XKI=1.81
IC1=0.073
IC2=0.65
GAMMA=3.*(1.-EPS)/(2.*EPS)
DYNAMIC
C1=INTGRL(IC1,DC1DT)
CB=INTGRL(IC2,DCBDT)
DC1DT=A12*(CB-C1)*2./(h*(1.+h*X1))+A22*(CB-C1)/h**2-...
XKMAX/(XK/C1+1.+C1/XKI)
DCBDT=(SIG*(CBIN-CB)+GAMMA*(A22*(CB-C1)/h**2-XKMAX/(XK/CB+1.+CB/...
XKI)))/(1.+GAMMA)
*DCBDT=SIG*(CBIN-CB)-3*(1-EPS)*A22*(CB-C1)/(h*EPS*(1+h))
TIMER FINTIM=400.,OUTDEL=5.,PRDEL=5.
RELERR C1=1.0E-6
ABSERR C1=1.0E-6,CB=1.E-6
PRTPLT CB
PRINT C1,CB
END
STOP
ENDJOB
```

POLES3.FOR

```
C       THIS FILE DETERMINES WHETHER THE POLES OF A
C       TRANSFER FUNCTION ARE REAL OR COMPLEX.  TO USE
C       IT, THE VALUES OF THE PARAMETERS AND THE STEADY-
C       STATE VALUES OF THE DEPENDENT VARIABLES MUST BE
C       INPUT AT THE TOP OF THE FILE.
C
        IMPLICIT REAL(A-H,O-Z)
C
        CB=.13
        C1=.0178
        XK=0.005
        XKI=04.
        XKMAX=1.76
        CBIN=.5
        SIG=0.14666
        EPS=0.95
        h=.682
C
C       EVALUATE THE PARTIAL DERIVATIVES
C
        A12=2.29129
        A22=3.5
        X1=.654654
        BETA=3.*(1.-EPS)*A22/h*EPS*(1.+h)
        DF1DC1=-A12*2./(h*(1+h*X1))-A22/h**2+XKMAX*(1./XKI-
     1       XK/C1**2)/(XK/C1+1.+C1/XKI)**2
        DF1DC2=A12*2./(h*(1.+h*X1))+A22/h**2
        DF2DC1=BETA
        DF2DC2=-SIG-BETA
C
C       CALCULATE THE VALUE OF THE RADICAL
C
        RAD=(DF1DC1+DF2DC2)**2-4.*(DF1DC1*DF2DC2-DF2DC1*DF1DC2)
C
C       OUTPUT THE RESULTS
C
        WRITE (5,*)RAD
        WRITE (5,*)DF1DC1,DF1DC2
        WRITE (5,*)DF2DC1,DF2DC2
        WRITE (5,100)XK
 100    FORMAT(X,'KX=    ',G15.6)
        WRITE (5,200)XKI
 200    FORMAT(X,'KI=    ',G15.6)
        WRITE (5,300)XKMAX
 300    FORMAT(X,'KMAX=    ',G15.6)
        WRITE (5,400)SIG
 400    FORMAT(X,'SIGMA=    ',G15.6)
        WRITE (5,500)EPS
 500    FORMAT(X,'EPS=    ',G15.6)
        WRITE (5,600)h
 600    FORMAT(X,'h=    ',G15.6)
        WRITE (5,700)C1
 700    FORMAT(X,'C1SS=    ',G15.6)
        WRITE (5,800)CB
 800    FORMAT(X,'CBSS=    ',G15.6)
        STOP
        END
```

```
    THESIS.FOR
C       A DISPLA FILE TO PLOT DATA WHICH ARE STORED UNFORMATTED
C       IN TABULAR FORM IN FOR40.DAT.  MULTIPLE CURVES MAY BE
C       CREATED ON THE SAME PAGE.
C       TO EXECUTE, USE EX DISPLA.FOR,@SYS:DIS90
C
C
C       INITIALIZATION
C
        IMPLICIT REAL (A-H,O-Z)
        DIMENSION Y1(100),Y2(100),Y3(100),Y4(100),Y5(100),
        1 X1(100),X2(100),X3(100),X4(100),X5(100)
C
        N1=6
        N2=7
        N3=10
        N4=10
        N5=10
C
        XMAX=100.
        YLMAX=35.
        YRMAX=60.
C
C       READ IN THE DATA (UP TO FIVE SETS)
C
        DO 100 I=1,N1
C       READ (40,*)X1(I),Y1(I),Y2(I)
        READ (11,*)X1(I),Y1(I)
 100    CONTINUE
C
        DO 200 I=1,N2
C       READ (12,*)X2(I),Y2(I),Y3(I)
 200    CONTINUE
C
        DO 300 I=1,N3
C       READ (13,*)X3(I),Y3(I)
 300    CONTINUE
C
        DO 400 I=1,N4
C       READ (14,*)X4(I),Y4(I)
 400    CONTINUE
C
        DO 500 I=1,N5
C       READ (15,*)X5(I),Y5(I)
 500    CONTINUE
C
C       BELOW ARE THE OUTPUT DEVICE OPTIONS. THEY ARE:
C               DIRECT TO TEKTRONIX 4025 TERMINAL
C               ROUGH PLOT TO FOR20.DAT DATA FILE
C               COMPRESSED DATA FILE (.DMF EXTENSION)
C
```

```
C       CALL PRTPLT(80,5)
        CALL COMPRS
C
C       THE PLOTTING DIMENSIONS, LABELS, ETC:
C
        CALL PAGE (8.,10.5)
C       CALL PAGE (10.5,8.)
        CALL NOBRDR
        CALL AREA2D(6.,7.)
C       CALL AREA2D(8.,5.)
        CALL HEIGHT(.20)
        CALL DUPLX
C
C       NAME THE LEFT AXIS
C
C       CALL YNAME ('SPECIFIC REACTION RATE (MG/G CELLS MIN)$',100)
C       CALL YNAME ('PHENOL CONCENTRATION (mg/L)$',100)
C       CALL YNAME ('OD (400 nm)$',100)
C       CALL YNAME ('COLOR YIELD (ODU/ml cells)$',100)
        CALL YNAME ('REACTION RATE (mg/L min)$',100)
C       CALL YNAME ('ln[OD(490nm or 560nm)]$',100)
C
C       NAME THE X AXIS
C
C       CALL XNAME ('SAMPLE VOLUME (ml)$',100)
C       CALL XNAME ('DRY WEIGHT (g/L)$',100)
C       CALL XNAME ('TIME (min)$',100)
C       CALL XNAME ('INT CONCENTRATION (%)$',100)
        CALL XNAME ('PERCENT OXYGEN SATURATIONS',100)
C
C       SCALE THE AXES
C
        CALL GRAF(0.0,'SCALE',XMAX,0.0,'SCALE',YMAX)
C
C       THE TYPE OF INTERPOLATION DESIRED:
C               SMOOTHED
C               LINEAR
C
        CALL RASPLN(10.)
C       CALL LINEAR
C
C       FIRST PLOT--IS INTERPOLATION DESIRED?
C               YES--WITH POINTS DRAWN IN
C               YES--WITHOUT POINTS DRAWN IN
C               NO
C       CALL CURVE (X1,Y1,N1,1)
C       CALL CURVE (X1,Y1,N1,0)
        CALL CURVE (X1,Y1,N1,-1)
```

```
C
C       CALL CURVE (X1,Y3,N1,-3)
C       CALL CURVE (X1,Y2,N1,1)
C       CALL CURVE (X2,Y4,N2,1)
C       CALL CURVE (X1,Y1,N1,0)
C
C       NAME THE RIGHT AXIS
C
C       CALL YGRAXS(-1.5,'SCALE',YRMAX,7.,'ln[DRY WEIGHT (mg/L)]$'
C       1 ,-100,5.30,0.)
C       CALL YGRAXS(0.0,'SCALE',YRMAX,7.,'REACTION RATE (mg/L min)$'
C       1 ,-100,5.3,0.)
C       CALL YGRAXS(0.0,'SCALE',YRMAX,5.,'PHENOL CONCENTRATION
C       1 (mg/L)$',-100,8.0,0.)
C
C       THE TYPE OF INTERPOLATION DESIRED:
C               SMOOTHED
C               LINEAR
C
        CALL RASPLN(10.)
C       CALL LINEAR
C
C       FIRST PLOT--IS INTERPOLATION DESIRED?
C               YES--WITH POINTS DRAWN IN
C               YES--WITHOUT POINTS DRAWN IN
C               NO
C       CALL CURVE (X2,Y3,N2,1)
C       CALL CURVE (X1,Y2,N1,0)
C       CALL CURVE (X1,Y3,N1,-1)
C
C       CREATE THE OTHER PLOTS
C
C       CALL CURVE(X2,Y3,N2,1)
C       CALL CURVE(X4,Y4,N4,-1)
C       CALL CURVE(X5,Y5,N5,-1)
C
C       END THE PROGRAM
C
        CALL ENDPL(0)
        CALL DONEPL
        STOP
        END
```

```
    3DPLOT.FOR
C       A DISPLA PROGRAM FOR 3-DIM. PLOTS.  IT READS DATA FROM
C       FOR51.DAT.
C
        DIMENSION Y(11),X(11),Z(11,11)
        NX=11
        NY=11
        XMAX=1.0
        YMAX=20.
        ZMAX=0.8
C
C       READ IN THE DATA MATRIX
C
        DO 100 I=1,NY
               DO 50 J=1,NX
                      READ (51,25)Y(I),X(J),Z(J,I)
 25                   FORMAT ( 2F4.1,2X,F4.3)
 50            CONTINUE
 100    CONTINUE
C
C       BELOW ARE THE OUTPUT DEVICE OPTIONS. THEY ARE:
C              DIRECT TO TEKTRONIX 4025 TERMINAL
C              ROUGH PLOT TO FOR20.DAT DATA FILE
C              COMPRESSED DATA FILE (.DMF EXTENSION)
C
C       CALL TEKALL (4025,240,0,0,0)
C       CALL PRTPLT(80,5)
        CALL COMPRS
C
C       THE PLOTTING DIMENSIONS, LABELS, ETC:
C
        CALL PAGE (8.,10.5)
        CALL NOBRDR
        CALL AREA2D(6.,7.)
        CALL HEIGHT(.20)
        CALL DUPLX
        CALL VOLM3D(.9,.9,1.)
        CALL X3NAME('   RADIAL POSITION$',100)
        CALL Y3NAME('TIME$',100)
        CALL Z3NAME('CONCENTRATION$',100)
        CALL VUABS(4.8,6.,2.)
        CALL GRAF3D(0.,0.2,XMAX,0.,4.,YMAX,0.,0.2,ZMAX)
        CALL SURMAT (Z,0,11,0,11,0)
C
C       END THE PROGRAM
C
        CALL ENDPL(0)
        CALL DONEPL
        STOP
        END
```

APPENDIX 6

NOMENCLATURE

A_s Total surface area of biofilm particles (cm^2)

D_o Effective diffusivity of oxygen in the biofilm (cm^2/s)

D_p Effective diffusivity of phenol in the biofilm (cm^2/s)

F Volumetric flow rate of fresh feed (cm^3/s)

h Dimensionless biofilm thickness

h_o Initial dimensionless biofilm thickness

K_I Phenol inhibition constant (g/cm^3)

K_La Volumetric oxygen-transfer coefficient (s^{-1})

K_{max} Maximum specific phenol degradation rate (g phenol/g cells•s)

K_o Monod constant for oxygen (g/cm^3)

K_p Monod constant for phenol (g/cm^3)

m Mass of biofilm (g)

N_o Mass flux of oxygen ($g/cm^2•s$)

N_p Mass flux of phenol ($g/cm^2•s$)

O Oxygen concentration in the biofilm (g/cm^3)

O_b Oxygen concentration in the bulk liquid (g/cm^3)

O_{in} Oxygen concentration in the feed (g/cm^3)

O* Liquid-phase oxygen concentration in equilibrium with the gas phase (g/cm^3)

P Phenol concentration in the biofilm (g/cm^3)

P_b Phenol concentration in the bulk liquid (g/cm^3)

P_{in} Phenol concentration in the feed (g/cm^3)

r Radial position (cm)

r_i Inner radius of the biofilm (cm)

r_o Outer radius of the biofilm (cm)

R_o Oxygen consumption rate within the biofilm ($g/cm^3•s$)

R_p Phenol degradation rate within the biofilm ($g/cm^3 \cdot s$)

t Time (s)

V_{bed} Total volume of settled bed of bioparticles (cm^3)

V_f Volume of biofilm (cm^3)

V_ℓ Volume of liquid phase (cm^3)

V_s Volume of solid phase (cm^3)

$V_{s,o}$ Initial volume of solid phase (cm^3)

V_T Total wetted volume of reactor (cm^3)

X Concentration of active cells within the biofilm (g/cm^3)

$Y_{o/p}$ Stoichiometric coefficient (g oxygen/g phenol)

$Y_{x/p}$ Yield coefficient (g biomass/g phenol)

Greek Symbols

α Fraction of total wetted volume contained within the stirred tank

ε_g Volume fraction of gas phase

ε_ℓ Volume fraction of liquid phase

ε_s Volume fraction of solid phase

$\varepsilon_{s,o}$ Initial volume fraction of solid phase

τ Mean liquid-residence time (s)

PART II

DEVELOPMENT OF AN ACTIVE-BIOMASS ASSAY FOR BIOLOGICAL FIXED FILMS

CHAPTER I

INTRODUCTION

The concentration of active cells within a fixed-film bioreactor is a fundamental system parameter. It expresses the amount of "biological catalyst" available to carry out a desired chemical reaction and is important to the rational design, optimization and control of biofilm reactors.

Under a given set of environmental conditions, cells typically exhibit behavior which is characteristic of their species. This behavior may be described in terms of kinetic constants such as the specific growth rate, specific substrate-consumption and product-formation rates, etc. These constants are normalized on a per-unit-quantity-of-active-cells basis.

In chemostat culture, where all cells are exposed to conditions which encourage growth, virtually all of the cells remain viable, and dry weight is a suitable basis for normalization. However, in fixed-film systems, where the penetration depth of an essential nutrient may be less than the biofilm thickness, cell death from starvation can result. If the proportion of dead cells becomes significant, biomass assays which are not specific for viable cells will overestimate the active-cell concentration. Therefore, biomass-assay techniques which are specific to active cells need to be developed to enhance the accuracy of biofilm analysis and modeling. For the purposes of this study, an "active" cell may be loosely defined as one capable of

exhibiting metabolic activity in the presence of suitable environmental conditions.

The features desired in such an assay should be considered in the development of a methodology. As mentioned previously, the assay should be specific to active cells. It should measure some quantity which would serve as a suitable normalization basis, such as viable-cell number, viable-cell mass, enzyme-activity level, or the concentration of a particular intracellular component. Ideally it should also be quick to perform, inexpensive, sensitive, and should not require highly specialized or expensive laboratory equipment.

A primary objective of this study was to develop a methodology for determining the active-cell concentration in a biological fixed film. A second objective was to evaluate the suitability of the assay for applications such as process analysis and control of biofilm reactors.

CHAPTER II

REVIEW OF ACTIVE-CELL ASSAY TECHNIQUES

A description of several biomass-assay methodologies that have been used in suspended-cell systems is given below. A comparison of their relative merits can aid in choosing the one best suited for adaptation to fixed-film systems. Assays which are not specific for viable organisms, such as carbon, nitrogen, and protein assays are not included.

Adenosine Triphosphate

Adenosine triphosphate (ATP) is an energy-storage compound which is found in all living cells.[1] Its primary role is to energetically couple chemical reactions by transferring chemical energy from exergonic reactions to endergonic ones which may occur in different parts of the cell. The energy is stored in reversible pyrophosphate linkages that can be hydrolyzed when energy is needed. The chemical structure of ATP is shown in Figure 1.

Several methods for estimating viable biomass have been developed based upon ATP.[2] When organisms die, their reserves of ATP are consumed and not replenished. Thus the presence of ATP is indicative of life, and its measurement may be useful in quantifying the active biomass present.[3]

DeSha and Bostick,[4] using the luciferin-luciferase technique,[5] monitored the adenosine phosphate levels of a mixed culture for denitrification following the addition of toxic concentrations of

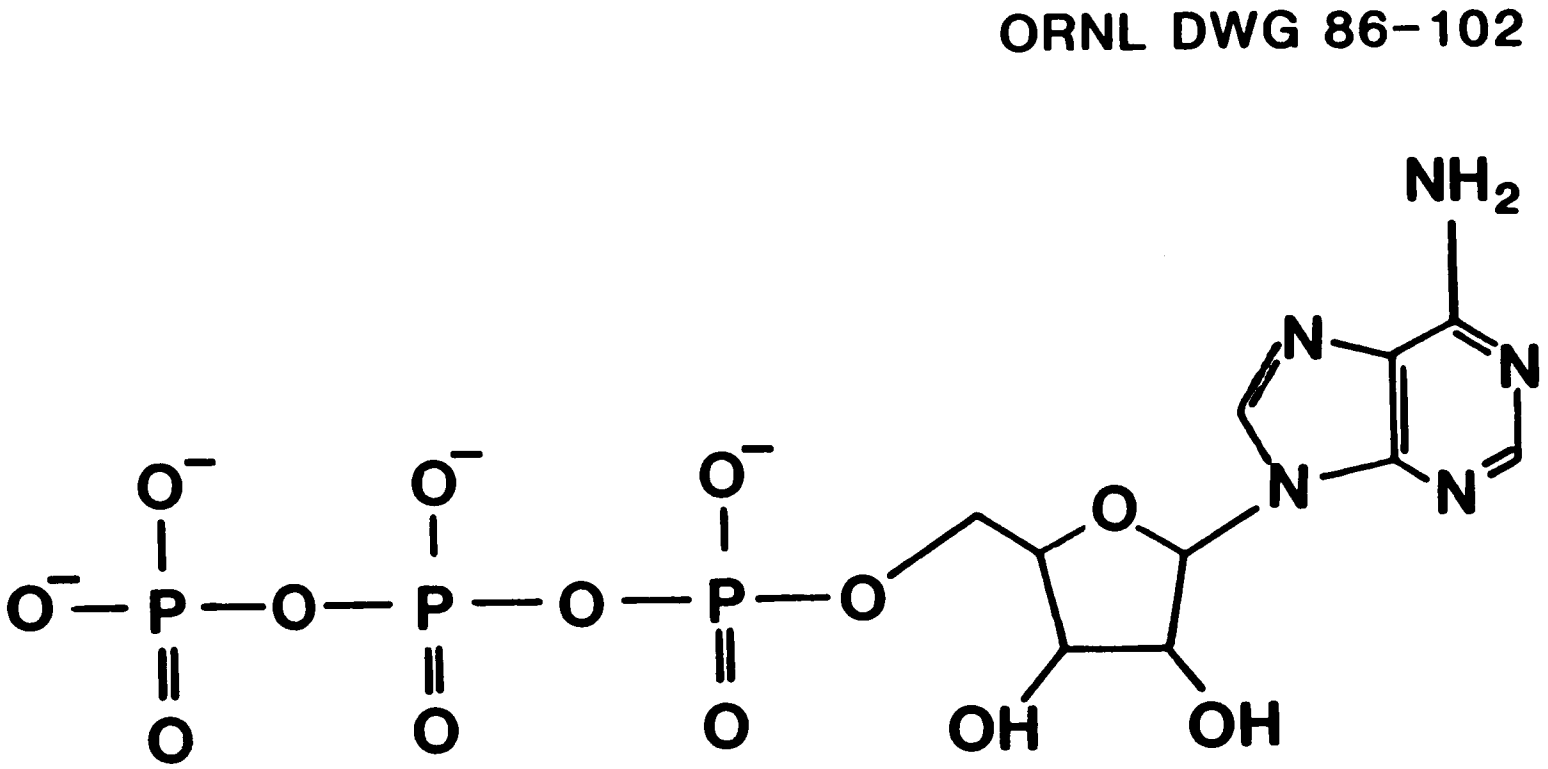

Figure 1. Chemical structure of ATP.

nickel ions. The resulting drop in adenosine phosphate levels paralleled a similar drop in the observed denitrification activity. This trend has also been noted by Patterson et al.[5] after adding toxic heavy-metal ions to activated-sludge systems.

The effects of short-term cell starvation on the ATP content of cells was investigated by Strange.[6] After 40 hours of starvation, Aerobacter aerogenes cells maintained virtually 100% viability via endogenous respiration, although starvation decreased the production rate of ATP. Forrest[7,8] found that a critical ATP concentration was required for exponential growth of Streptoccocus faecalis, and that lower levels of ATP provided only a linear growth rate.

DeSha and Dozier[9] found that in batch denitrification the luciferin-based ATP assay better reflected the eventual decline in active-cell concentration than did the standard mixed-liquor volatile suspended solids (MLVSS) assay. Franco et al.[19] have reported that at the end of a batch-growth cycle of Saccharomyces cerevisiae the ATP concentration declines.

Statham and Langton[3] have used the luciferin-luciferase method to measure the ATP content of activated sludge and have correlated these measurements with the solids retention time. They concluded that ATP measurements could successfully be used for the practical control and monitoring of the activated sludge process. NASA has developed an ATP-based on-line sensor[11] which automatically analyzes aqueous streams for microbial contamination. It uses the luciferase reaction and is linear with cell number above a concentration of 10^6 cells/mL.

Nucleic Acids

The nucleic acids (RNA and DNA) are information-storage polymers composed of nucleotides. Each nucleotide contains phosphate, a sugar molecule, and a ring-shaped organic molecule having several nitrogen atoms.[12] Assays specific to nucleic acids have been tested as indicators of active biomass in free-cell culture.

Koliander et al.[13] selectively hydrolyzed the RNA content of several species of cells and measured the resulting guanylic acid (a nucleotide) concentration using high-pressure liquid chromatography. This parameter was then used to calculate the RNA concentration. An excellent correlation was observed between RNA concentration and mycelial dry weight for Penicillium chrysogenum. However, the authors pointed out that the RNA content of a cell can vary with the metabolic state of the cell. A similar observation has been made by others. Ataai and Shuler[14] reported that Escherichia coli cells responded to an increase in growth-limiting substrate concentration by increasing the components of the protein biosynthetic machinery, including the RNA content. Karl[15] cites that the rate of RNA synthesis is proportional to the rate of protein synthesis and that the concentration of ribosomal RNA is directly related to the rate of protein synthesis.

Because the RNA content is strongly affected by the physiological state of the cell, it is not an ideal indicator of active-cell concentration. Preferably the method should be independent of growth rate, substrate concentration, etc.

DNA concentration is less affected by the physiological state. Intracellular DNA concentration has been reported to be a characteristic of each species and not significantly affected by the environmental condition.[16] Solomon et al.[17] found that DNA measurement was a satisfactory indicator of Candida utilis concentration in a solids-containing medium. Their analytical technique included reacting the hydrolyzed DNA nucleotides with diphenylamine to obtain colored complexes and then measuring the color formed.

Fluorometry has also been used to quantify the DNA content of a free-cell suspension. Tharakan and Chan[18] have employed ethidium bromide to stain the DNA of lysed H1 fibroblast cells. The induced fluorescence of the stained DNA was linear with the number of cells in the sample in the range of 0.5×10^6 to 8×10^6 cells/mL.

Flow microfluorometry can rapidly estimate both the protein and the DNA content of suspended cells. Rates on the order of 10^4 cells/s can be processed with this technique. Bailey et al.[19] measured the protein and DNA distributions of Bacillis subtilis at several intervals during batch culture. They found that during the exponential-growth phase the cells contained somewhat more protein and more DNA than during the stationary phase. Boye et al.[20] used fluorescence to measure the DNA content and light scattering to measure protein in Escherichia coli cells with a microscope-based flow cytometer. They reported that the presence of antibiotics strongly affected both parameters. Also, during batch growth the amount of DNA per cell varied; at higher cell concentrations, greater DNA content was observed.

Electron-Transport Activity

The electron-transport system (ETS) is a sequence of oxidation-reduction reactions through which electrons are transferred from Krebs-cycle intermediates through a sequence of intermediate carriers that include the cytochromes, and finally to the terminal electron acceptor (typically oxygen). ATP is formed as a result of this process. The ETS is common to virtually all bacteria,[21] and its activity can be measured using artificial electron acceptors such as 2-(p-iodophenyl)-3-(p-nitrophenyl)-5-phenyl tetrazolium chloride (INT). INT, a water-soluble, organic salt, has a low redox potential which allows it to successfully compete with the cytochromes for electrons. Its reduced form (INT-formazan) is an insoluble red dye which precipitates intracellularly. The chemical structure of INT is shown in Figure 2, and its interaction with the ETS is depicted in Figure 3. Since the formation of the red product requires an active ETS, dead cells are not detected.

INT-based techniques have been developed to visually distinguish between living and dead cells.[21-26] These techniques require microscopic inspection of the INT-treated cells. Both the total cell concentration and the concentration of living cells can be measured using these methods.

Alternatively, the red formazan may be extracted from cells using an organic solvent, and the red color can then be measured spectrophotometrically. This method was used by Arcuri[27] to estimate the concentration of Zymomonas mobilis cells trapped within porous

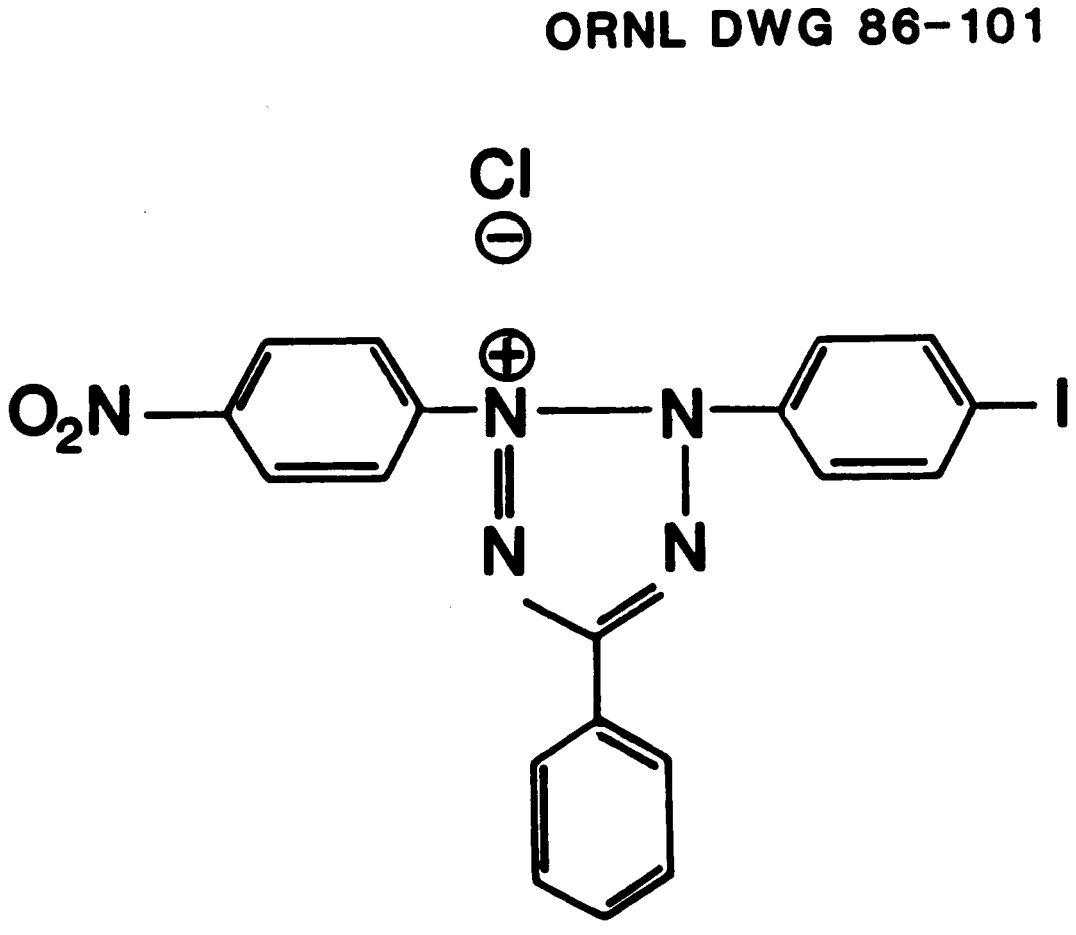

Figure 2. Chemical Structure of INT.

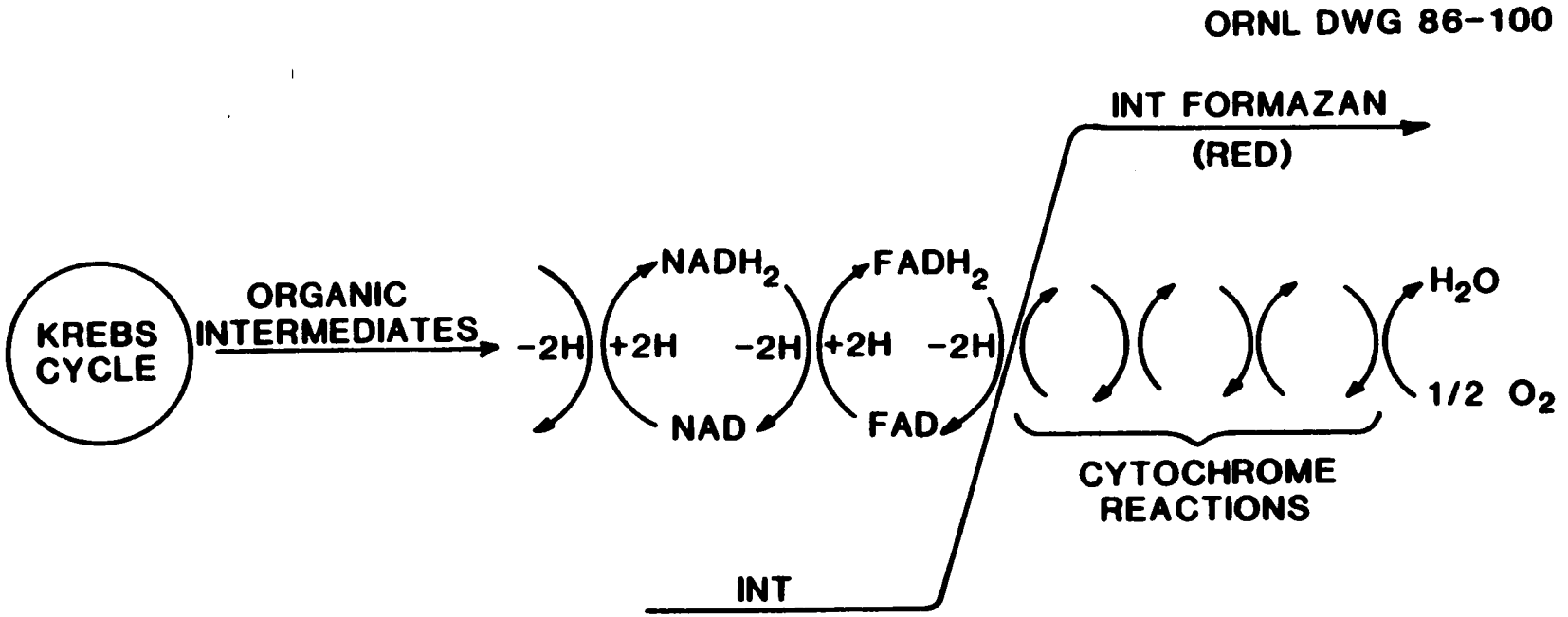

Figure 3. Interaction of INT with the electron-transport system.

glass-fiber pads. He found that the cell concentrations measured with INT and dry-weight methods were in reasonable agreement over two orders of magnitude.

A third approach to quantifying the red color produced has been used by DeSha and Bostick[2] and DeSha and Dozier[9] in studying mixed-culture denitrification in stirred-tank reactors. They incubated a sample of the suspended-cell culture with an equal volume of INT solution and then directly measured the absorbance of the mixture at 490 nm; this wavelength corresponds to the maximum absorptivity of INT-formazan. They found that this INT method was a faster, easier, and more accurate indicator of active biomass than the volatile suspended solids (MLVSS) method.

Comparison of Active-Cell Assays

Relative merits of the various techniques can now be compared. RNA-based methods are unattractive due to the large fluctuations in RNA concentration which follow changes in substrate concentration. Ideally, the assay response should be relatively independent of growth rate.

Although the DNA content of cells is reported to be less transient than the RNA concentration, it is uncertain how long after cell death DNA remains intact. Cell death would eventually result in lysis, and the DNA would likely be utilized as a carbon and energy source by other organisms. If this process is relatively slow, however, artificially high cell-concentration measurements would result. Further study is needed to resolve this issue.

The ATP and electron-transport activity assays do not indicate dead cells. The relative advantages of two techniques have been directly compared for suspended-cell cultures. DeSha and Bostick[4] concluded that the INT method gave approximately the same accuracy as the ATP method, was easier to perform, and required only basic laboratory equipment. Pohland and Kang[28] found both methods to be sensitive and accurate measures of active biomass. However, they concluded that the ATP method was less satisfactory, because the intracellular ATP concentration varied with the cell growth rate and because it was more complicated and costly to perform.

For the reasons listed above, the electron-transport activity approach using INT was selected in the present study as a basis for the development of an active-cell biomass assay for biological fixed films.

CHAPTER III

MATERIALS AND METHODS

Microbial Film

The biofilm used in this study is a mixed culture of phenol-oxidizing microorganisms attached to 30 to 60 mesh anthracite coal particles. It has been maintained during several years of use at the Oak Ridge National Laboratory (ORNL) in the development of fluidized-bed bioreactors for phenol degradation.[29] Several microbial species have been isolated from the mixed culture and are listed in Table 1.

Medium

The medium on which the biofilm was sustained consisted primarily of monohydric phenol, trace elements and micronutrients. Its composition is given in Table 2.

Bioreactor

Continuous fixed-film experiments were conducted using the bioreactor depicted in Figure 4. It has two primary components: a small fluidized bed of biofilm particles and a stirred tank. Phenol was consumed within the fluidized bed, while addition of fresh medium and oxygen, mixing of reagents, and temperature control occurred in the stirred tank. A liquid-recycle loop transported medium between the two components. By keeping the fluidized bed relatively small, a differential reactor was approximated; all biofilm particles were exposed to approximately identical conditions.

Table 1

Cultures Isolated From Phenol-Degrading Biofilm

Pseudomonas fluorescens
Pseudomonas mendocina
Pseudomonas stutzeri
Pseudomonas alcaligenes
Pseudomonas sp.
Alcaligenes sp. (two isolates)
Flavobacterium ferrugineum
Arthrobacter globiformis
Endomycopsis sp.
Four unidentified bacteria

Source: Donaldson, T. L., Strandberg, G. W., Hewitt, J. D., and Shields, G. S. (1984), "Biooxidation of Coal Gasification Wastewaters," *Environmental Progress*, *3*, p. 248.

Table 2

Composition of Experimental Medium

Component	Concentration (g/cm^3) × 10^6
Phenol	50 to 100 (varied between experiments)
Salts	
NH_4NO_3	200
K_2HPO_4	64
$MgSO_4 \cdot 7H_2O$	20
KI	2
Micronutrients	
H_3BO_3	0.02
$ZnSO_4 \cdot 7H_2O$	0.008
$(NH_4)_6Mo_7O_{24} \cdot 4H_2O$	0.004
$MnSO_4 \cdot 7H_2O$	0.008
$CuSO_4 \cdot 5H_2O$	0.009
$FeSO_4 \cdot 7H_2O$	0.005
Thiamine HCl	0.013

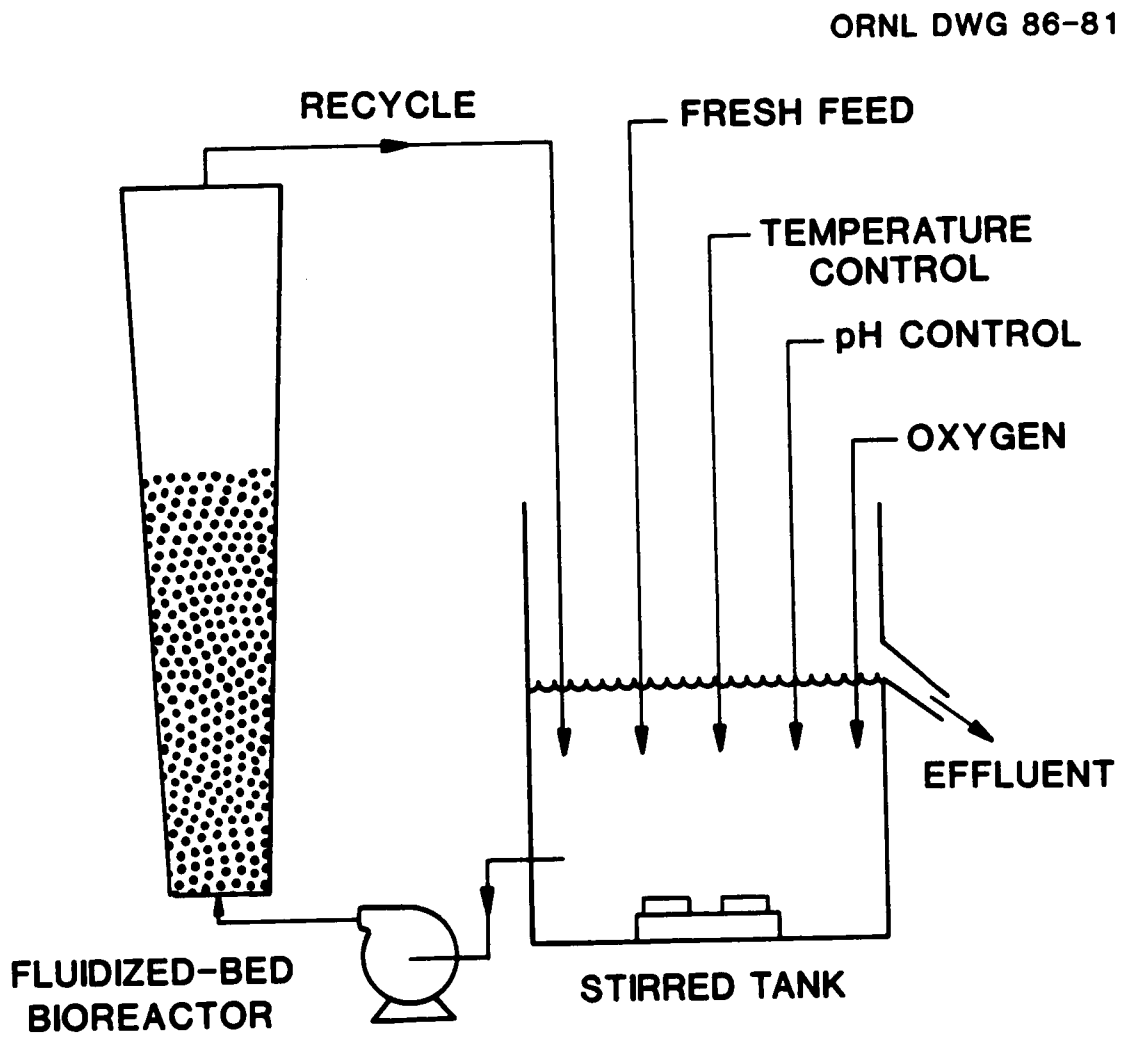

Figure 4. Experimental Bioreactor.

Assay Procedure

The 0.1% (w/v) INT solution was prepared as follows. 0.500 g INT (Calbiochem #40795) was dissolved in 500 mL distilled water. Dissolution was facilitated by first wetting the INT with 1 mL of 95% ethanol. After adding approximately half of the water, the pH was adjusted to 7.5 using 0.01 M Na_2CO_3 solution. Once the remainder of the water was added, the solution was magnetically stirred until dissolution was complete, then filtered through Whatman No. 40 filter paper to remove any residual solids, and stored at 4°C in a dark bottle to prevent photoreduction of the INT.

The basic procedure for the active-biomass assay is described below. Slight variations of this procedure were tested in an attempt to optimize the technique for biofilm applications, and the effects of these variations will be discussed.

1. A sample of the coal-biomass (typically 0.5 to 2.0 mL) was measured into each 10 mL test tube.

2. Excess liquid above and between the settled bioparticles was removed using gentle suction through a hypodermic needle or disposable pipette tip having an inner diameter less than 0.1 mm.

3. An aliquot (typically 2 to 5 mL) of 0.1% INT solution was added to each test tube.

4. The tubes were incubated in a water-bath shaker at 30°C for the desired length of time (typically between 20 and 150 min) and inverted occasionally.

5. The residual INT solution was withdrawn using gentle suction through a pipette tip.

6. The contents of each tube were transferred into a labeled 50 mL graduated cylinder.

7. Acetone was added to a final volume of 50.0 mL in each graduated cylinder.

8. Thirty minutes were allowed for complete extraction of the red INT-formazan color into the acetone. During this time the graduated cylinders were inverted occasionally.

9. The amount of reduced INT formazan was measured via optical density (OD) of the acetone extract at 490 nm versus an acetone blank. The OD (490 nm) was taken to be indicative of the amount of active biomass in the sample.

CHAPTER IV

PRELIMINARY EXPERIMENTS

Acetone Extraction Time

In order to determine the time required for complete extraction of the red INT formazan from 2.0 mL biomass samples, the optical density of the acetone extract was measured at several time intervals. The volume of INT solution added to the 2 mL coal-biomass samples and the time of incubation of the biofilm with INT varied among the samples. The results are plotted in Figure 5.

The extraction process was essentially at equilibrium after 30 minutes for all of the samples. Thus a 30 minute acetone extraction was incorporated as a part of the standard assay procedure. However, in subsequent experiments with a pure culture of Pseudomonas alcaligenes, 30 minutes was insufficient for complete color extraction. It is therefore important to determine the necessary extraction time for each microbial system used.

Interference by Coal Support Particles

Control experiments were conducted to determine whether the coal support particles could induce significant color formation in the absence of either INT or active biomass. The assay was performed on 1.0 mL samples of clean coal using 30 and 90 minute INT incubation times. The same procedure was also performed on other clean-coal samples using distilled water instead of 0.1% INT solution. For comparison, identical procedures were also performed on 1.0 mL samples of

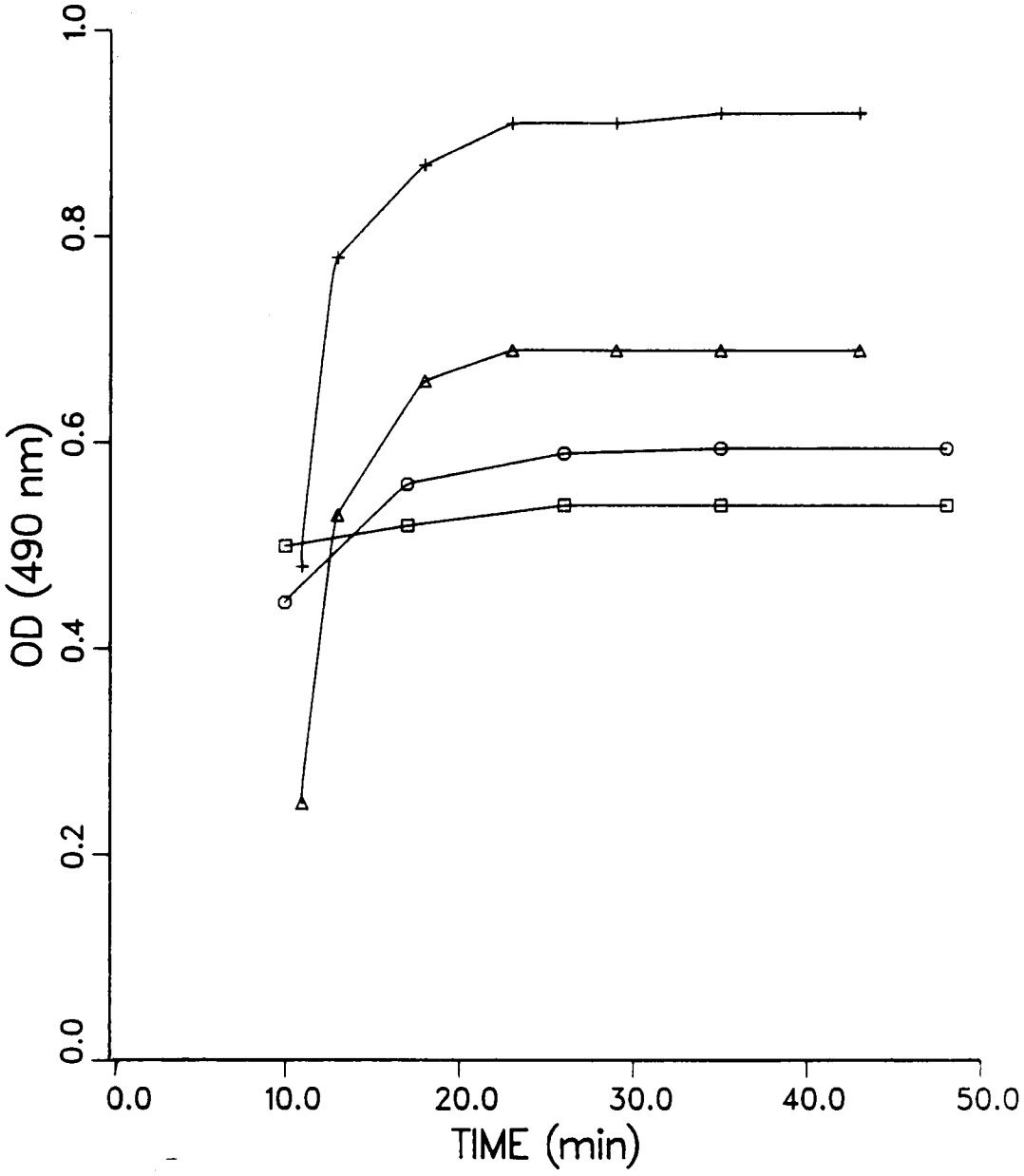

Figure 5. Rate of color extraction from INT-treated biomass.

Squares: 20 min incubation in 2 mL INT solution;
Circles: 20 min incubation in 5 mL INT solution;
Triangles: 40 min incubation in 2 mL INT solution;
Crosses: 40 min incubation in 5 mL INT solution.

active coal-biomass. The results are shown in Table 3. Clearly the amount of color produced in the presence of both active biomass and INT is far greater than that produced in the absence of either. Under the experimental conditions, approximately 99% of the measured color is due to biomass-catalyzed INT reduction.

Another control experiment was performed to determine whether a significant amount of the red formazan produced might be adsorbed by the coal particles. Erroneously low assay values would result under these circumstances. Clean coal (0.5 mL) was added to 25 mL of a solution of INT formazan in acetone which had an OD (490 nm) of 0.260. The mixture was capped and magnetically stirred gently for 30 minutes. A 5.0 mL sample of the liquid was then centrifuged at 2500 rpm in an IEC Centra 7R centrifuge for 10 minutes to remove coal particlates. The OD (490 nm) was measured to be 0.250. Thus the amount of color taken up by the coal was quite small, approximately 4%.

Red Color Lost in the Aqueous Phase

In the standard assay procedure, the aqueous phase is discarded following the INT-incubation step, and the biofilm is then extracted with acetone. However, the aqueous phase contains a small amount of red color which is trapped within suspended cells. Several experiments were conducted to establish whether the fraction of color lost in the aqueous phase is significant.

Coal-biomass samples of 0.5 and 1.0 mL volumes were prepared in triplicate. Each was incubated with 2.5 mL of INT solution for 20 minutes. The aqueous portions were then removed and centrifuged to

Table 3

Control Experiments in the Absence of Biomass and INT

	OD (490 nm)			
	30 minute incubation		90 minute incubation	
	clean coal	coal-biomass	clean coal	coal-biomass
With INT	0.009	0.467	0.001	0.750
Without INT	0.006	0.036	0.002	0.010

settle the suspended cells. The supernatants were removed, and the cell pellets were extracted with 5.0 mL of acetone. The biofilm particles were extracted with 50 mL acetone as usual. The OD (490 nm) of the aqueous supernatant, the 5 mL acetone extract and the 50 mL acetone extract were measured for each sample, and the results are shown in Table 4. The percentage of the total color contained within each of the fractions was calculated from these data. The amount of color in the i'th fraction was obtained by multiplying the volume of that fraction (V_i) and the relative concentration (OD_i). The percentage of the total color in the i'th fraction (P_i) was then calculated as follows:

$$P_i = \frac{(V_i)(OD_i)}{\sum_{j=1}^{3} (V_j)(OD_j)} ,$$

where the summation is over all three fractions. Percentage values are shown in Table 5. For the 0.5 mL coal-biomass samples, an average of 5.6% of the total red color was contained in the aqueous fraction, and for the 1.0 mL samples, the value was 8.6%. Greater than 90% of this color was recovered through centrifugation. Whether this centrifugation step should be included in the assay procedure depends upon the degree of accuracy required by the researcher.

Interference by Inactive Biomass

To ensure that the observed red color is due to cell activity rather than a chemical reaction nonspecific to active cells, several

Table 4

Color Content of Various Fractions

Biomass Volume (mL)	Aqueous Supernatant	Acetone Extract (5 mL)	Acetone Extract (50 mL)
0.5	0.017	0.178	0.258
0.5	0.023	0.112	0.247
0.5	0.043	0.125	0.259
1.0	0.068	0.268	0.386
1.0	0.080	0.373	0.430
1.0	0.123	0.537	0.407

Table 5

Percentage of Total Color Contained in Each Fraction

Biomass Volume (mL)	Percentage of Total Color		
	Aqueous Supernatant	Acetone Extract (5 mL)	Acetone Extract (50 mL)
0.5	0.2	6.3	93.5
0.5	0.3	4.7	95.0
0.5	0.6	4.8	94.6
1.0	0.6	6.4	92.8
1.0	0.7	7.9	91.5
1.0	1.0	11.5	87.5

control experiments were conducted. Biofilm samples were treated with common metabolic inhibitors and poisons, and the INT assay was subsequently performed.

Rotenone and cyanide are known to be potent inhibitors of the electron transport system. Rotenone inhibits the transfer of electrons between flavoprotein molecules and the cytochromes, while cyanide blocks electron transfer from the cytochromes to molecular oxygen.[30]

Biofilm samples were incubated in the presence of either 0.5 mM KCN for 20 minutes or 5.0 mM KCN for 90 minutes. These samples, as well as control samples, were then INT-assayed. The results are shown in Table 6. Color formation was decreased an average of 63% by 0.5 mM cyanide and 42% by the 5.0 mM cyanide. Although color formation was reduced by approximately one half, it was not eliminated, because the inhibitory influence of cyanide occurs at the final reaction step of the electron-transport system. INT reduction can occur "upstream" of the inhibited step.

Rotenone would likely be a more potent inhibitor of INT reduction, since it inhibits an earlier reaction in the ETS sequence. It is insoluble in water, however, which requires that a different solvent system be used. Various aqueous solutions of ethanol and dimethyl sulfoxide were tested, but none was both completely non-toxic to the biofilm and also able to hold 0.5 mM rotenone in solution. The ethanol-water system yielded the results shown in Table 7. At both 0.01 mM and 0.1 mM concentrations, rotenone inhibited, but did not eliminate color formation. The 10% ethanol solvent required to

Table 6

Effect of Cyanide on INT Assay

Cyanide Concentration (mM)	Incubation Time (min)	OD (490 nm)
0	20	0.90 , 1.00
0.5	20	0.35 , 0.34
0	90	0.89 , 0.90
5.0	90	0.52 , 0.52

Table 7

Effect of Rotenone on INT Assay

Rotenone Concentration (mM)	Ethanol Concentration (% v/v)	OD (490 nm)
0	0	0.610
0	1	0.678
0.01	1	0.427
0	10	0.383
0.1	10	0.271

dissolve 0.1 mM rotenone was also somewhat toxic to the biofilm. Because of the solubility and solvent-toxicity problems encountered, higher concentrations of rotenone were not tested.

Two methods of totally inactivating the biofilm were found -- heat treatment and poisoning with $HgCl_2$. The heat treatment consisted of lowering a test tube with biofilm particles into boiling water for 15 minutes. The INT assay was performed after the samples were cooled to room temperature. The OD (490 nm) of the unheated controls averaged 0.112, while the heat-treated samples averaged 0.011. This latter value represents turbidity due to biomass residue in the extract. No red color was visible. Similarly, bioparticles treated for 1.5 hours with 0.1% (w/v) $HgCl_2$ yielded an average OD (490 nm) of 0.005, while untreated controls registered an average value of 0.895. The corresponding effect of $HgCl_2$ treatment on the phenol degradation rate of the biofilm is shown in Figure 6. Phenol concentration remains constant for the $HgCl_2$ treated samples and declines rapidly for the control samples. Thus the INT assay has the desirable feature of not responding to dead cells.

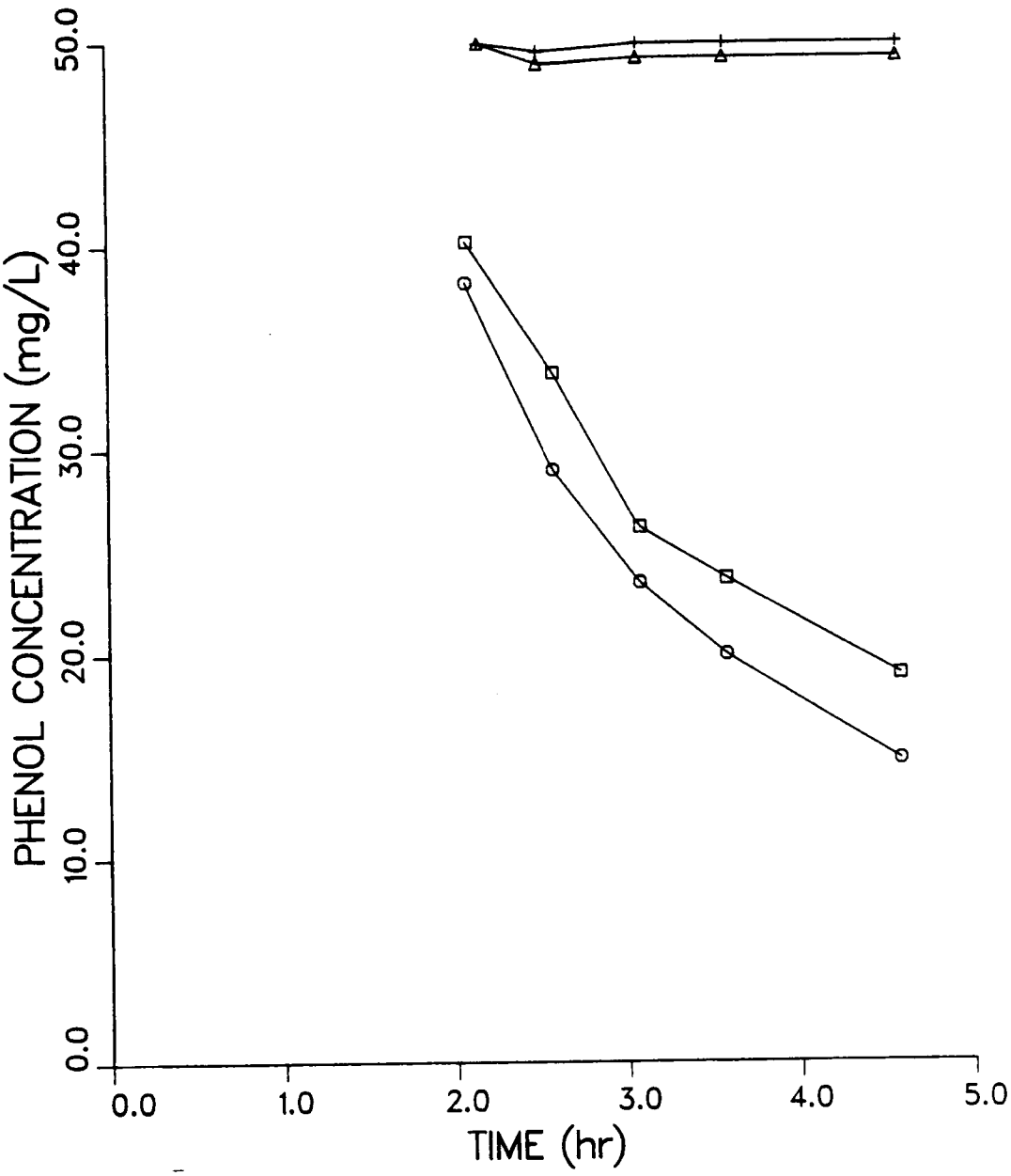

Figure 6. Effect of $HgCl_2$ treatment on biofilm activity.

Triangles and crosses: Samples treated with $HgCl_2$;
Squares and circles: Untreated samples.

CHAPTER V

OPTIMIZATION OF ASSAY PROCEDURE

Nutrient Requirements

Electron transport activity and the resulting reduction of INT to the red formazan product requires the oxidation of high-energy substrate materials. These substrates may be from extracellular sources (e.g., phenol) or, during periods of starvation, the cell will break down its own internal energy reserves (i.e., endogenous respiration). An experiment was conducted to determine whether nutrients were required during the INT-incubation step for maximum color production.

Biofilm samples (1.0 mL) were incubated in 2.5 mL of INT solution for times ranging from 45 to 225 minutes, both with and without the presence of nutrients. The INT-nutrient solution contained 0.1% INT plus 50 mg/L phenol and the mineral salts and micronutrients listed in Table 2, page 136. Prior to the INT incubation, the coal-biomass was gently rinsed in a mineral-salts solution to remove residual phenol. Results are plotted in Figure 7. The presence of nutrients was associated with only a slightly higher degree of color formation. Therefore, the inclusion of nutrients was deemed unnecessary.

Volume of INT Reagent

To determine whether the assay response was sensitive to the volume of INT reagent used, the assay procedure was performed on 2.0 mL biomass samples using both 2.0 and 5.0 mL aliquots of INT solution.

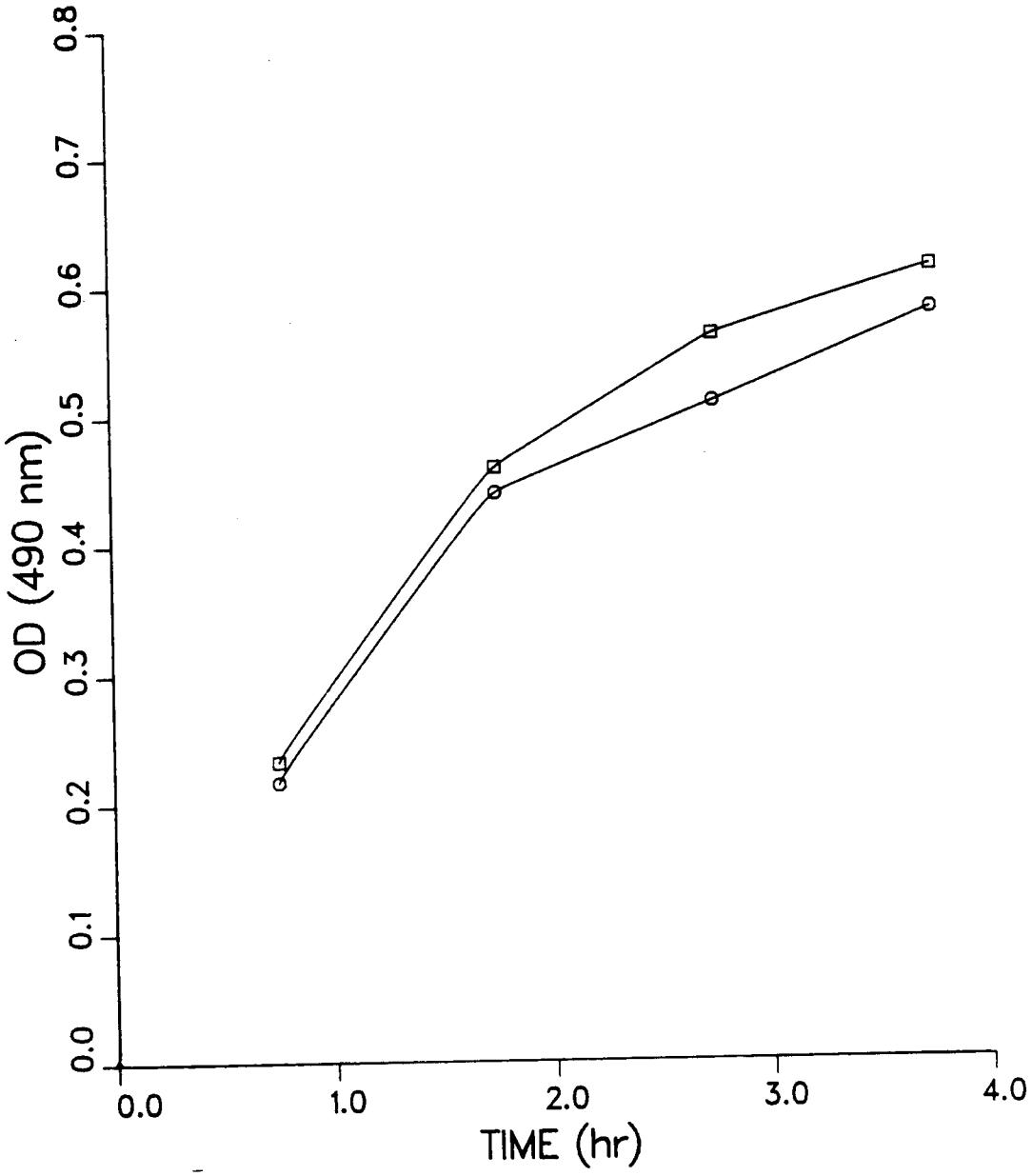

Figure 7. Effect of nutrients on color formation.

Squares: With nutrients; Circles: Without nutrients.

Incubation times of 20 and 40 minutes were tested. The results are listed in Table 8. Larger aliquots of INT resulted in more color being produced, probably due to a dilution effect. After washing the biomass samples into test tubes, the liquid above the biomass was discarded, but that between the particles was not removed. When the 0.1% INT solution was added, INT diffused into the biofilm and interstitial liquid, eventually reaching an equilibrium. The equilibrium concentration of INT in the liquid was then less than 0.1%. The decrease in concentration would be greater for the smaller (2.0 mL) aliquot of INT. Assuming the color formation rate is dependent upon INT concentration, the reduced concentration should result in a lower overall production of red color for the 2.0 mL sample — as was observed experimentally. This phenomenon is considered in more detail in Appendix 1. To minimize dilution effects in subsequent experiments, the interparticle liquid was removed prior to the addition of INT, and a volume of INT solution at least double the biomass volume was used.

Kinetic Versus Endpoint Assay

As seen in Figure 7, the reaction does not come to equilibrium within four hours. The dynamics of color formation during this initial four-hour period were measured in two subsequent experiments. In the first experiment (Figure 8-a), 2.0 mL of biomass and 5.0 mL of INT solution were used. In the second experiment (Figure 8-b), the respective volumes were one-half as large.

Table 8

Effect of Quantity of INT Added on Color Produced

Incubation Time (min)	OD (490 nm)	
	INT Solution	
	(2.0 mL)	(5.0 mL)
20	0.54	0.60
40	0.69	0.92

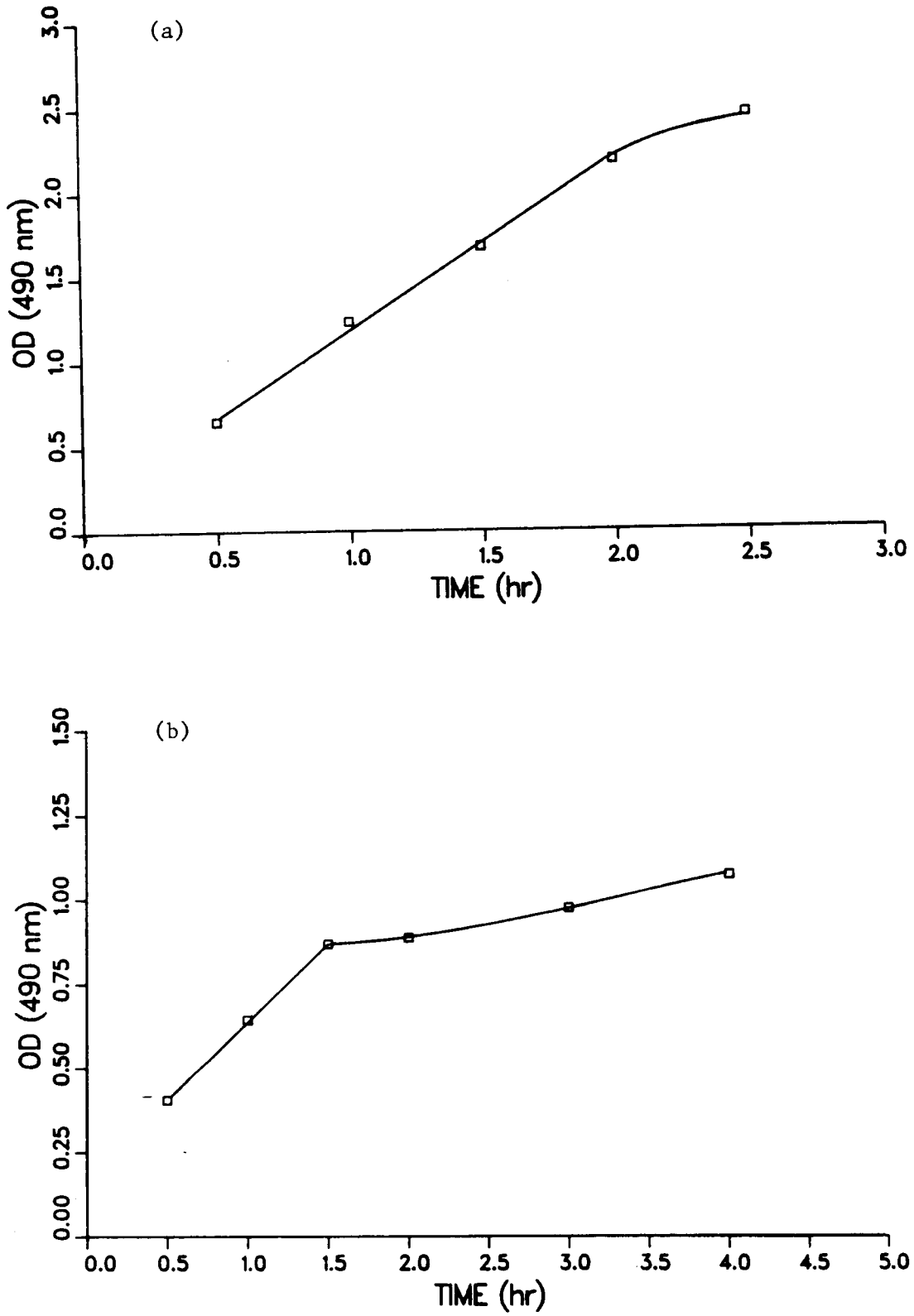

Figure 8. Dynamics of color formation.

In both graphs, an initial period of high linearity is followed by a reduced rate of color production. Figure 7 is also consistent with this observation. The reason for the abrupt change in the rate of color formation after two hours is unknown.

The ratio of the slopes of the initial portions of Figures 8-a and 8-b is 2.2, and the ratio of the respective volumes of biopar-ticles was 2.0. This observation suggested that the initial slope of the color-production curves might be a suitable indicator of biomass concentration. Assays based upon such "kinetic" approaches are not uncommon.[31,32] Two further experiments were conducted to test this hypothesis. In each experiment, samples containing either 1.0 mL coal-biomass, 0.5 mL coal-biomass, or 0.5 mL coal-biomass plus 0.5 mL clean coal were incubated in 2.5 mL of INT solution. The results are plotted in Figures 9-a and 9-b.

In both instances, the curve for the 0.5 mL coal-biomass sample was in good agreement with the curve for the 0.5 mL coal-biomass plus 0.5 mL clean coal sample, reinforcing the previous finding that coal is inert to the assay reagents. However, the curves were in general not as linear as the initial portions of Figures 8-a and 8-b. When regression was applied to determine the best linear fit, the ratios of the slopes were 1.4 for Figure 9-a and 1.6 for Figure 9-b. Since the ratio of biomass content in the samples was 2.0, these values are significantly too small, even after dilution effects (see Appendix 1) are considered. In view of the rather large degree of error and the lack of consistent linearity in the experimental data, the "kinetic" approach was deemed less satisfactory than the standard "endpoint" method.

Figure 9. Effect of quantity of biomass on the rate of color formation.

Squares: 1.0 mL coal-biomass; Circles: 0.5 mL coal-biomass; Triangles: 0.5 mL coal-biomass plus 0.5 mL clean coal.

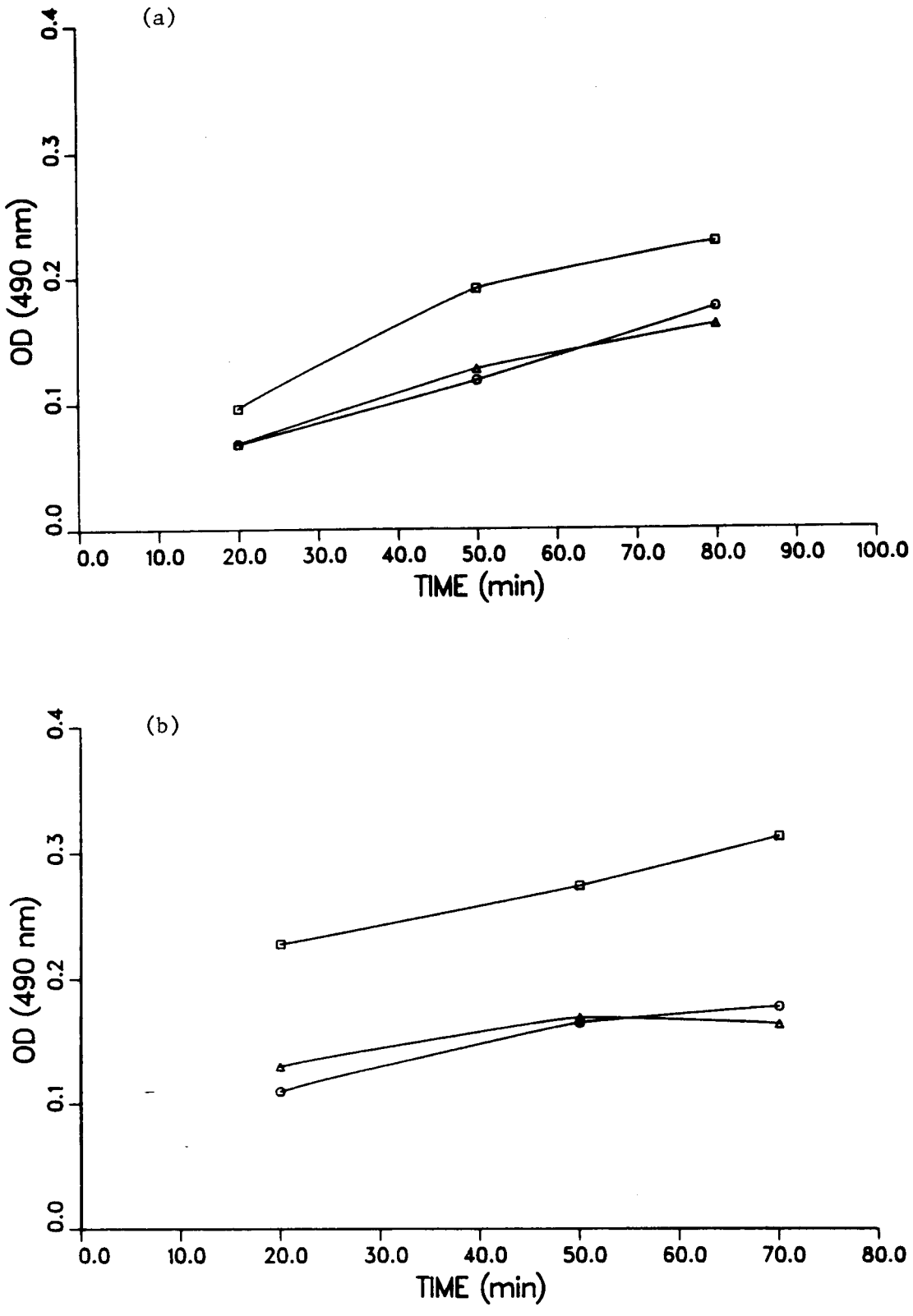
(a)
OD (490 nm)
0.0
0.1
0.2
0.3
0.4
0.0
10.0
20.0
30.0
40.0
50.0
60.0
70.0
80.0
90.0
100.0
TIME (min)
(b)
OD (490 nm)
0.0
0.1
0.2
0.3
0.4
0.0
10.0
20.0
30.0
40.0
50.0
60.0
70.0
80.0
TIME (min)

Figure 9.

INT Incubation Time

Since over a four-hour period the INT reaction does not come to equilibrium, an incubation period must be chosen which provides a satisfactory combination of accuracy and convenience. Based upon Figures 9-a and 9-b, there appear to be two distinct rates of color production — a higher rate, which occurs in the first two hours, and a lower rate, which occurs after two hours. To determine whether locating the assay endpoint before or after the point of transition would provide more accuracy, several endpoint assays were performed using either a 20 minute or a 2.5 hour incubation period. In each experiment, both 0.5 and 1.0 mL samples were assayed. The results are shown in Tables 9 and 10.

The average color ratio was 1.78 for the 20 minute incubation period and 1.85 for the 2.5 hour incubation period. The standard deviations (using an "N-1" weighting factor) were 0.167 and 0.246, respectively. The "correct" color ratio has been estimated in Appendix 1 to be 1.8. This figure includes a correction for the dilution of INT due to the use of different sample volumes. Thus, within experimental error, both of the incubation periods provide linear responses. The 20 minute incubation provides somewhat better reproducibility and is quicker to perform, making it a preferable alternative for this biofilm.

Table 9

Linearity of the Assay Using a 20 min INT Incubation

Sample Volume (mL)	OD (490 nm)	OD (1.0 mL Sample) / OD (0.5 mL Sample)
0.5	0.200 , 0.195	1.99
1.0	0.392 , 0.395	
0.5	0.165 , 0.167	1.90
1.0	0.301 , 0.321	
0.5	0.223 , 0.222	1.52
1.0	0.346 , 0.331	
0.5	0.242 , 0.228 , 0.240	1.67
1.0	0.345 , 0.412 , 0.409	
0.5	0.180 , 0.191 , 0.184	1.81
1.0	0.330 , 0.349 , 0.324	
0.5	0.157 , 0.151 , 0.148	1.79
1.0	0.267 , 0.276	

Table 10

Linearity of the Assay Using a 2.5 hr INT Incubation

Sample Volume (mL)	OD (490 nm)	OD (1.0 mL Sample) / OD (0.5 mL Sample)
0.5	0.142 , 0.148	2.2
1.0	0.321 , 0.311	
0.5	0.515 , 0.504	1.90
1.0	0.940 , 0.995	
0.5	0.592 , 0.580	1.85
1.0	1.09 , 1.08	
0.5	0.743 , 0.745	1.43
1.0	1.04 , 1.09	
0.5	0.655 , 0.563	1.83
1.0	1.11 , 1.12	
0.5	0.431 , 0.467 , 0.463	1.89
1.0	0.879 , 0.843 , 0.858	

CHAPTER VI

STABILITY OF ASSAY RESPONSE

Ideally, the INT assay should provide consistent results over a wide range of the important process variables. Two such variables for the biofilm system under investigation are the phenol and oxygen concentrations. The continuous fluidized-bed bioreactor (Figure 4, page 137) was operated at a variety of phenol and oxygen concentrations. Periodically biomass samples were withdrawn and INT-assayed to determine the effects of these key variables on the assay response.

Effect of Phenol Concentration

Figure 10 depicts a continuous experiment in which the phenol concentration in the reactor was varied between essentially 0 and 170 mg/L, while the oxygen concentration was maintained above 60% saturation. Biomass samples were withdrawn periodically and assayed. The amount of color produced remained relatively constant throughout the experiment. The standard deviation of the entire data set was 8% of the mean. This degree of consistency may be quite satisfactory, depending upon the needs of the researcher.

Effect of Oxygen Concentration

To explore the influence of oxygen concentration, INT assays were performed following exposure to either high (~70%) or low (<0.3%) oxygen saturation. The high concentration was obtained by sparging the

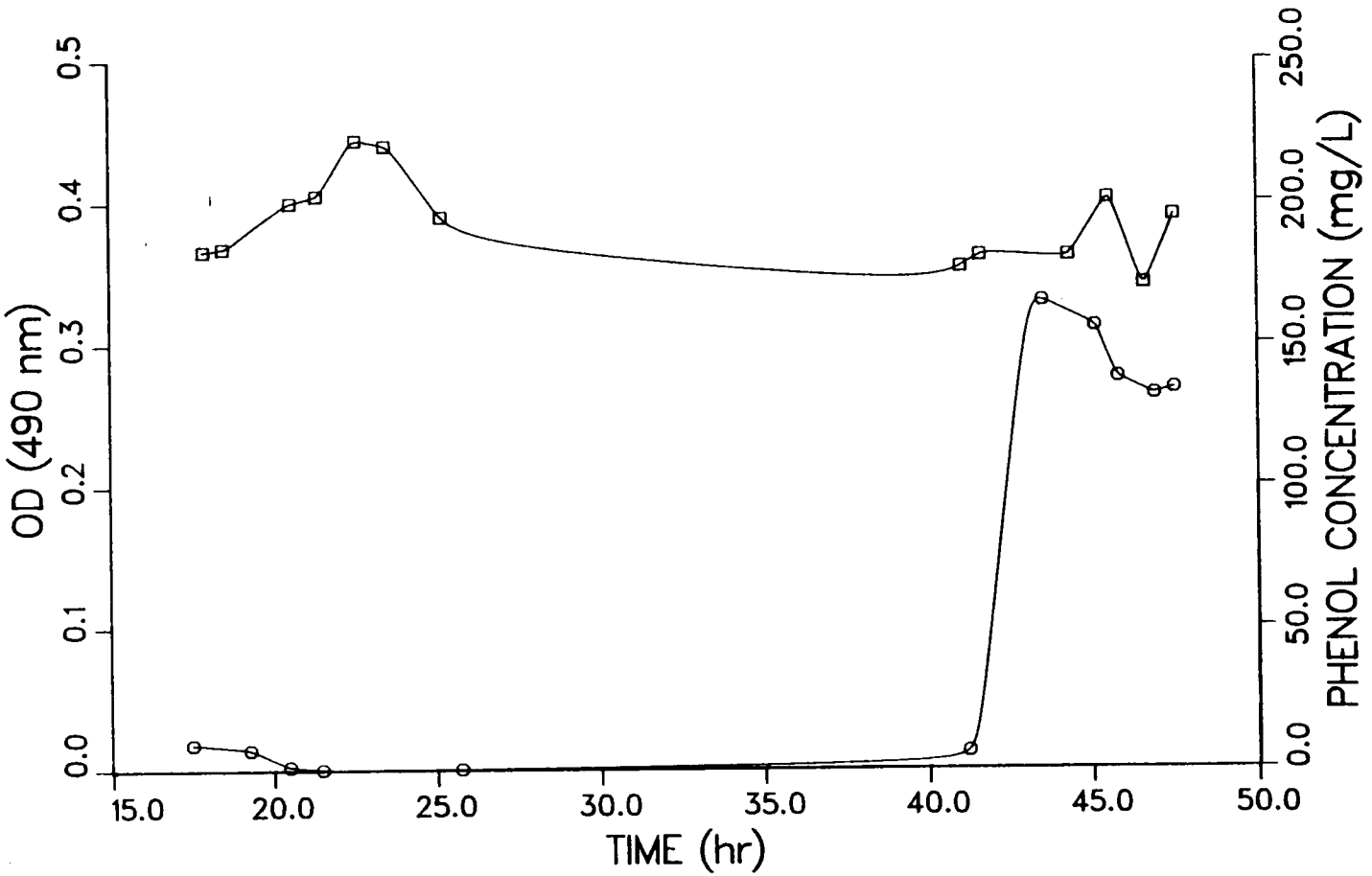

Figure 10. Effect of phenol on color formation.

stirred tank with pure oxygen at a rate of 75 mL/min, while the low concentration was achieved by sparging the stirred tank and the fresh-feed storage tank with nitrogen gas. Thick-walled Tygon tubing was used in place of silicone tubing, since the latter was found to be oxygen-permeable. The results of this continuous experiment are shown in Figure 11.

Although the INT-assay values of Figure 11 varied over a somewhat wider range than in Figure 10 (the standard deviation of the data was 15% of the mean), there was no consistent pattern to the fluctuations. In one instance an increase in oxygen concentration was associated with a decrease in color formation. When the same change was later repeated, however, color production increased. Thus, the scatter in the data was likely due to unknown factors other than oxygen concentration.

During 44 hours of continuous oxygen deprivation, no significant decrease in INT color formation was observed. The phenol degradation rate during this period was less than 5% of the original rate, and once oxygen sparging was resumed, the rate returned to its original level. The biofilm thus seems to be resilient to extended periods of oxygen deficiency.

Effect of Nitrate Concentration

One possible explanation for this resiliency was that the biofilm could be utilizing nitrate as a terminal electron acceptor in place of oxygen. Nitrate reduction by biofilms has been demonstrated, and is being exploited as a process for wastewater denitrification.[33]

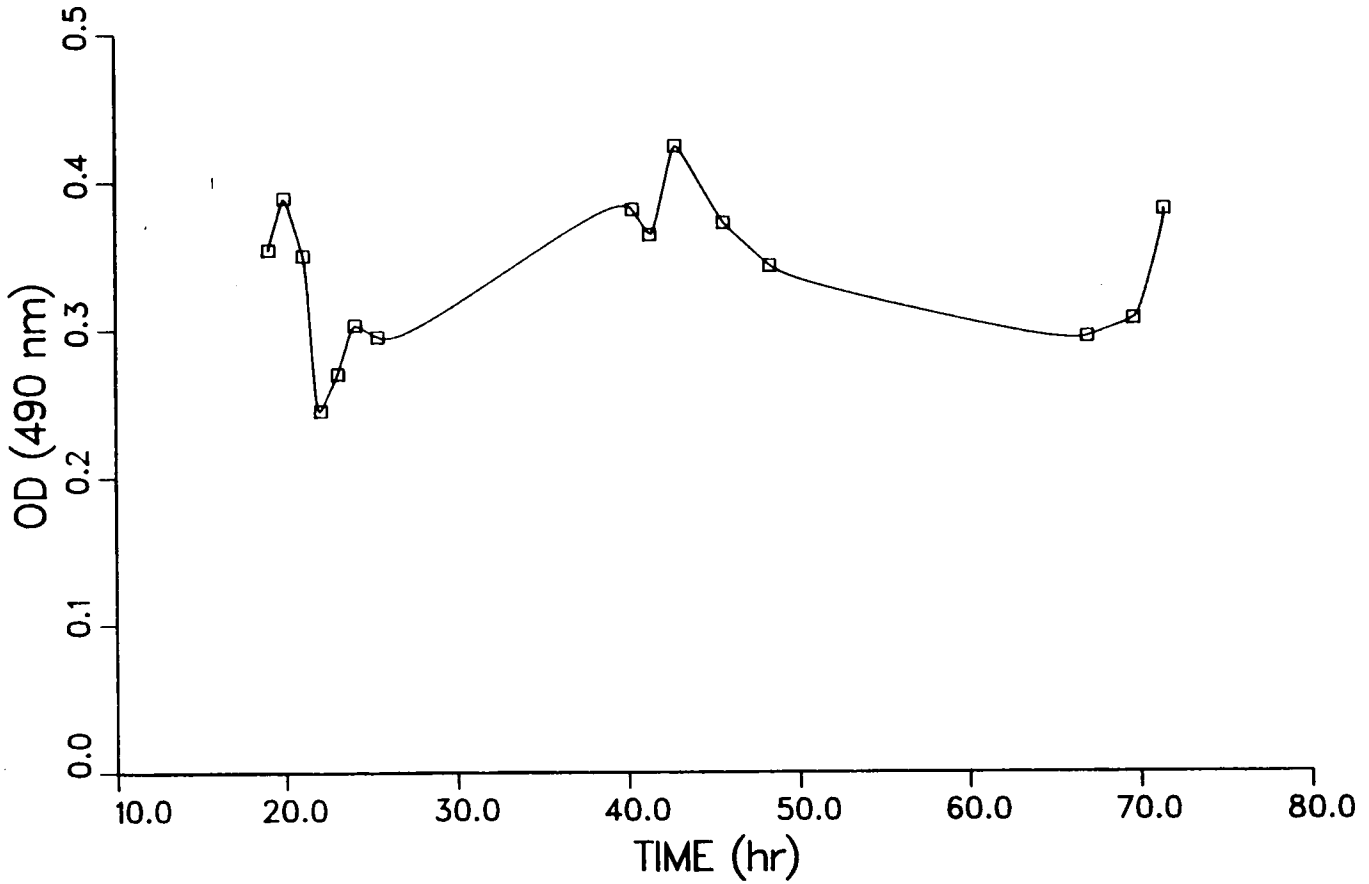

Figure 11. Effect of oxygen on color formation.

0 to 21 hr: Oxygen off; 21 to 23 hr: Oxygen on; 23 to 67 hr: Oxygen off; 67 to 72 hr: Oxygen on.

To test this hypothesis, a series of anaerobic batch experiments were conducted in the presence of 90 mg/L phenol and various concentrations of nitrate. The media were initially deoxygenated by sparging with nitrogen gas. Phenol concentration was monitored periodically, and after four days, a sparge of oxygen was begun. The results are shown in Figure 12.

The presence of nitrate did not enhance the rate of phenol degradation. Whether the gradual disappearance of phenol prior to oxygen sparging was due to the seepage of traces of oxygen into the reactors or to an anaerobic reaction mechanism is not known. The addition of oxygen greatly accelerated the biofilm activity, as expected.

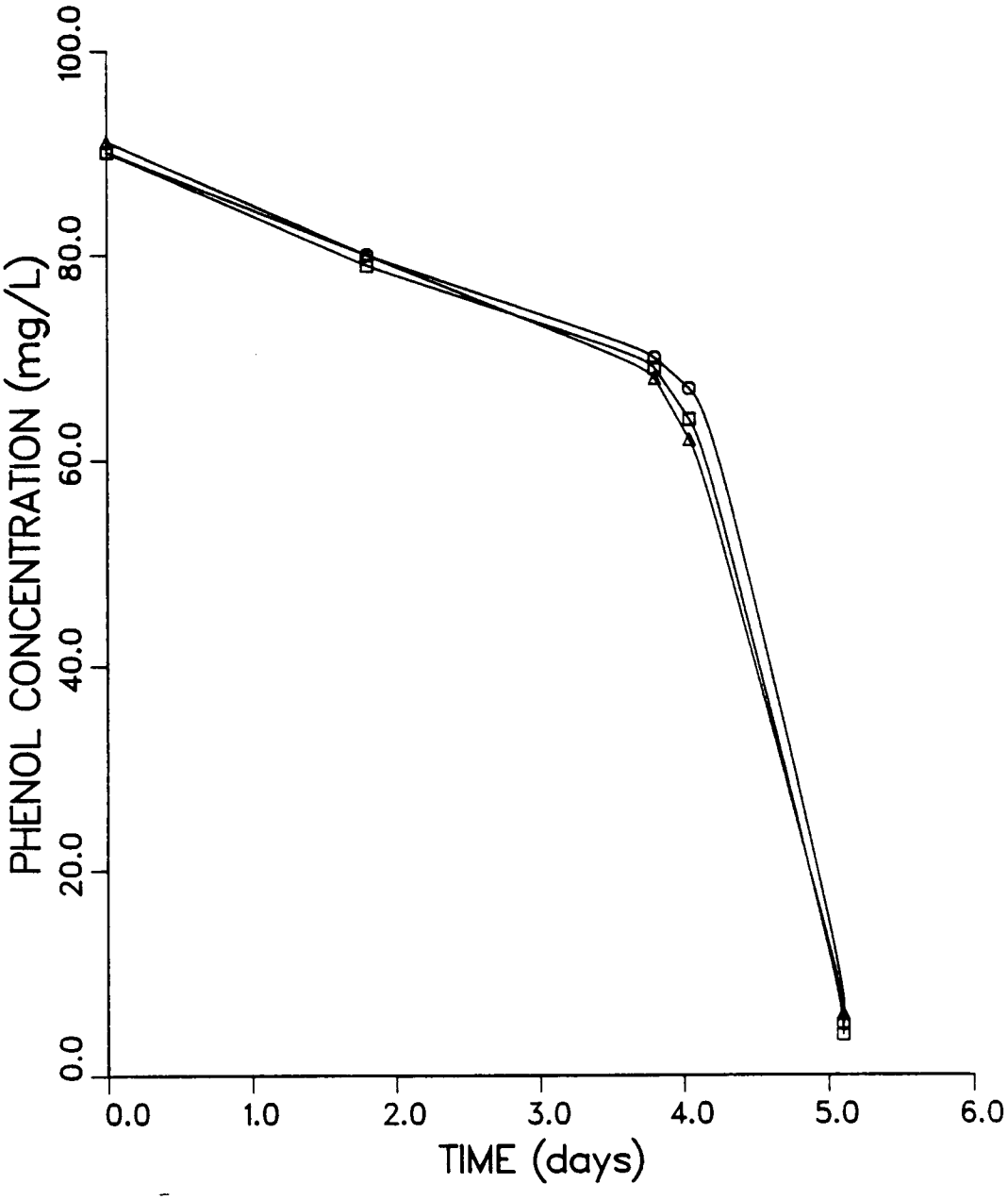

Figure 12. Effect of nitrate on color formation.

Squares: Without KNO_3; Circles: 250 mg/L KNO_3; Triangles: 500 mg/L KNO_3.

CHAPTER VII

CALIBRATION OF ASSAY RESPONSE

The INT assay provides a colorimetric means of measuring the amount of active cells within a biological fixed film. A calibration technique for converting OD (490 nm) into some standard units of active biomass, such as cell number or cell mass, would enhance the utility of the assay. To develop such a technique, the INT assay was compared with some of the traditional biomass assays for Pseudomonas alcaligenes. This species has been identified as a component of the phenol-degrading biofilm.

P. alcaligenes was grown at 30°C in batch culture using a Tryptic Peptone medium. The composition of this medium is listed in Table 11. Cell concentration was monitored via dry weight, turbidity (560 nm), and INT assays. The INT procedure used for suspended cells is listed below.

1. 5.0 mL of cell broth were withdrawn.

2. The sample was centrifuged to settle the cells, and the supernatant was discarded.

3. The cell pellet was resuspended in 3.0 mL of 0.1% INT solution and incubated at 30°C for 20 min.

4. The suspension was centrifuged again, and the supernatant was discarded.

5. The cell pellet was resuspended in 50 mL of acetone to extract intracellular red color.

Table 11

Tryptic Peptone Medium

Component	Concentration (g/cm^3) × 10^3
Tryptone	17
Proteose peptone	3.0
Dextrose	2.5
NaCl	5.0
K_2HPO_4	2.5

6. 5.0 mL of the acetone extract was centrifuged to remove cell debris, and the OD (490 nm) was measured.

As shown in Figure 13, the specific growth rate of P. alcaligenes (which is numerically equal to the slope of the semi-log curve) varies during the course of the batch fermentation. Since the dry weight and turbidity curves remain approximately parallel, they are linear assays, as shown in Figure 14. The INT-based growth curve, however, is not proportional to the other two. It exhibits sudden changes in slope, and generally depicts a lower growth rate.

During the course of the experiment, the INT-containing supernatant contained a quantity of red color which, for one sample, was measured to be 9% of the total color. To provide better accuracy, a second batch-growth experiment was conducted with two modifications. First, the centrifugation step was conducted at a higher speed in order to better pelletize the cells; this change greatly reduced the amount of red color lost in the supernatant. Second, the cells were incubated in the INT solution for 120 rather than 20 minutes. The growth curve is shown in Figure 15. As before, the INT curve is not parallel to the turbidity curve, and it exhibits a sharp decrease in slope at the same cell density as did Figure 14.

To ascertain whether the observed change in slope is a real phenomenon, an experiment was performed to estimate the precision of the suspended-cell assay procedure. Aliquots of 0.5, 1.0, 2.0, and 4.0 mL of actively growing P. alcaligenes culture were INT-assayed. INT concentrations of 0.014, 0.05, and 0.1% (w/v) were used for comparison. As seen in Figure 16, the assay is quite linear over the

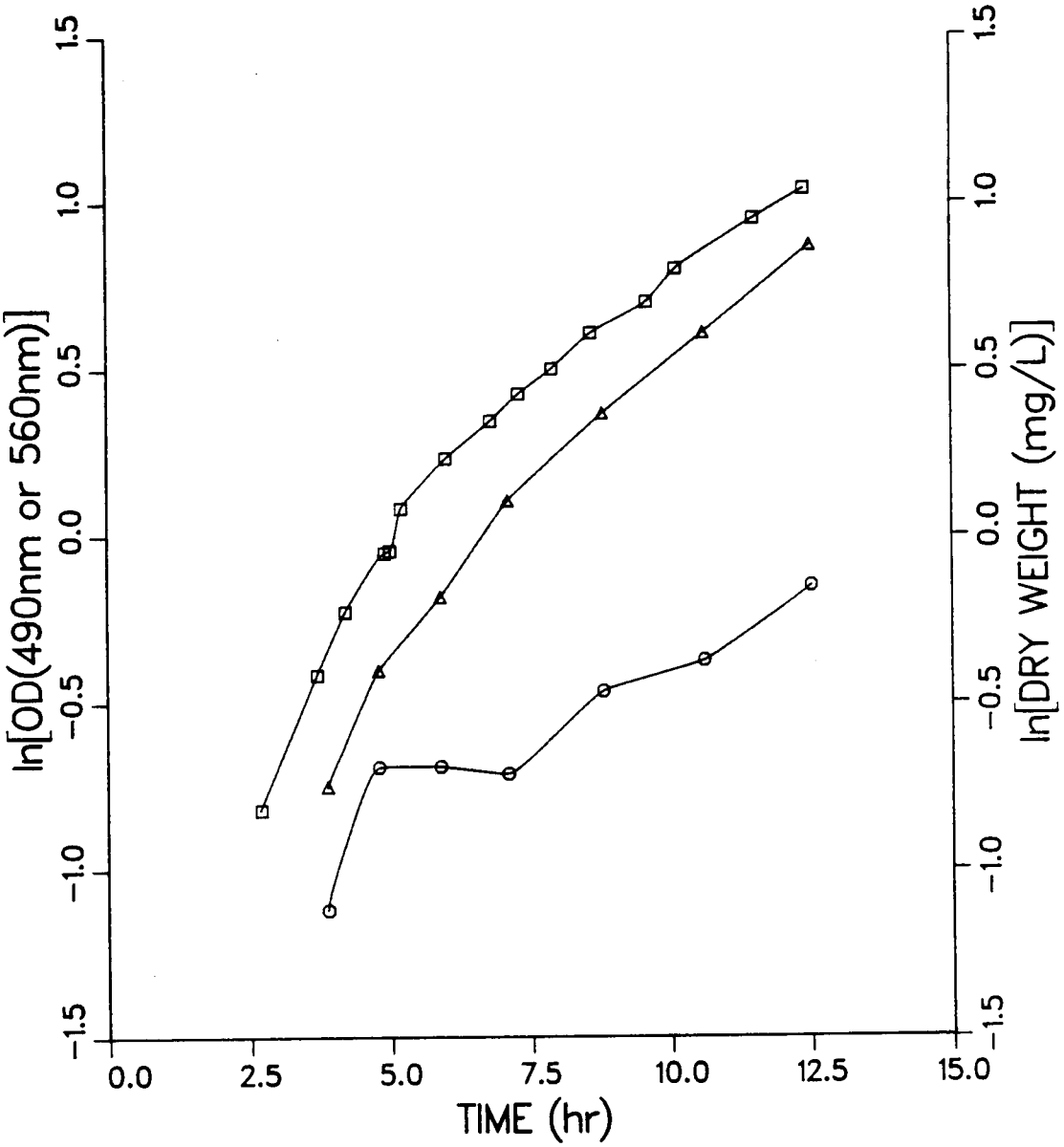

Figure 13. Comparison of dry-weight, turbidity and INT biomass assays.

Squares: Turbidity assay; Triangles: Dry-weight assay; Circles: INT assay.

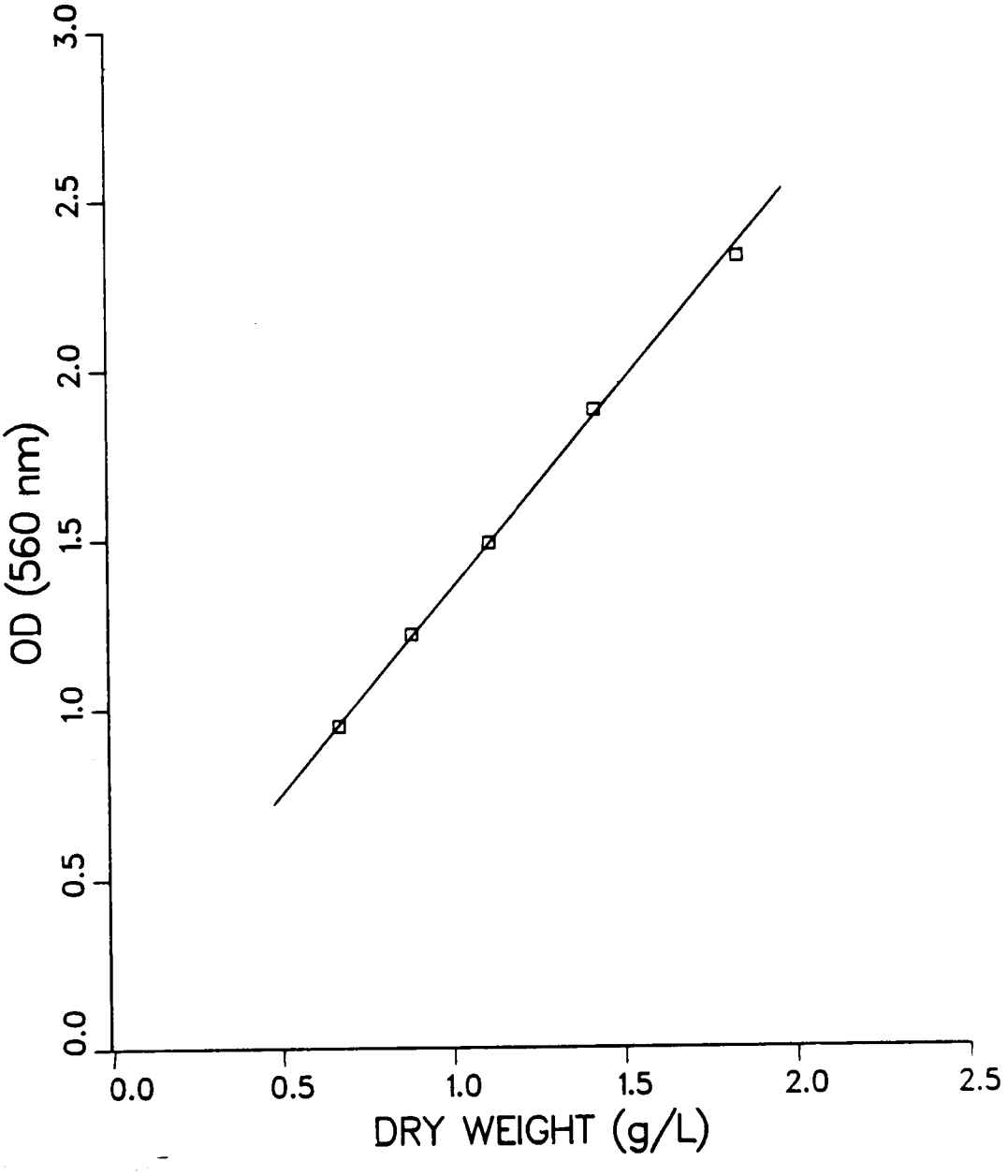

Figure 14. Linear relationship between dry-weight and turbidity biomass assays.

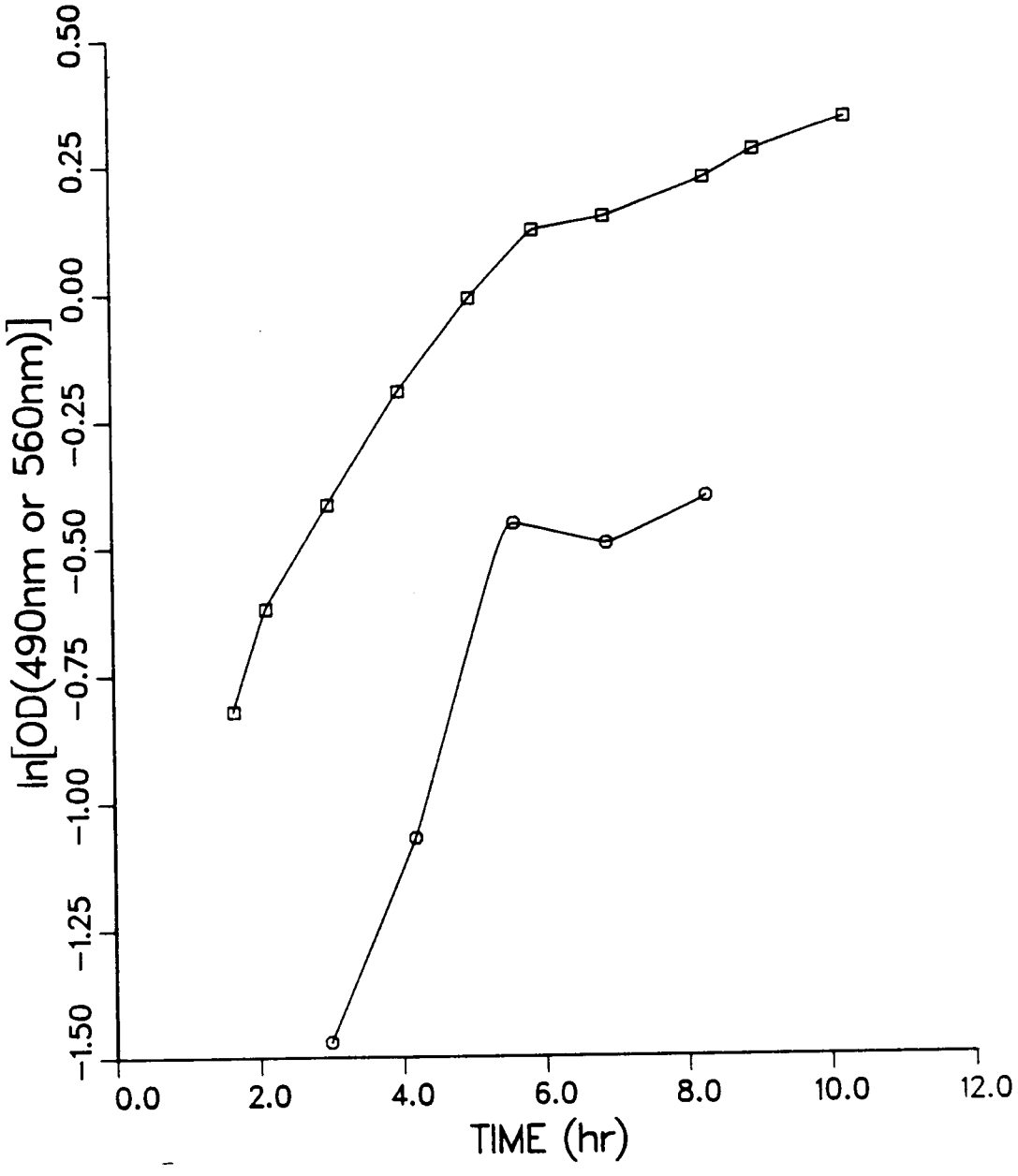

Figure 15. Comparison of turbidity and INT biomass assays.

Squares: Turbidity assay; Circles: INT assay.

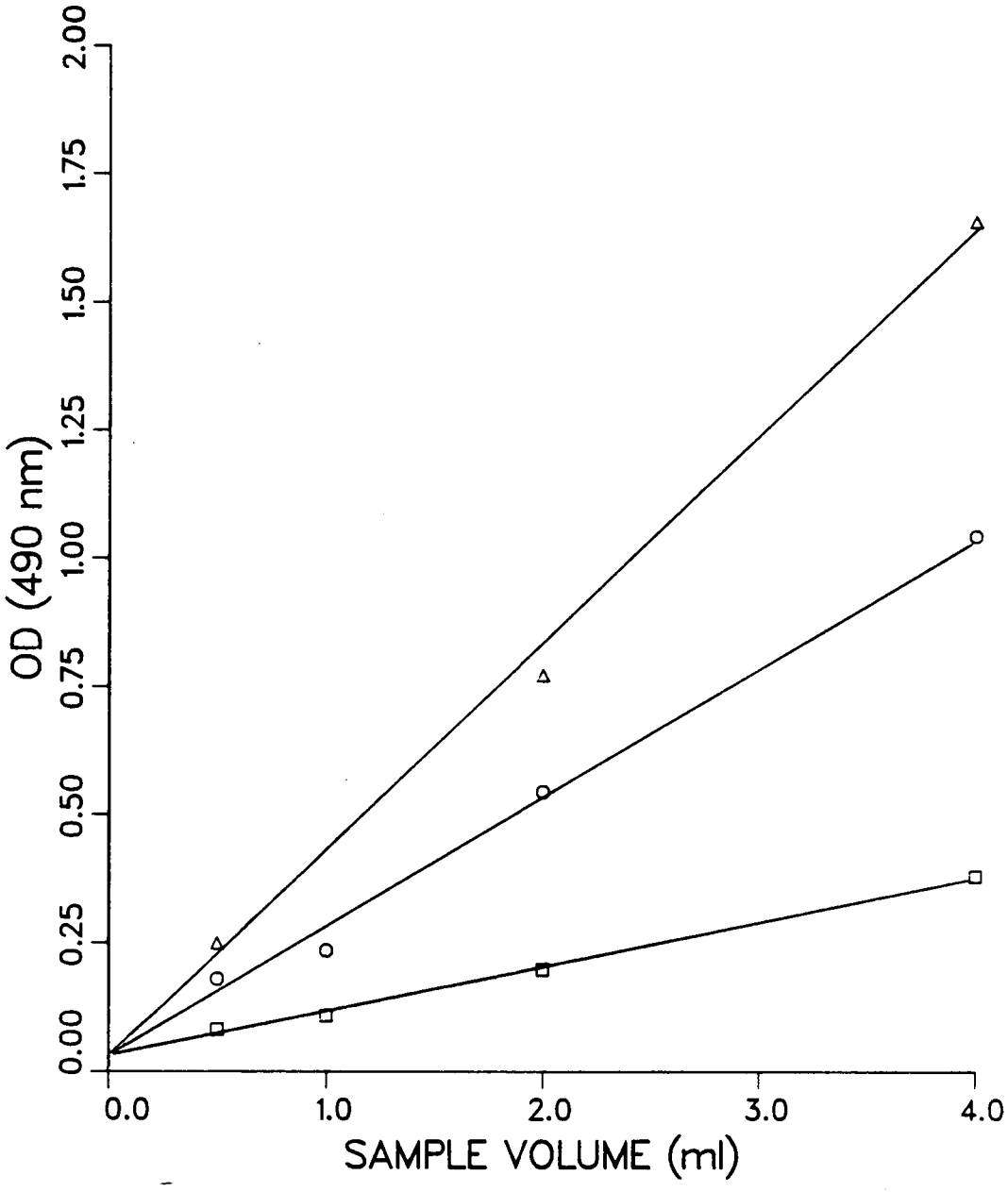

Figure 16. Precision of INT assay for suspended-cell samples. Squares: 0.014% INT; Circles: 0.05% INT; Triangles: 0.10% INT.

range of sample volumes tested for all three INT concentrations. The maximum deviation observed between the data points and the linear regression line is ~0.04 OD units, and the correlation coefficients for a linear fit are 0.9985, 0.9970, and 0.9979 for the 0.014, 0.05, and 0.10% INT curves, respectively. This relatively high degree of precision suggests that the sharp decrease in slope is a real phenomenon. Apparently changes in cell metabolism are being reflected in the amount of red color produced per cell. These changes are likely due to diauxic phenomena, since the cells are being grown on a complex medium having a variety of potential carbon sources.

Because the INT assay did not remain proportional to the dry weight and turbidity assays throughout the growth curve, calibration of the INT assay relative to P. alcaligenes was unsuccessful. However, for growth of other organisms, preferably on a medium with a single carbon source, such calibration may be possible.

CHAPTER VIII

INFLUENCE OF DIFFUSIONAL RESISTANCE

Figure 16 demonstrates that the concentration of INT has a strong bearing on the total color produced for suspended cells. The slopes of the linear regression lines through the data may be interpreted as color yields per unit of cells. These yield values are almost proportional to the INT concentration, as shown in Figure 17.

A physical interpretation of this finding is that the number of electrons consumed in the INT reaction is a relatively small fraction of the total number of electrons being processed in the electron-transport system. Higher INT concentrations thus result in the capture of more electrons and consequently, the production of more color. If the solubility of INT were unlimited, excess INT could be used, and this concentration dependence would be eliminated. Unfortunately the solubility limit is a marginal 0.6% (w/v) at 23°C.

Resistance to diffusion of INT through the biological film could result in a significant concentration gradient within the biofilm. Since the INT concentration is rate limiting, this gradient would cause a reduced rate of color formation deep within the film, and consequently, an erroneously low estimate of the total quantity of active biomass.

To determine whether such a gradient is likely, the criterion of Hudgins was employed.[34] Details of this analysis are included in Appendix 2. The calculations indicated that if first-order reaction kinetics are assumed, as suggested by Figure 17, there would be a

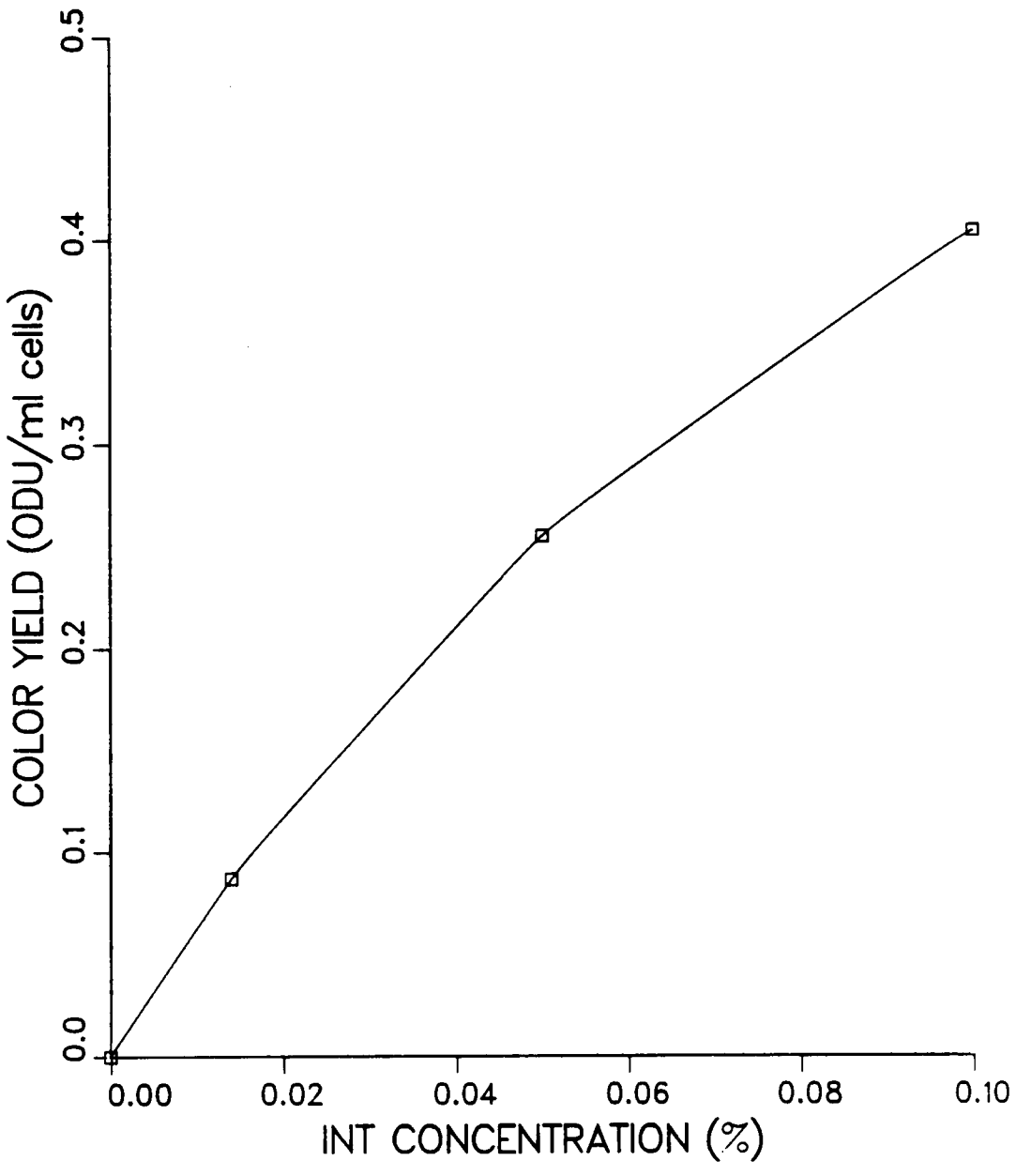

Figure 17. Effect of INT concentration on color yield.

slight (~5%) deviation from a flat concentration profile within the biofilm.

For biofilms that do exhibit significant INT concentration gradients, the biofilm should be dispersed prior to the INT incubation step. Dispersion may be achieved mechanically using gentle ultrasound treatment, or chemically, using detergents or enzymes. The Hudgins' criterion may be used to determine the need for such pretreatment.

CHAPTER IX

CONCLUSIONS

The INT assay was found to be quite specific for active biomass. In the absence of either biomass or INT, negligible red color was formed. Following biomass inactivation by heat treatment or $HgCl_2$, there was no INT response. Cyanide and rotenone were found to reduce, but not eliminate, color formation.

Interference due to the presence of coal support particles was negligible. Coal neither reacted with INT nor adsorbed the colored reaction product to any appreciable degree.

Several variations of the assay procedure have been evaluated to allow experimental flexibility, depending upon the needs of the researcher. Nutrients may be included in the INT solution. Their presence resulted in a slight increase in the assay response. The color contained in unattached cells following the INT-incubation step may be either discarded or recovered and measured. Up to 10% of the total color was found to be contained in these cells. A kinetic approach based upon the initial rate of INT reduction may be used. However, this approach was found to be no more accurate than an end-point method and more complicated to perform. In a comparison between 20 and 150 minute INT incubation times, the shorter incubation time provided equivalent accuracy and better reproducibility.

When using biofilm samples of different volumes, the assay produced results which appeared to be slightly nonlinear. However, this trend was shown to be due to a dilution effect and is easily corrected.

A high degree of linearity was observed when suspended cells were centrifuged and put on an equal-volume basis prior to being assayed.

Phenol and oxygen are the two primary substrates in the fixed-film biooxidation reaction. Over a range of phenol concentration from 0 to 170 mg/L, the assay exhibited a relatively stable response. The standard deviation was 8% of the mean. No consistent pattern was observed in response to oxygen concentration changes between 0 and 70% saturation, although the standard deviation was larger in this case — 15% of the mean. During 44 hours of oxygen deprivation, the biofilm exhibited no appreciable decrease in INT color production. Denitrification activity was not significant during this period.

Calibration of the INT assay via correlation of assay response to the concentration of active Pseudomonas alcaligenes cells was unsuccessful due to changes in the cell color yield during batch growth on a mixed substrate. Such calibration may be possible using a single substrate or other microorganisms.

The rate of color formation was found to be strongly dependent upon the concentration of INT. Thus the existence of INT concentration gradients in the biofilm could cause significant underestimation of biomass content. If diffusional limitations are indicated by the Hudgins' criterion, the biofilm should be dispersed before the assay is performed.

The INT assay is quite suitable for application to biofilm-process analysis. In addition to the features previously mentioned, the assay is also relatively quick to perform, inexpensive, and does not require highly specialized laboratory equipment.

LIST OF REFERENCES

LIST OF REFERENCES

1. Curtis, H. (1975), Biology, Worth, New York, p. 57.

2. Bostick, W. D., and Ausmus, B. S. (1978), "Methodologies for the Determination of Adenosine Phosphates," Anal. Biochem., 88, p. 78.

3. Statham, M., and Langton, D. (1975), "The Use of Adenosine Triphosphate Measurements in the Control of the Activated Sludge Process by the Solids Retention Time Method," Process Biochem, 10, p. 25.

4. DeSha, C. M., and Bostick, W. D. (1978), Unpublished Research, Oak Ridge National Laboratory.

5. Patterson, J. W., Brezonik, P. L., and Putnam, H. D. (1970), "Measurement and Significance of Adenosine Triphosphate in Activated Sludge," Environ. Sci. Technol., 4, p. 569.

6. Strange, R. E., Wade, H. E., and Dark, F. A. (1963), "Effect of Starvation on ATP Concentration in Aerobacter aerogenes," Nature, 199, p. 55.

7. Forrest, W. W., and Walker, D. J. (1965), "Synthesis of Reserve Materials for Endogenous Metabolism in Streptococcus faecalis," J. Bacteriol., 89, p. 1448.

8. Forrest, W. W. (1965), "ATP Pool During Growth Cycle in Streptococcus faecalis," J. Bacteriol., 90, p. 1013.

9. De Sha, C. M., and Dozier, B. J. (1979), "A Direct Counting Method for Assessing the Performance of Denitrification Bioreactors," Developments in Industrial Microbiology, Vol. 20, Soc. of Indus. Microbiol, Arlington, p. 617.

10. Franco, C. M. M., Smith, J. E., and Berry, D. R. (1984), "Changes in Intermediate Levels During Batch Culture of Saccharomyces cerevisiae," Biotech. Letters, 6, p. 803.

11. Johnson, R. E. (1978), "Chemiluminescence and Bioluminescence Microbe Detection," Nasa Tech Briefs, p. 244.

12. Dyson, R. D. (1975), Cell Biology, Allyn and Bacon, Inc., Boston, p. 112.

13. Koliander, B., Hampel, W., and Roehr, M. (1984), "Indirect Estimation of Biomass by Rapid Ribonucleic Acid Determination," Appl. Microbiol. Biotechnol., 19, p. 272.

14. Ataai, M. M., and Shuler, M. L. (1985), "Simulation of CFSTR through Development of a Mathematical Model for Anaerobic Growth of Escherichia coli Cell Population," Biotech. and Bioeng., 27, p. 1051.

15. Karl, D. M. (1979), "Measurement of Microbial Activity and Growth in the Ocean by Rates of Stable Ribonucleic Acid Synthesis," Applied and Environ. Microbiol, 38, p. 850.

16. Lehninger, A. L. (1975), Biochemistry, 2nd ed., Worth, New York, p. 860.

17. Solomon, B. O., Erickson, L. E., and Yang, S. S. (1983), "Estimation of Biomass Concentration in the Presence of Solids for the Purpose of Parameter Estimation," Biotech. and Bioeng., 25, p. 2469.

18. Tharakan, J. P., and Chan, P. C. (1984), "Cell Number Estimation via Fluorescence Measurement," Biotech. Letters, 6, p. 793.

19. Bailey, J. E., Fazel-Madjlessi, J., McZuitty, D. N., Allred, J. C., Lee, L. Y., and Oro, J. A. (1977), "Characterization of Bacterial Growth by Means of Flow Microfluorometry," Science, 198, p. 1175.

20. Boye, F., Steen, H. B., and Skarstad, K. (1983), "Flow Cytometry of Bacteria: A Promising Tool in Experimental and Clinical Microbiology," J. Gen. Microbiol., 129, p. 973.

21. Tabor, P. S., and Neihoff, R. A. (1982), "Improved Method for Determination of Respiring Individual Microorganisms in Natural Waters," Applied and Environ. Microbiol., 43, p. 1249.

22. Zimmerman, R., Iturriaga, R., and Becker Birck, J. (1978), Simultaneous Determination of the Total Number of Aquatic Bacteria and the Number Thereof Involved in Respiration," Applied and Environ. Microbiol., 36, p. 926.

23. Britton, G., and Koopman, B. (1982), "Tetrazolium Reduction-Malachite Green Method for Assessing the Viability of Filamentous Bacteria in Activated Sludge," Applied and Environ. Microbiol., 43, p. 964.

24. Dutton, R. J., Bitton, G., and Koopman, B. (1983), "Malachite Green-INT (MINT) Method for Determining Active Bacteria in Sewage," Applied and Environ. Microbiol., 46, p. 1263.

25. Trevors, J. T., Merrick, R. L., Russell, I., and Stewart, G. G. (1983), "A Comparison of Methods for Assessing Yeast Viability," Biotech. Letters, 5, p. 131.

26. Harvey, R. W., and Young, L. Y. (1980), "Enumeration of Particle-Bound and Unattached Respiring Bacteria in the Salt Marsh Environment," Applied and Environ. Microbiol., 40, p. 156.

27. Arcuri, E. J. (1982), "Continuous Ethanol Production and Cell Growth in an Immobilized-Cell Bioreactor Employing Zymomonas mobilis," Biotech. and Bioeng., 24, p. 595.

28. Pohland, F. G., and Kang, S. J. (1975), "Measurements of Active Biomass Concentrations in Biological Waste Treatment Processes," National Technical Information Service, EPA-600/2-75-029.

29. Donaldson, T. L., Strandberg, G. W., Hewitt, J. D., and Shields, G. S. (1984), "Biooxidation of Coal Gasification Wastewaters," Environmental Progress, 3, p. 248.

30. Tribe, M., and Whittaker, P. (1982), Chloroplasts and Mitochondria, Edward Arnold Ltd., London, p. 17.

31. Bostick, W. D., and Burtis, C. A. (1980), "Hydroxylamine as a Competitive Inhibitor for the Kinetic Enzymatic Assay of Ethanol in Relatively Concentrated Solutions," Biotech. and Bioeng., 22, p. 2437.

32. Tiffany, F. O., Jansen, J. M., Burtis, C. A., Overton, J. B., and Scott, C. D. (1972), "Enzymatic Kinetic Rate and End-Point Analyses of Substrate, by Use of a GeMSAEC Fast Analyzer," Clinical Chemistry, 18, p. 829.

33. Hancher, C. W., Taylor, P. A., and Napier, J. M. (1978), "Operation of a Fluidized-Bed Bioreactor for Denitrification," Biotech. and Bioeng. Symp. No. 8, p. 361.

34. Butt, J. B. (1980), Reaction Kinetics and Reactor Design, Prentice Hall, Englewood Cliffs, p. 386.

35. Reid, R. C., and Sherwood, T. K. (1966), The Properties of Gases and Liquids, McGraw Hill, New York, p. 550.

APPENDICES

APPENDIX 1

DILUTION EFFECTS DUE TO VOLUME OF BIOFILM SAMPLE

In several instances, assays were conducted on samples of different volumes to study the linearity of the assay response. In the data of Tables 9 and 10, pages 161 and 162, average color ratios of 1.78 and 1.85 resulted from samples having volume ratios of 2.0. A correction for the dilution of the INT reagent should be made in the interpretation of these results.

Total bioparticle-sample volumes of 0.5 and 1.0 mL were used. These total volumes included the volume of the particles and the interstitial volume between the particles. The particle volume can be further divided into the biomass volume and the coal support-particle volume.

In the experimental procedure, the interstitial liquid was withdrawn by suction prior to the addition of the INT. Upon addition of 2.5 mL of 0.1% INT solution, the reagent diffused into the biofilm. Assuming equal partitioning of INT between the liquid and biofilm phases, the reagent became evenly distributed throughout the biofilm and liquid volumes at a concentration less than the original 0.1%.

There was a greater volume of biofilm in the 1.0 mL samples, causing the INT to be diluted more than in the 0.5 mL samples. Since the reaction rate is dependent upon INT concentration, the reaction rates observed in the 1.0 mL biomass samples should be less than in the 0.5 mL samples, as was observed experimentally.

The magnitude of this dilution effect may be estimated. A typical biofilm particle has an outer radius of 0.04 cm and an inner (coal particle) radius of 0.022 cm. The void fraction for the settled

particles in a biomass sample is ~0.1. The volume of biofilm in a 1.0 mL biomass sample is then

$$(1.0\ \text{mL})\ (0.9)\ \frac{[(0.04\ \text{cm})^3 - (0.022\ \text{cm})^3]}{(0.04\ \text{cm})^3} = 0.75\ \text{mL}\ .$$

Similarly, the biofilm volume in an 0.5 mL biomass sample is 0.38 mL. The concentrations of INT in the samples would be

$$0.1\%\ \frac{2.5\ \text{mL}}{(2.5 + 0.75)\text{mL}} = 0.077\% \quad \text{for a 1.0 mL sample ,}$$

$$0.1\%\ \frac{2.5\ \text{mL}}{(2.5 + 0.38\text{mL})} = 0.087\% \quad \text{for a 0.5 mL sample .}$$

Since the color produced is roughly proportional to the amount of biomass and to the concentration of INT, color ratio expected between the 1.0 and 0.5 mL samples would be

$$\frac{(1.0\ \text{mL})(0.077\%\ \text{INT})}{(0.5\ \text{mL})(0.087\%\ \text{INT})} = 1.77\ .$$

Within experimental error, this was the ratio observed experimentally.

APPENDIX 2

ESTIMATION OF DIFFUSIONAL RESISTANCE WITHIN THE BIOFILM

Hudgins' criterion[34] for the absence of concentration gradients within a catalyst particle (i.e., effectiveness factor > 0.95) may be written

$$\frac{R\ r^2}{C_b\ D} < \frac{1}{n} ,$$

where r is the radius of the particle, R is the observed rate of reaction per unit volume of catalyst, C_b is the liquid-phase concentration of the reactant, D is the effective diffusivity of the substrate in the catalyst, and n is the order of the reaction.

The order of reaction was taken to be approximately 1, based upon the nearly linear relationship exhibited between INT concentration and color formation in Figure 17, page 178. The diffusivity of INT in water was estimated to be 4.0×10^{-6} cm^2/sec using the correlation of Othmer and Thakar,[35] and the effective diffusivity of INT within the biofilm was assumed to be 25% of this value. The observed reaction rate was calculated to be 2.3×10^{-6} g $INT/cm^3 \cdot s$ from the initial slope of Figure 8-b, page 157, and the data in Table A-1. The catalyst particle radius was taken to be the biofilm thickness, 0.02 cm.

Substituting these values into Hudgins' criterion gives

$$\frac{R\ r^2}{C_b\ D} = 0.9 ,$$

which barely satisfies the criterion. Since there is uncertainty and time-variability in the values of several parameters, the results of this test are somewhat inconclusive but suggest that there is only a slight gradient within the biofilm.

Table A-1

Values Used in the Calculation of INT Reaction Rate

Parameter	Value
Initial slope of Figure 8-b	0.0078 ODU/min•mL biomass
Volume of acetone extract	50 mL
Void fraction of settled bioparticles	0.1
Outer radius of biofilm particles	0.04 cm
Inner radius of biofilm particles	0.02 cm
Molar absorptivity of INT-formazan	1.8×10^4 L/mole•cm at 490 nm
Molecular weight of INT	505.7 g/mole
Concentration of INT in liquid phase	0.1% (w/v)

VITA

Robert Mark Worden was born in Knoxville, Tennessee on September 20, 1956. He graduated from Farragut High School in June 1974 and the following September entered The University of Tennessee, Knoxville. In March 1979, he received a Bachelor of Arts degree with majors in Chemistry and Cell Biology.

In January of 1980, he accepted a teaching assistantship at The University of Tennessee, Knoxville and began study toward the Master of Science degree in Chemical Engineering. He was the recipient of an Eastman Kodak Fellowship for the 1980-1981 academic year and graduated in December 1982.

In January of 1983, he began study for the Doctor of Philosophy degree in Chemical Engineering at The University of Tennessee, Knoxville. During this time he was supported by a Union Carbide Fellowship and a research assistantship through the Oak Ridge National Laboratory. He graduated in March, 1986.

The author is a member of AIChE, ACS, Tau Beta Pi, Phi Beta Kappa, and Phi Kappa Phi. After graduation in March 1986, he will be employed by The Michigan State University and Michigan Biotechnology Institute.